POLYMER RESEARCH
Department of Chemistry,
University of Glasgow.
G12 8QQ

UNIVERSITY
of
GLASGOW

An Investigation into the Thermal Degradation of Poly(3-Hydroxy Butyric Acid)

Stuart Neil Rendall

for the degree of Ph.D.

submitted: March 1997

ProQuest LLC.
789 East Eisenhower Parkway
P.O. Box 1346
Ann Arbor, MI 48106 – 1346

Summary

Poly(hydroxybutyrate), or 'Biopol' as it is commercially known, is a naturally occurring , biodegradable thermoplastic, produced by bacterial culture. It can be processed and used in similar ways to conventional thermoplastics, offering the same versatility and convenience, whilst also being much more 'environmentally friendly'. Thus, as a marketable product it has sparked great interest, but to become a commercial success a number of intrinsic difficulties have to be overcome.

Although workable, pure PHB has relatively poor mechanical properties with respect to other thermoplastics, and it ages, worsening this situation. It is also difficult to work with because it decomposes at its melt temperature, again depressing its physical properties.

The aim of this project was to explore the possibility of using additives to improve the thermal stability of poly(hydroxybutyrate) to enable easier processing of the material. To enable this, new techniques were developed to examine the kinetics and mechanism of degradation, along with methods for determining the effect of additives. By screening a large number of additives, a number of compounds have been identified that demonstrate a stabilising effect, reducing the rate of degradation.

The new methods have included quantitative and kinetic measurements by FT-IR upon degrading systems by analysing either the molten polymer, using a heated mirror, or examining the volatile gases in a heated gas cell.

A number of modifications to the TVA (thermal volatilisation analysis) apparatus were explored. Internal thermocouples have been shown to be able to detect cold ring formation, and a thermal volatilisation mass spectrometry system (TVMS) was constructed and used to great effect.. A technique to quantitatively determine the degradation products from PHB by gas chromatography, was devised, successfully identifying PHB chain fragments up to six monomer units long. This operated by chemically forming derivatives of these degradation products

The effectiveness of the additives was examined in a number of ways. Many techniques were discarded, either being too unwieldy or of poor reproducibility. It turned out that weight loss measurements were the most straightforward and reliable, and proved to be effective for rapidly assessing additives. Kinetic measurements were also made using this technique. Molecular weight determinations were performed on degraded samples prepared using the same apparatus, allowing further comparisons and kinetic measurements to be made.

A system was designed that made it possible to record IR spectra of a degrading film of the polymer, in real time, that was being heated on a reflective surface. Loss of material from the polymer and changes in its chemical nature could be observed easily, and allowed further comparison of additives.

In summary, a number of new and novel techniques have been successfully developed to assess the kinetics and mechanism of degradation, and a number of additives have been identified that demonstrate stabilising effects.

Contents

Acknowledgements

During the course of my studies and the writing of this thesis, I have been supported and encouraged by a variety of people. In particular, the guidance and knowledge imparted by my supervisor, Dr. Ian McNeill, has been invaluable and I would like to take this opportunity to thank him.

I also acknowledge the support given by my sponsors, Zeneca Bio Products, both financial and practical in nature. The quarterly meetings with Dr Tim Hammond and Dr John Liggat were particularly beneficial in directing my studies and offering other avenues for research. It was through these meeting I became acquainted with Robert Williams, and his supervisor Dr Roy Lehrle of Birmingham University, who also had significant influence on this work.

Working in the polymer lab introduced many colleagues and friends: Shafique Ahmed, Gordon Seeley, Mussarrat Mohammed, Angus Alston, Livia Memetea, Lev Raminovsky, Alexandre Polischuk and Eugene Davydov. These people provided not only valuable ideas and criticism , but also good humour and repartee.

When it comes to repartee and good humour in the polymer lab, the technician Jim Gorman deserves particular mention. Many others of the chemistry department staff also influenced my thoughts and opinions: Ewan MacPherson, Josie Douglas, Isa Kelly, Derek Sellars, Brigitte Thompson and Kim Wilson.

Many of the technical aspects of this thesis could not have been attained without the assistance from experts within the department: Dr Kelvin Tyler, Computing and Physical chemistry; Dr John Cole, GC and GC-MS; William McCormack, Glass Blowing; Neil McLachan, Mechanical Workshop; Jarnail Bhumbra, Electronics Workshop; George McCulloch, IR-Lab; Stuart Niven, Henderson lab (diazomethane); Andrew Gliddle, IR; Tony Ritchie, MS.

It is impossible to list everyone who has helped, provided ideas or expertise, or even just moral support, but to them I also extend my gratitude and wish them well in the future.

Section 1: Introduction

Plastics have become an integral part of modern day life. They are found in a wide variety of applications, such as mouldings, films, packaging, construction materials, fabrics, coatings, etc. They are extremely versatile, and can be tailored to suit any particular application.

However, most of the plastics in use today are derived from oil or fossil fuels, which are valuable feedstocks of potentially limited supply. Some would say that squandering this natural resource for such trivial uses is wasteful and inconsiderate, particularly considering that this feedstock is used for pharmaceuticals and will be required by future generations.

Not only that, but most of these materials are extremely stable, an advantage in some applications, but this aspect poses serious problems when it comes to their disposal.

Incineration is expensive and can produce toxic by-products either in the form of volatile gas or hazardous residue which, in turn, also has to be disposed of. It also contributes to global warming, by converting 'trapped carbon' (i.e. carbon unavailable to the ecosystem because it is buried deep underground) into carbon dioxide which is a powerful greenhouse gas.

Disposal by burial is also unsuitable as landfill sites are limited and the material is bulky.

In addition, discarded material in the form of litter does not decompose, is dangerous to wildlife and leaves many rural and urban areas unsightly.

Although plastics have invaluable properties, it is clear that in our 'disposable' society they may be creating problems that, in the very near future, outweigh their benefits. Hence, there is a continued search to find new and better disposal methods, recycling methods or even materials that do not have these intrinsic problems.

One such material is poly(hydroxybutyrate). It is a naturally occurring polymer that can be used as a conventional thermoplastic, in that it can be moulded, extruded and spun, using established techniques. However unlike its olefinic counterparts, e.g. polyethylene, polypropylene. this polymer can be manufactured from renewable resources and is biodegradable.

Poly(hydroxybutyrate), PHB

Overview

Poly(hydroxybutyrate) was first isolated by Lemoinge at the Pasteur Institute in 1925[1] and was discovered to be a condensation polyester of 3-hydroxybutyric acid.

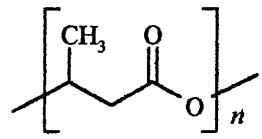

poly(3-hydroxy butyrate)

It is found as discrete spherical granules[2] within various bacteria, such as estuarine microflora and cyanobacteria[3] which produce this polymer as an energy store for when nutrients are scarce. This is analogous to the use of fat by mammals.

Commercially it is manufactured by fermenting glucose in culture with Alcaligene eutrophus and then extracting the polymer by dissolving it in chloroform[4,5] or propylene carbonate[6,7] and filtering off the bacterial residues. Alternatively the cellular material can be dissolved by use of hypochlorite[8] and filtering off the polymer. However this process degrades the PHB and the hypchlorite residues are difficult to remove.

Each monomer unit of the main polymer backbone contains an asymmetric carbon. The bacterially produced polymer is optically pure with the carbon atom in question being in the R form. Thus, by hydrolysis a large enantiomeric excess of R-3-hydroxybutyric acid can be produced. This has

been used commercially to produce intermediates for the pharmaceutical industry.[9,10]

It is possible to synthesis the poly(hydroxybutyrate) from β-butyrolactone by ring opening polymerisation[11-15], giving a polymer with similar properties to the biologically produced material, including its biodegradability[16], but it is not optically active. It cannot be synthesised by condensation polymerisation of 3-hydroxybutyric acid due to competing cyclisation and dehydration reactions, giving butyrolactone and 2-butenoic acid[17].

Early studies of the homopolymer[1] showed that the polymer is unstable at its melt temperature(~180°C), and it was concluded that it was unworkable by traditional melt methods.[18,19] However, it has been shown that the polymer is injection mouldable and can even be blown into film, provided care is taken to minimise the melt temperatures and residence times.[20] These techniques are much easier to implement by the use of poly(hydroxybutyrate-valerate) copolymers.

Valerate copolymers

The regularity in chemical structure leads to the solid polymer being highly crystalline, raising its melting point, and lowering its mechanical properties. These effects can be overcome by introducing alternative monomer units into the chain. A range of copolymers are commercially produced where 3-hydroxypentanoic acid (valeric acid) units are incorporated into the main chain. These are known as poly(hydoxybutyrate/valerate) (PHB/V) copolymers and are produced by careful control of fermentation conditions[21,22]. These valeric acid monomer units have ethyl side groups as opposed to methyl ones which disrupt the close packing of the chains in solid polymer lowering its crystallinity, and hence its melting point and fracture properties. This enables the material to be processed at lower temperatures thereby reducing the rate of degradation due to heat: maintaining its mechanical properties. However, this does not address the fundamentals of the

degradation. The copolymers degrade at similar rates to the homopolymer with the degradation reduced by utilising the lower melt temperature.

In this work, experiments were performed largely using pure PHB homopolymer, rather than the various PHB/V copolymers. This is because the copolymers produce a much more complex range of degradation products, due to the presence of valeric acid monomer units, making analysis much more difficult. However, it is generally accepted that degradation of the homopolymer and copolymers proceeds via similar mechanisms and any data obtained for the homopolymer should also be relevant to the copolymers.

Applications

This polymer has captured the imagination of many people and has led to novel uses for the polymer. Ideally it can be used as packaging materials[23-26], i.e. plastic, bottles bags, etc. but it has been suggested that it could be used as an environmentally friendly abrasive in cleaning agents[27], or biodegradable filters for cigarettes[28]. As a natural product it is completely food safe and can be used as a support in water treatment works for denitrifying bacteria[29]. In fact it is possible to buy the polymer as 'Bio Balls' for home aquariums to remove nitrates, i.e. nitrogenous fish waste, from the water. The polymer acts as a carbon source, consumed by bacteria which also use nitrogen from the water to grow, hence reducing the need for such frequent water changes.

The genes for producing the polymer have successfully been transferred to various plants[30], so that in the future the polymer could be grown directly as a cash crop by farmers, rather than from the specialised fermentation process it is today. In a science fiction novel[31], this technology was used by a community, living in space stations isolated from the earth, to produce new polymer when repeated recycling had reduced existing stocks to very low quality rendering it useless.

It would appear that the future of the polymer as a commodity plastic is quite attractive, if its intrinsic problems can be surmounted or eliminated.

Thermal Degradation of PHB

It is accepted that polyhydroxybutyrate and its copolymers are melt unstable[1], and degrades quantitatively to crotonic acid at temperatures slightly higher than its melting point[19,32].

In the temperature range 170-200°C, is has been found[33] that the molecular weight of the polymer does not fall smoothly with respect to time. In the early stages, after an initial drop, it increases significantly before, again declining. This is attributed to condensation of the initial hydroxyl endgroups with existing carbonyl endgroups and those formed by chain scission. Chain scission does not create new hydroxyl end groups and so only a finite number of condensation bonds can be formed, after which the decomposition proceeds as expected. Additional evidence is that water is produced upon degrading the polymer in vacuum[34], which is a product of condensation reactions and cannot be explained by the decomposition.

On heating to temperatures up to 300°C, the principal products are butenoic acid, commonly known as crotonic acid, its isomers and small oligomers of this type[34].

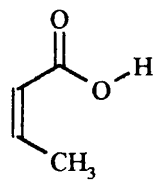

cis-crotonic acid

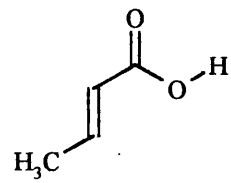

trans-crotonic acid

Other degradation products appear at higher temperatures up to 500°C. Propene and carbon dioxide are observed, which are probably decomposition products of crotonic acid whist a rearrangement reaction would produce isocrotonic acid. Butyrolactone can also be observed in small amounts, which can be formed by way of a six membered transition state, but it is very unstable, and decomposes to form ketene and acetaldehyde[35].

The most important stage, from a practical point of view, is that of the melt processing temperatures (circa 170 to 300°C). As described above, at these

temperatures, molecular weight drops rapidly, by multiple chain scissions, eventually producing small chain fragments, or oligomers, and ultimately crotonic acid with complete wieght loss from the polymer. There are a number of possible mechanisms at work here.

free radical depolymerisation

Recent work by McNeill and Brounekhel[36] on the degradation of PET has suggested a case for a radical homolysis with H abstraction. During the degradation of PET CO and CO_2 are produced throughout the degradation process. However, this mechanism seems unlikely, or at least unimportant, in the case of PHB as CO_2 is only produced at relatively high temperatures, similar to that of the degradation of PET.

ester exchange

Montaudo and Puglisi[37] believe that intramolecular exchange to be among the most frequent processes responsible for the thermal cleavage of condensation polymers. Intramolecular exchange reactions result in the formation of cyclic oligomers. Products of this type have been also been observed by Carothers in other condensation polymers[38].

beta elimination

It is generally accepted that the dominant degradation mechanism is β–elimination[39], which is involved in the pyrolysis of simple alkyl esters such as isopropyl acetate[40], and similar to that observed in the decompositon of poly(vinyl acetate) at 200-250°C[41]. Crotonic acid and its oligomers are produced by repeated β–elimination reactions (Figure 1.1).

Figure 1.1 *β–elimination reaction*

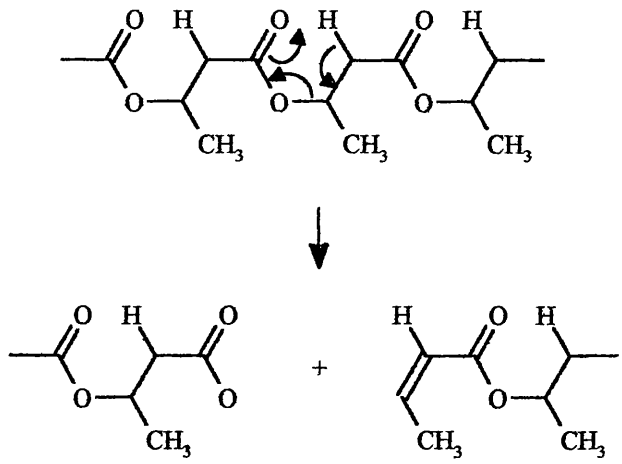

This mechanism is aided by the neighbouring carbonyl groups which weaken the hydrogen-carbon bond by keto enol tautomerism.(Figure 1.2). This means that the temperature of degradation is very much lower than that of other polyesters with longer carbon chains. It also explains why the hydrogens of the backbone are attacked in preference to those on the methyl sidegroup.

Figure 1.2 *Keto enol tautomerism*

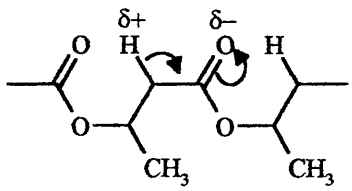

Further substantiating evidence has been demonstrated by Iwabuchi[42] with poly(β–propiolactone) and poly(pivalolactone). By substituting the β hydrogens of poly(β–propiolactone) with alkyl groups as in poly(pivalolactone) (Figure 1.3), degradation is effectively prevented.

Figure 1.3

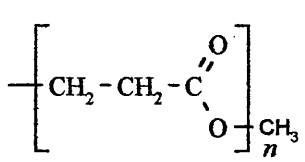

poly(β–propiolactone)

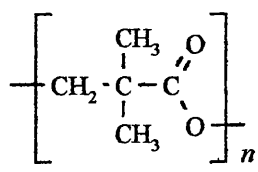

poly(piviolactone)

Kinetics of random scission

It is expected that β–elimination is a random process and can take place at any position on the polymer chain, with equal preference. It is relatively easy to generate a model[43] of such a system mathematically, which can then be compared with experimental results to test this hypothesis.

Assume that the original chain length is $(N+1)$ units, so that it has N bonds present that may be broken. If S of these bonds are broken the degree of degradation α is given by S/N. The probability that the kth bond will be broken is $w_k = S/N = \alpha$; hence the probability of this bond remaining intact will be $w_k = (N - S)/N = 1 - \alpha$. So the probability that a section of n consecutive units will be isolated will be

$$w_n = \alpha^2(1 - \alpha)^{n-1}$$

i.e. the probability of two bonds breaking in the desired place times the probability of the desired $n - 1$ bonds not breaking

This fragment of n units may be built up in $(N - n + 1)$ different ways so that the total number of these fragments will be

$$Z_n = (N - n + 1)\alpha^2(1 - \alpha)^{n-1} \qquad (1)$$

i.e. the total number of ways that the event can occur times the probability of that event.

If N is very large compared to n then (1) will reduce to

$$Z_n = N\alpha^2(1 - \alpha)^{n-1} \qquad (2)$$

Let the reaction rate constant be k

The number of bonds remaining after a degree of degradation α has been attained will be

$$N' = (1 - \alpha)N \qquad (3)$$

If the reaction is unimolecular

$$N' = N \exp\{-kt\} \qquad (4)$$

Combining (3) and (4)

$$\alpha = (1 - \exp\{-kt\}) \qquad (5)$$

equation (4) can then be substituted into equation (2) to form the complete expression for the formation of n-unit fragments with respect to time.

$$Z_n = N (1 - \exp\{- kt\})^2 (1- (1- exp\{-kt\}))^{n-1}$$

A plot of this expression for monomer and small oligomer production (Figure 1.4), displays some interesting features.

As expected, monomer production starts off slowly as there will be relatively few chain ends from which it can be formed. Production then increases to a maximum where there is clearly a large number of chain ends generated by scissions of larger polymer chains. The rate of monomer formation then slows and levels off as all of the available material is converted to monomer.

A similar situation occurs for the oligomers. Production starts slowly, reaches a maximum , but then instead of just levelling off it becomes a depletion, as each particular oligomer is consumed to produce smaller fragments.

What is less apparent from the model, is that initially, fragments of all sizes are produced with equal probability and that the observed abundance of smaller fragments results specifically from decomposition of fragments one unit larger. For example, the abundance of monomer over dimer is the result of dimer decomposing to monomer. Thus if it was possible to remove both monomer and dimer from the degrading influence they would be present in equal quantities.

Figure 1.4 *Graph of quantity of n-unit fragments produced by the random scission expression*

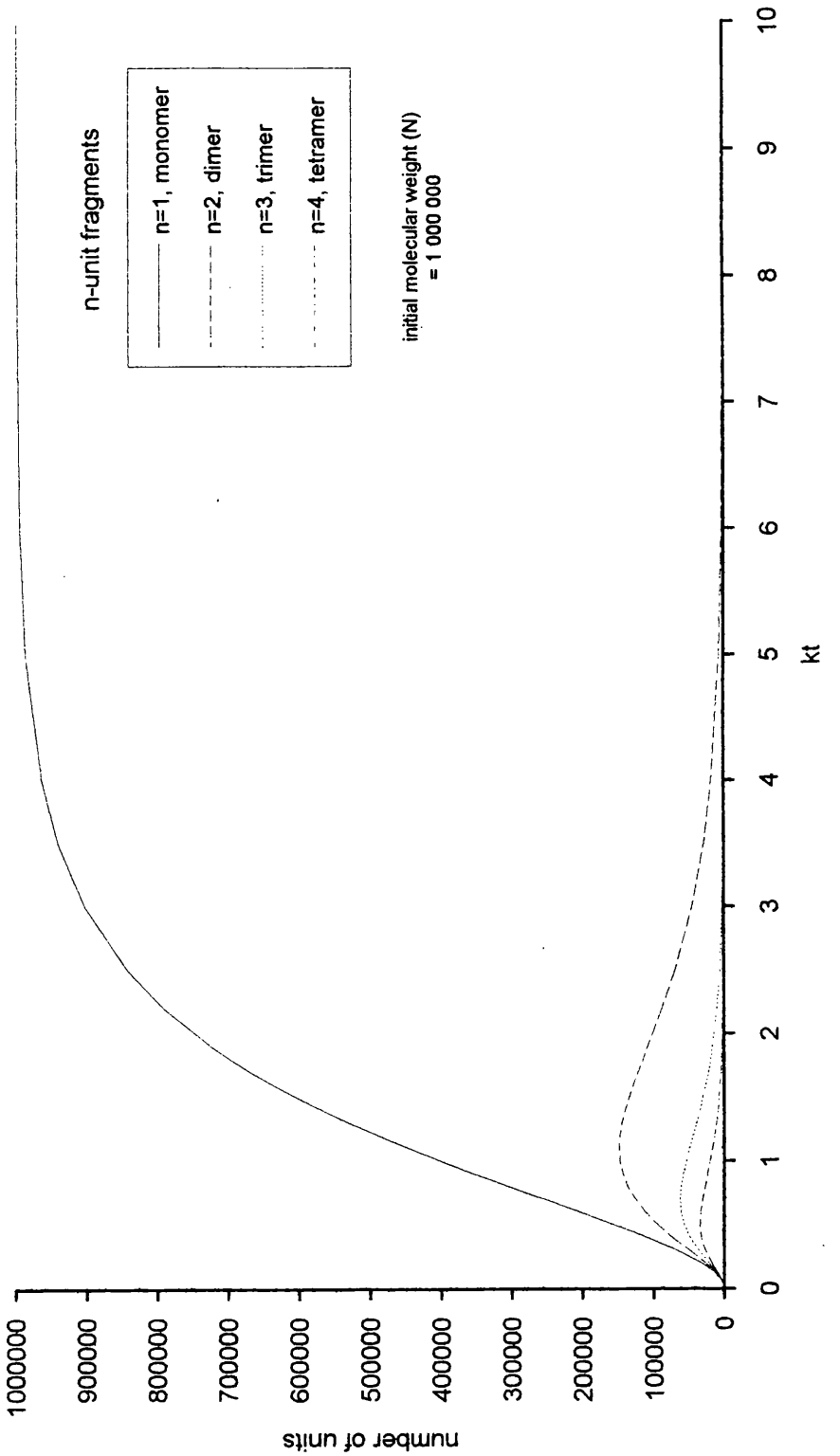

Objectives

A major problem with poly(hydroxybutyrate) is that it is difficult to process because of its thermal instability. The aim of this project is to examine and determine the degradation processes that take place at temperatures around 200°C and to investigate methods for preventing, or slowing degradation at these processing temperatures.

To achieve this, methods had to be tested for their suitability, and developed to fully optimise them for PHB use. This includes techniques to analyse the degradation products, the residual polymer and the associated kinetics.

In an attempt to stabilise the polymer an investigation into the use of additives was carried out. Again techniques to do this had to be developed which were required to be robust, reliable and allow rapid screening of possible compounds.

Compounds showing stabilising effects were subjected to further examination, to precisely determine their effect under processing conditions.

Section 2: Techniques of mechanistic study

Over the course of this investigation a large number of techniques have been examined to determine their suitability to assess the degradation of PHB.

In this section the techniques discussed were used to examine the degradation of PHB without additives in an attempt to establish the degradation patterns and mechanisms. In all cases the polymer used was high purity technical grade homopolymer, batch number G044.

The techniques included thermal volatilisation analysis (TVA), Pyrolysis-Mass Spectrometry, FT-IR spectroscopy and GC-MS.

TVA was carried out conventionally under isothermal and programmed heating conditions. The use of a thermocouple was investigated as a method for determining formation of the relatively involatile products (cold ring fraction).

The Pyrolysis-Mass Spectrometry apparatus was constructed to help to elucidate the complex trace observed in TVA. A sample was subjected to programmed heating, whilst the mixture of volatile products was fed directly into a mass spectrometer. The mass spectral data can be deconstructed to give detailed gas composition throughout heating. These results confirm and extend the TVA data, demonstrating different volatilisation patterns between isothermal and programmed heating methods.

FT-IR spectroscopy has been used to quantitatively determine volatile degradation products and kinetic analysis has been performed. This has been compared with a mathematical model for 'random chain scission'.

Thermal Volatilisation Analysis (TVA)

Thermal Volatilisation Analysis was originally created in this department by Dr Ian C. McNeill[44], and has been continuously developed over the years.

The technique offers many advantages over other analytical methods as it gives access to all of the product fractions, plus information on the stages of breakdown and threshold temperatures. It has been used with great success in various investigations related to polymer stability and mechanisms of breakdown.

A sample is heated under vacuum, either isothermally or under programmed temperature control, whilst Pirani gauges measure pressure changes caused by the evolution of volatile products. Non-condensable gases are identified by an on-line quadropole mass spectrometer. Condensable gases and volatile liquids (liquid fraction or LF) are collected in condensation traps and are later separated into their constituent compounds by a sub-ambient distillation procedure (sub-ambient thermal volatilisation analysis or SATVA). Less volatile material (referred to as cold ring fraction or CRF) condenses onto a water cooled surface (the cold ring), adjoining the oven.

These collected materials: i.e. the components of the liquid fraction, the cold ring fraction and the residue, are then available for subsequent analysis by other methods such as FT-IR spectroscopy, GC, MS or HPLC.

TVA and PHB

Earlier work showed that the usual TVA method was unsuitable for analysis of PHB[45]. Typically the oven is programmed from 0 to 500°C at 10°C/min. However, as the oven temperature rises the region around the cold ring warms. In the case of PHB, the viscosity of the collected material is lowered and it then falls into the hot chamber, where it degrades rapidly producing uncharacteristic spikes on the TVA trace.

Initially this was overcome by inserting a cold finger into the degradation tube that used solid CO_2 as the coolant. This provided a fixed temperature cold surface for the volatile materials to condense and prevented further secondary degradation. This system was used for long term isothermal experiments at 200°C for four and five hours. The TVA traces show little variation, whilst the SATVA trace shows small amounts of CO_2 and H_2O. This was attributed to minor leakage in the vacuum system and it was concluded that there is no significant direct formation of these products.

A much simpler solution to avoid degradation of the cold ring fraction was to heat the sample to only 250°C at 5°C/min. This temperature does not affect the cold ring significantly but is perfectly adequate for complete degradation of the PHB sample. The TVA trace shows some response by this method, and this was used to advantage in later work.(see *TVA comparison of impure samples from each stage of the production process, p86*)

In both experiments there is almost complete weight loss of sample leaving very little residue and producing a large quantity of cold ring fraction (CRF) which was a light brown coloured, thick syrupy liquid with a smell very like crotonic acid. The residue was a black char that smelt of burnt potatoes and was analysed by IR, whilst the CRF was a thick syrupy liquid that smelled of crotonic acid and was analysed by FT-IR spectroscopy and GC-MS.

IR spectrum of residue

The IR spectrum of the black char shows a broad peak in the NH stretching region and strong similarities to the spectra of polyamides by comparison with the IR database. Hence it is concluded that the char consists mainly of proteinaceous material, remnants of the cultured bacterial cells used to manufacture the polymer.

IR spectrum of cold ring fraction

The spectrum of the cold ring fraction(Figure 2.2) appears to be intermediate between that of pure PHB(Figure 2.1) and crotonic acid(Figure 2.3). There are two types of ester carbonyl stretch present, as in pure PHB at 1740cm^{-1} and 1720cm^{-1} but the carbonyl absorption is much broader, extending past 1700cm-1, the region for acidic carbonyls. There is a strong unsaturation peak at 1655cm^{-1}, as for crotonic acid. Similarly a broad OH band is present at 3000-3500cm-1. The finger print region shows strong similarities with both crotonic acid and PHB. Hence the CRF is believed to consist of small oligomers, fragmented PHB, which have vinyl and acidic end groups like crotonic acid.

GC-MS of cold ring fraction

The cold ring fraction was also investigated using the departmental GC-MS service. The GC trace (Figure 2.4) showed three peaks with virtually the same mass spectrum: that of crotonic acid. To eliminate 3-hydroxybutyric acid as a possible product, mass spectra and retention times were compared for the sample and a reference sample of 3-hydroxybutyric acid (Figure 2.5). The retention data clearly showed that 3-hydroxybutyric acid was not present and so it is assumed that only oligomers of crotonic acid were present in the sample.

Figure 2.1 *Infra-red spectrum of PHB homopolymer, taken as KBr disc.*

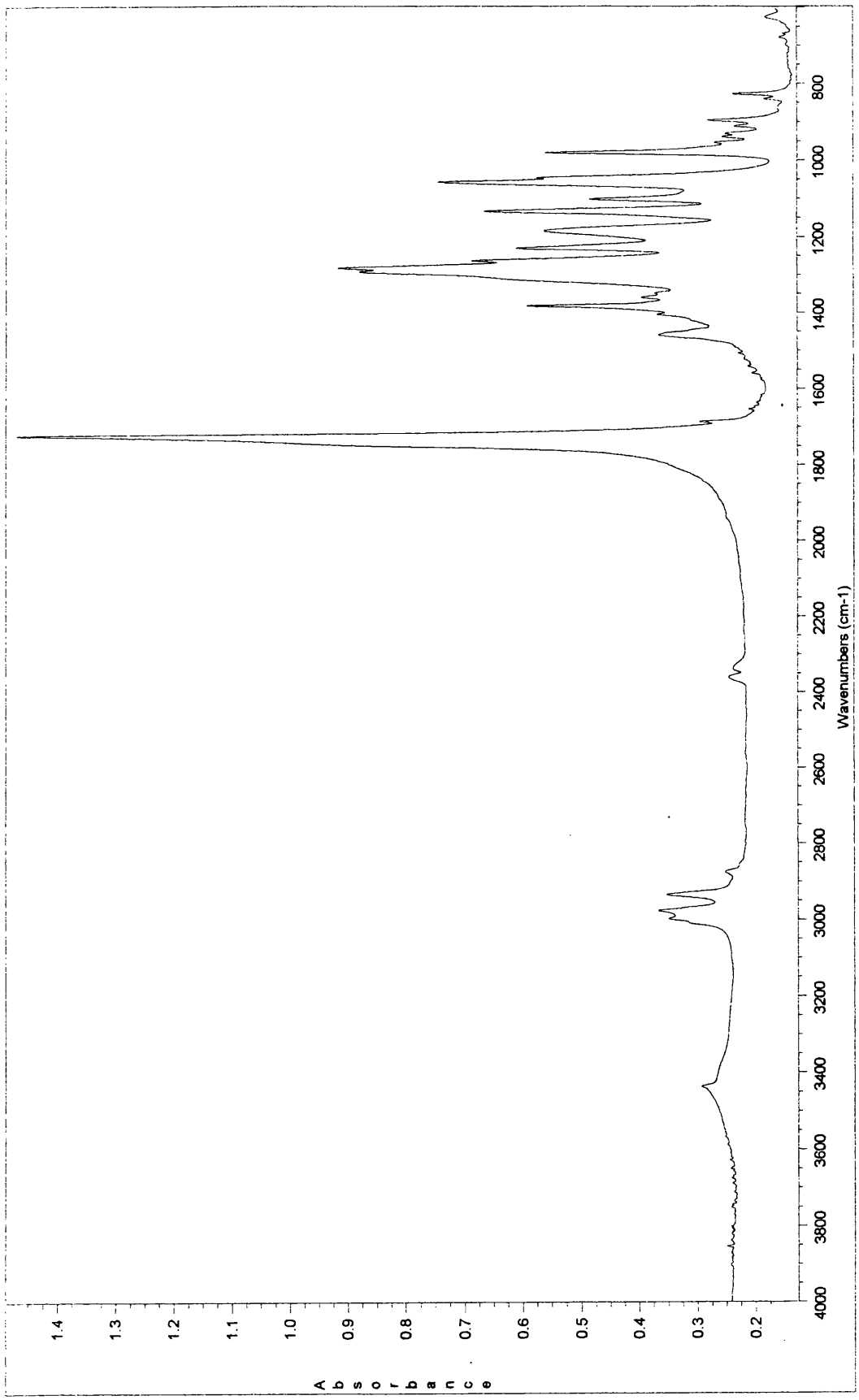

Figure 2.2 *Infra-red spectrum of cold ring fraction from a TVA experiment of PHB heated to 250°C, on a NaCl window.*

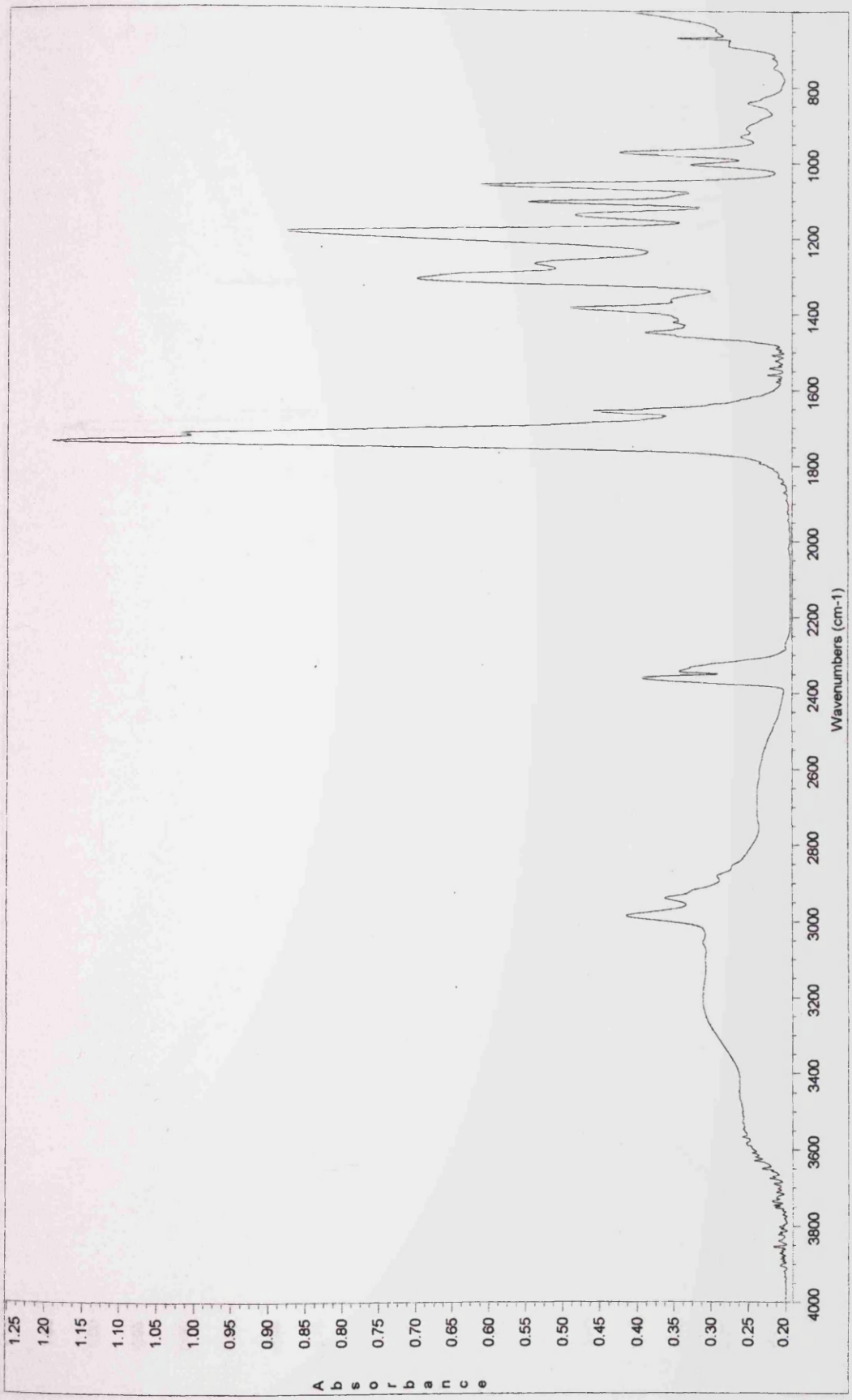

Figure 2.3 *Infra-red spectrum of crotonic acid, cast from a methanol solution onto a NaCl window*

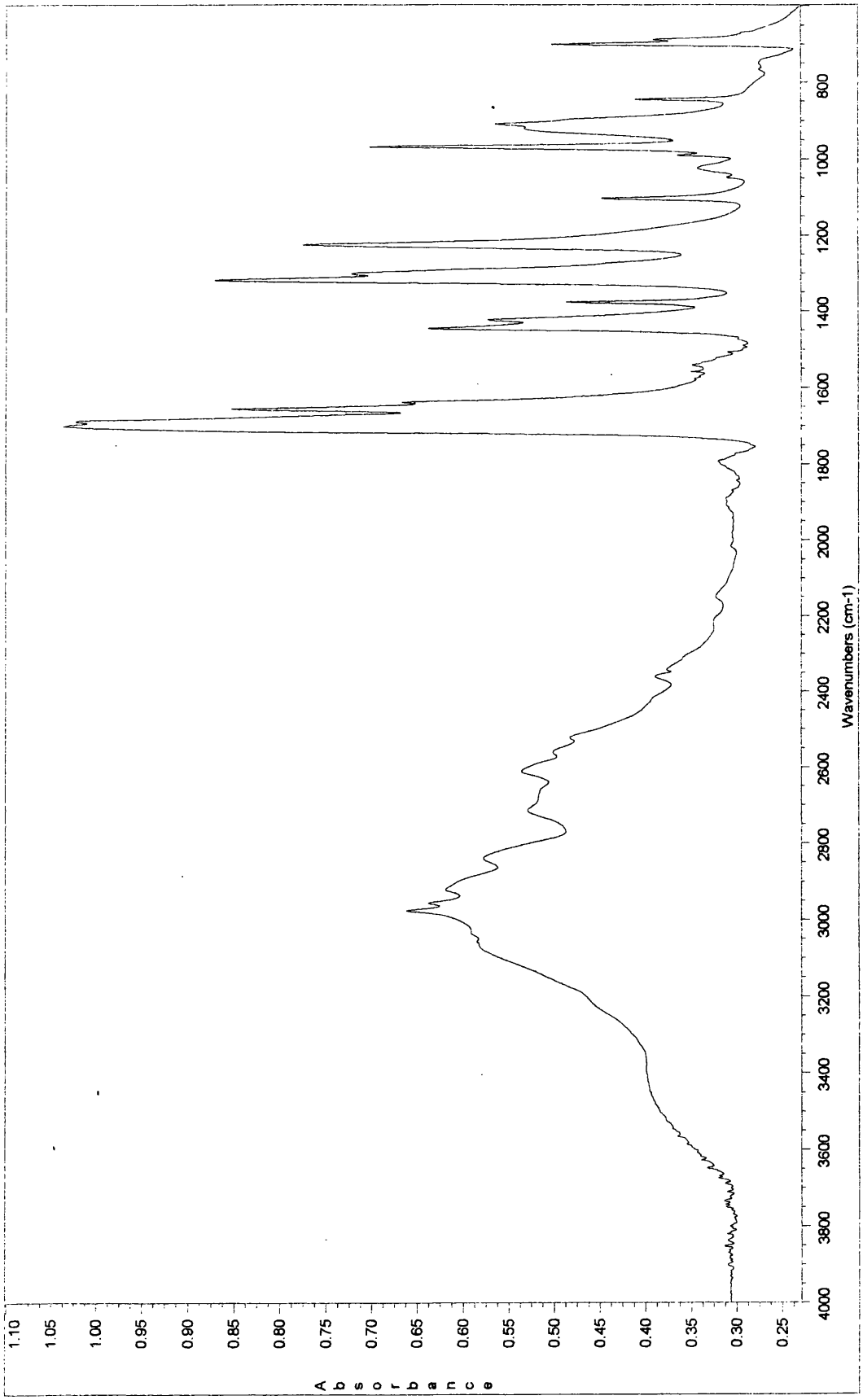

Figure 2.4 *GC trace of cold ring fraction from a TVA experiment of PHB heated to 250°C*

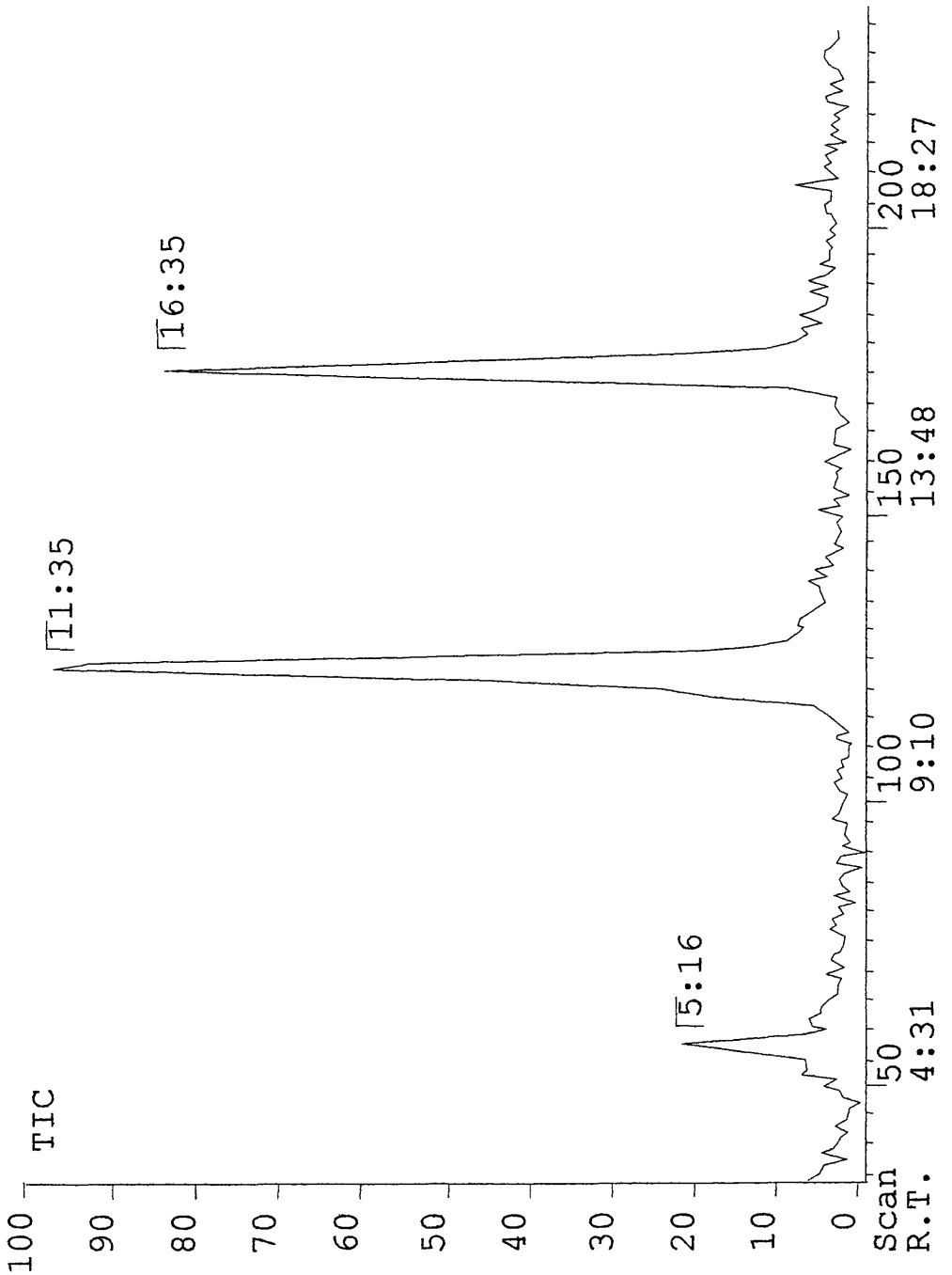

Figure 2.5 GC trace of 3-hydroxybutyric acid

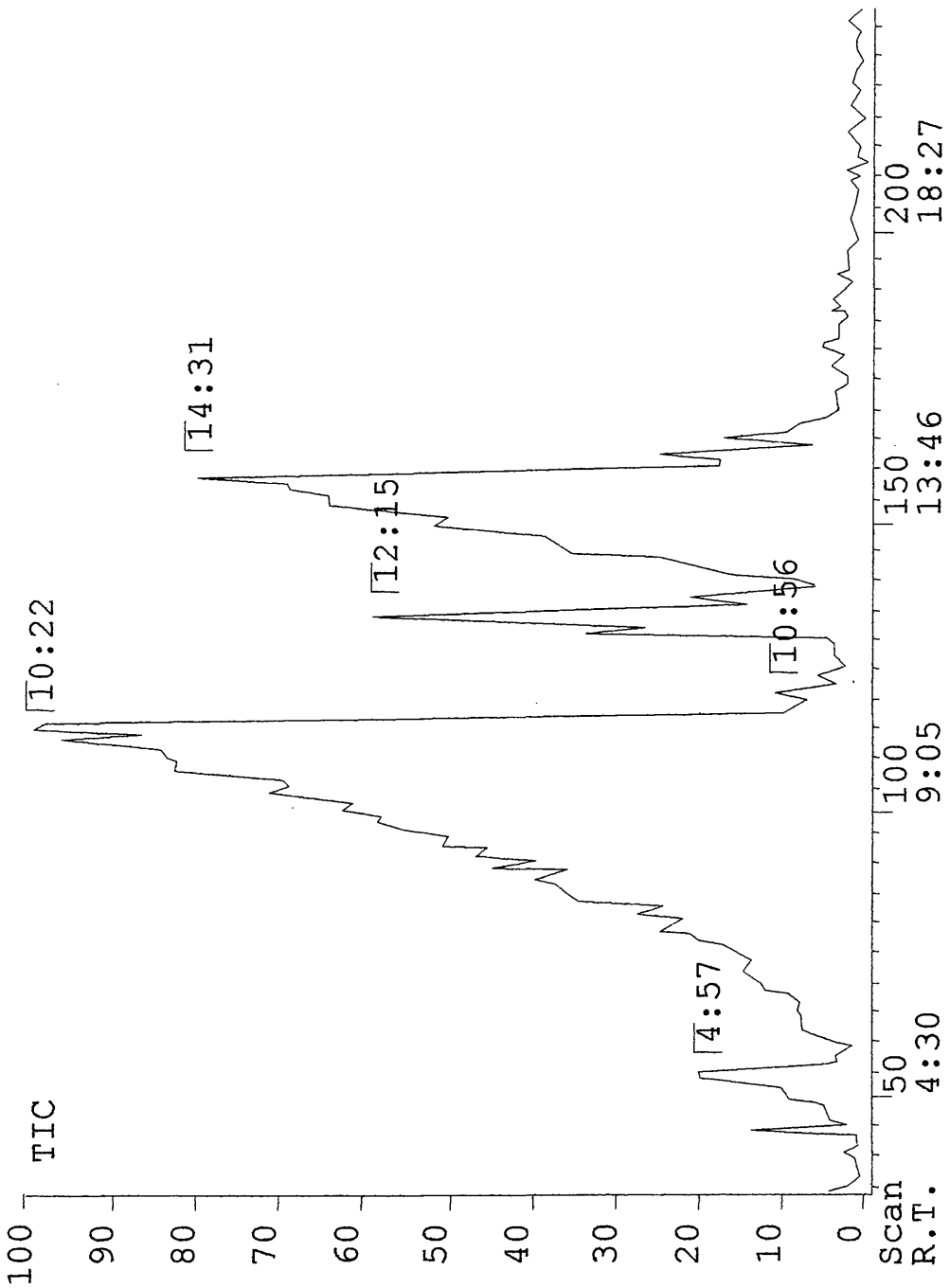

Oven Thermocouple Calibration

The current TVA setup uses a number of Pirani gauges along with two thermocouple pairs. These are attached to a computer which records their responses throughout the heating programme.

The thermocouples consist of a pair of chromel/alumel junctions, one of which is placed in the oven and the second is placed in an ice bath as a reference. A temperature dependant contact potential develops at each of the two junctions, but as the junctions are the reverse of each other the potentials oppose. The resulting potential difference is roughly 4mV per 100°C temperature difference.

The Pirani control units possess an output port that produces a voltage proportional to the gauge reading.

The voltages from the Pirani guages and thermocouples are passed to amplification/attenuation circuits and read by an Analogue to Digital Converter (ADC) in the computer. The ADC returns a value from 0 to 4095 for each reading, so the attenuation/amplification has been calculated such that the response is maximised. Thus, there is an arbitrary integer produced for each measurement. This is ideal for the Pirani gauges as it is the relative pressure in the system that is measured. However, to establish degradation temperatures the exact temperature in the oven must be calculated. Hence, it is necessary to calibrate the response from the thermocouple pair.

To calibrate the thermocouple reading a millivolt source was used to generate the expected potential from the thermocouple. It was connected directly to the amplifier/attenuator circuit and the potential adjusted to correspond to various temperatures according to literature values[46].

It is clear that the relationship between temperature and ADC reading takes the form

$$\text{ADCresponse} = \text{factor} \times \text{Temperature}(°C) + \text{constant}$$

The factor can be calculated by performing a linear regression analysis (Figure 2.7) on the readings taken from the millivolt source(Figure 2.6). The constant was obtained by shorting the contacts on the amplifier to produce a zero voltage. This was done as we cannot be sure that there is not an intrinsic voltage introduced by the source.

The resulting conversion is:

$$\text{ADC response} = \text{Temperature}(°C) \times 6.59 + 338$$

or

$$\text{Temperature}(°C) = 0.152 \times (\text{ADC response} - 338)$$

Figure 2.6 *Comparison of ADC values with millivolt source (raw experimental data*

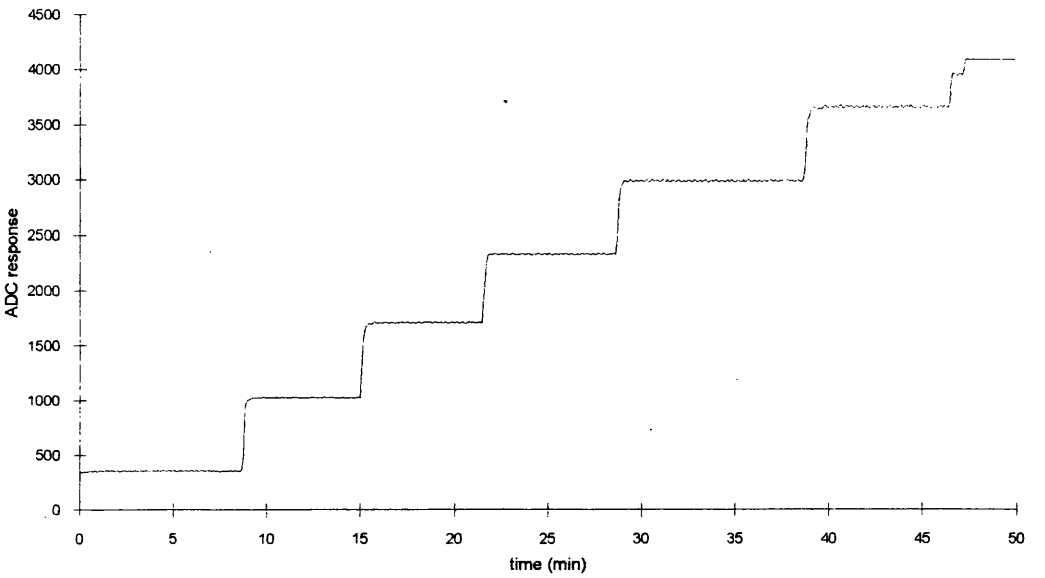

Figure 2.7 *ADC response versus temperature (calculated from millivolt source settings*

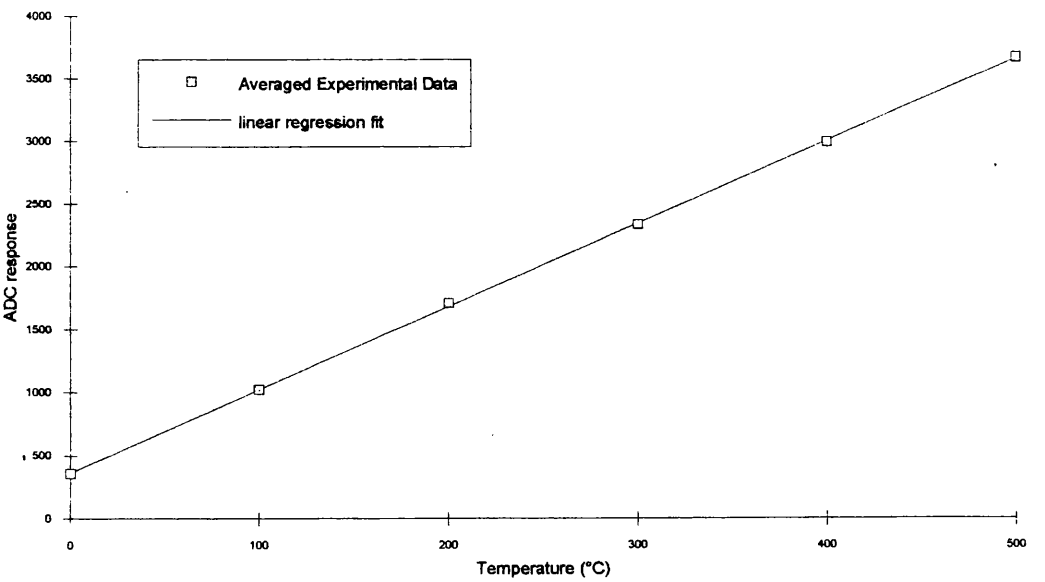

Viability of an internal thermocouple as a detector of CRF formation

In differential thermal analysis (DTA) a sample is heated at a constant rate and the temperature of that sample is measured and compared with that of a standard. Absorption or evolution of heat by the sample as the temperature is raised is detected by endotherms or exotherms on the plot of ΔT versus T.

A typical example of what is seen would be an endotherm, caused by melting, followed by an exotherm due to sample decomposition.

The same principle could, in theory, be used to detect volatilisation from a hot sample in a TVA experiment, using a thermocouple junction located just above the sample. When volatile products leave the hot sample and pass the thermocouple junction, it should register a small increase in temperature. In this way, it was hoped to detect formation of cold ring products (crotonic acid and oligomers) which are not detectable by the Pirani gauges.

A system for measuring this effect was incorporated into conventional TVA apparatus with relatively simple hardware and software modifications.

The original TVA data collection system is set up such that 5 channels of the analogue to digital converter (ADC) are used for the Pirani heads, one channel is used for the oven thermocouple and another for the SATVA thermocouple. In this arrangement both thermocouple circuits are a back to back pair using an ice bath as a reference. The SATVA thermocouple has been calibrated to be much more sensitive than the oven thermocouple as it operates over a smaller temperature range. As there are two thermocouple channels attached to the computer one of the circuits could be used for recording the oven temperature, and the other (normally used for SATVA) used to measure the temperature difference, by putting the reference junction in the oven, instead of in an ice bath, and the other in the sample tube positioned above the sample. The difference could thus be measured with the sensitivity of the SATVA thermocouple.

The experiment was carried out as in a normal TVA experiment at a heating rate of 5°C/min up to 250°C. The arms of the extra thermocouple circuit were positioned 2mm above the sample (inside the TVA tube), and the reference junction inside the oven was positioned as close to the internal thermocouple as possible i.e. just below the tube base.

The trace on the computer is also as normal but with the added difference thermocouple trace. This trace is such that when its ordinate is zero it will represent an equal temperature between the inside and outside of the sample tube, and the larger the ordinate response the cooler the internal thermocouple is with respect to the oven thermocouple.

When the system was tried with a sample of PHB a response similar to the typical one described above was observed (Figure2.9). However, when the experiment was repeated with no sample present, the initial exotherm remained (Figure 2.10). This technique clearly showed up a very minor anomaly in the heating rate, caused by the temperature programmer. When this anomaly is taken into account, the thermocouple response was very poor: showing a slight exotherm during vapourisation of the products. An attempt to amplify this effect, by reducing the size of the tube used, did not have the desired effect.

On shortening the internal thermocouple to 20cm(Figure 2.8) the resulting difference thermocouple trace showed a large exotherm i.e. the temperature of the internal junction warmed towards the temperature of the oven junction. This was possibly due to a warming effect of the cold ring fraction condensing onto the junction. An internal thermocouple 25cm long showed very little response to the degradation. It was also observed that the position of the junction inside the oven had little effect on the sensitivity.

Figure 2.8 *Schematic diagram of TVA tube with the associated internal thermocouple measurements*

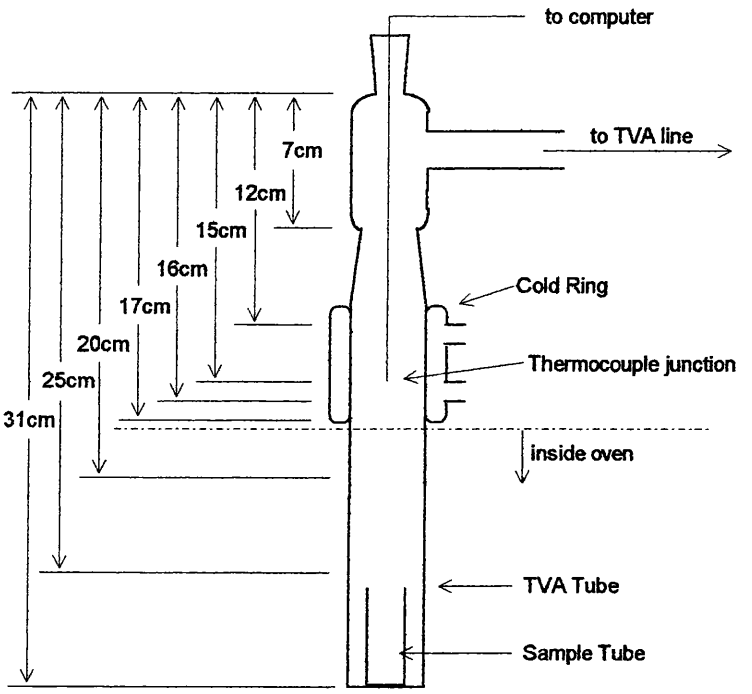

When the internal junction was 16cm long, the reading from the thermocouple pair went off scale i.e. the temperature difference was very large. At this point the difference pair was adapted to take a direct temperature reading of the inside of the tube using an ice bath as a reference.

Using the thermocouple to measure the absolute temperature of the internal junction produced much more satisfactory results. With the 16cm thermocouple, positioned just inside the cold ring, the trace clearly shows a cooling effect followed by warming. This is thought to be caused by volatile gases passing the junction, cooling it, followed by warming due to condensation of cold ring products (relatively non-volatile) onto the junction.

This theory would appear to be confirmed by later experiments. As the thermocouple junction is raised above the cold ring the warming effect is lessened as the cold ring product is condensed on the cold ring and so does not reach the junction, hence only the cooling is observed. As the thermocouple is lengthened, the cooling effect is lessened and only the warming effect of the non-volatile products condensing is observed (Figure 2.11).

The heating and cooling effects were confirmed by repeating each run without sample to obtain background traces. These runs gave rise to smooth curves (Figure 2.12).

Note that in the experimental run with the 20cm thermocouple the junction got so warm that the reading went off scale. In a repeat of the experiment, this was prevented by wrapping foil around the outside of the top of the TVA tube with aluminium foil, reducing the amount of radiant heat reaching the junction. This kept it cool enough for acceptable readings to be made.

It is apparent that a thermocouple placed in the cold ring region can be used to detect CRF formation and a thermocouple placed above detects the flow of gases past that point. The recorded information suggests that the degradation of PHB takes place in two stages: the initial stage is the formation of volatile products, causing the peak on the Pirani trace and a cooling effect on the 12cm thermocouple, the second stage produces predominantly cold ring, detected by the 20cm difference thermocouple. This idea is supported by later experiments using thermal volatilisation mass spectroscopy (*see p36*).

Figure 2.9 TVA run of PHB with difference thermocouple

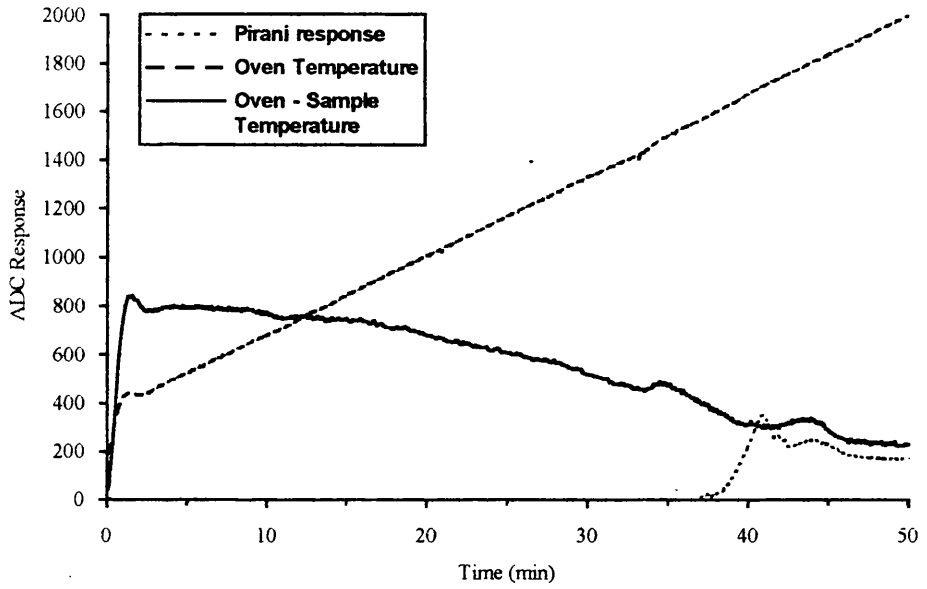

Figure 2.10 TVA run of empty tube with difference thermocouple

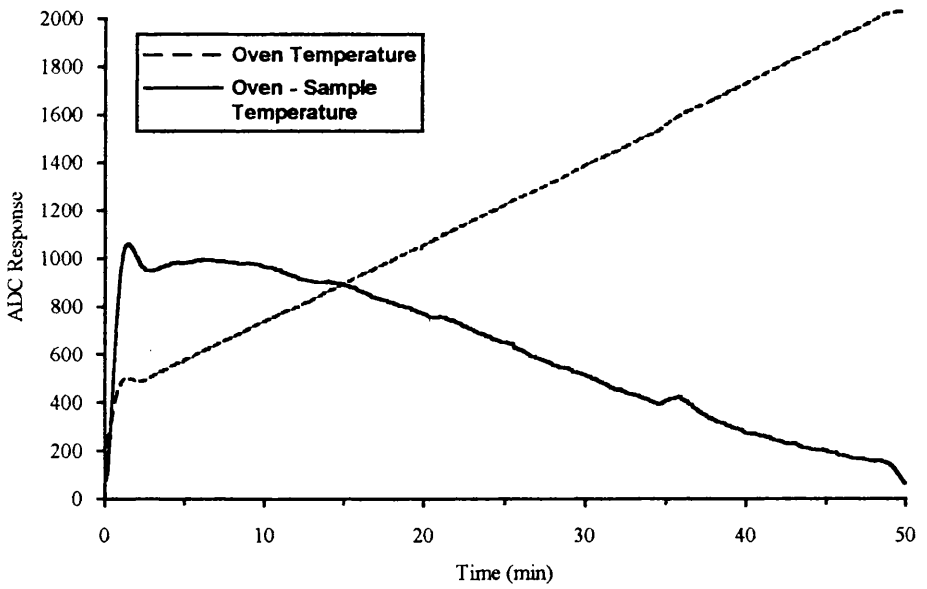

Figure 2.11 TVA traces of G044 degradation at heating rate of 5°C/min with internal thermocouple at various heights

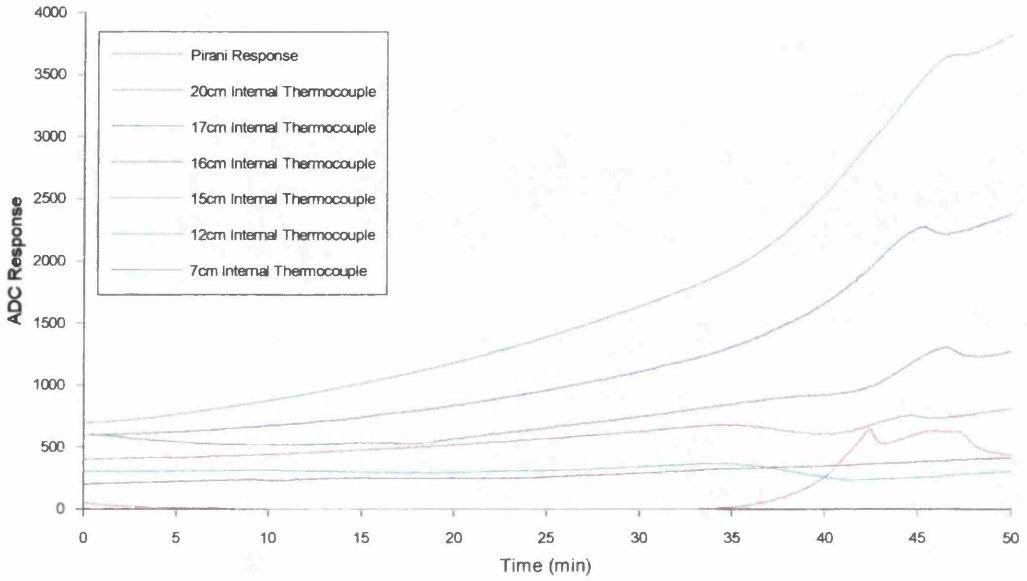

Figure 2.12 TVA traces with no sample at heating rate of 5°C/min with internal thermocouple at various heights

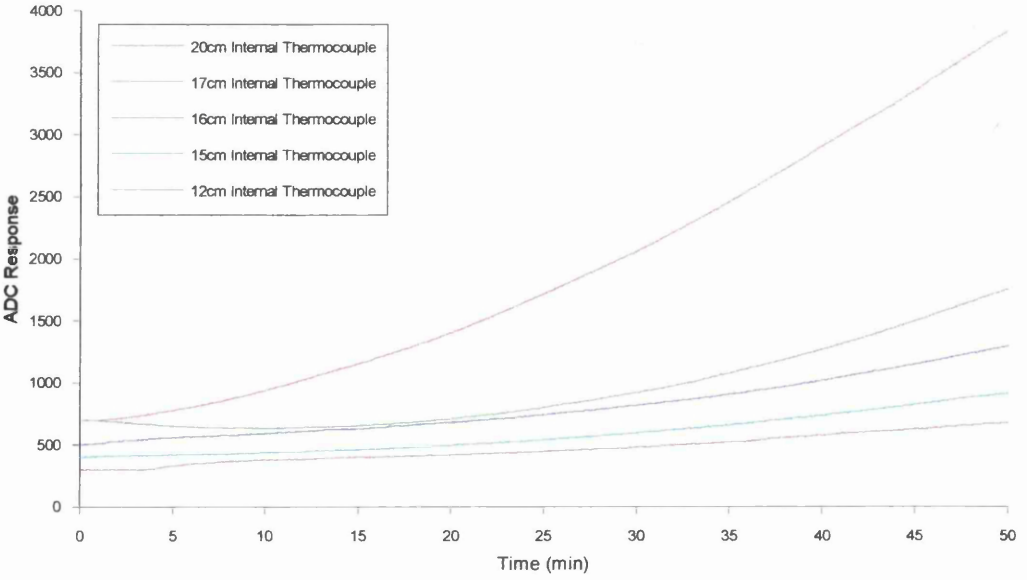

Thermal volatilisation mass spectrometry (TVMS)

It has been established that the TVA apparatus, although a very useful tool for examining polymers, poses a number of problems when faced with PHB. This is mainly because of the nature of the degradation products, crotonic acid and its oligomers, which sublime readily from the CRF yet adhere strongly to the walls of any container, even under high vacuum.

The conventional technique used in the lab for analysing the degradation products, SATVA, is also of limited use as the method relies upon the examination of all the products after complete degradation and gives no indication at which temperatures or the rate at which they formed. This is of particular importance in this case as a complex mixture of products is given off in a small temperature region.

The TVA apparatus has a gas analysis quadropole mass spectrometer connected for the purpose of identifying components of the SATVA trace. Normally this records a sample spectrum from each peak of the trace. However, with appropriate software, it can collect a series of spectra which can be manipulated at a later date. By allowing the spectrometer to sample volatile products throughout an experiment, either TVA or SATVA, it is possible to determine the nature and relative quantity of the volatile products as they evolve, leading to a much more detailed analysis.

A system such as this has been used to great effect by Shafique Ahmed[47] but was unsuitable for PHB because of the distance between the degradation oven and the mass spectrometer which provides many surfaces for the sublimate to adhere. In addition, the TVA peaks in the aforementioned system were quite well resolved and the products of completely different nature making interpretation of the data relatively simple.

To eliminate these long path lengths a thermistor element (Pyroprobe) was used to heat the sample and was connected directly to the mass spectrometer. The Pyroprobe consists of a small coiled filament, the temperature of which is controlled by measuring its resistance. It is an extremely powerful tool and

can heat a sample to over 1000°C at a rate of 2000°C/sec. However, 'flash' heating is not always desired and much finer control can also be achieved. The nature of this technique means that it is impossible to determine the exact temperature of the sample, but if the heating is ramped then the accuracy of the measurements are less crucial because all temperatures in the program will be achieved at some point. This contrasts with an isothermal experiment where exact sample temperature control is critical as a small temperature difference can affect reaction rates significantly.

A special chamber to house the Pyroprobe was constructed out of 'Swagelok' fittings (Figure 2.13). This consisted of a short piece of large bore tubing connected to the 'Nupro' valve on the spectrometer with a PTFE ferrule forming the seal on the probe. The probe itself was not airtight, being designed to operate in 'positive' gas pressures, and had to be dismantled and sealed with epoxy resin.

Figure 2.13 Schematic diagram of pyroprobe/mass spectrometer connector

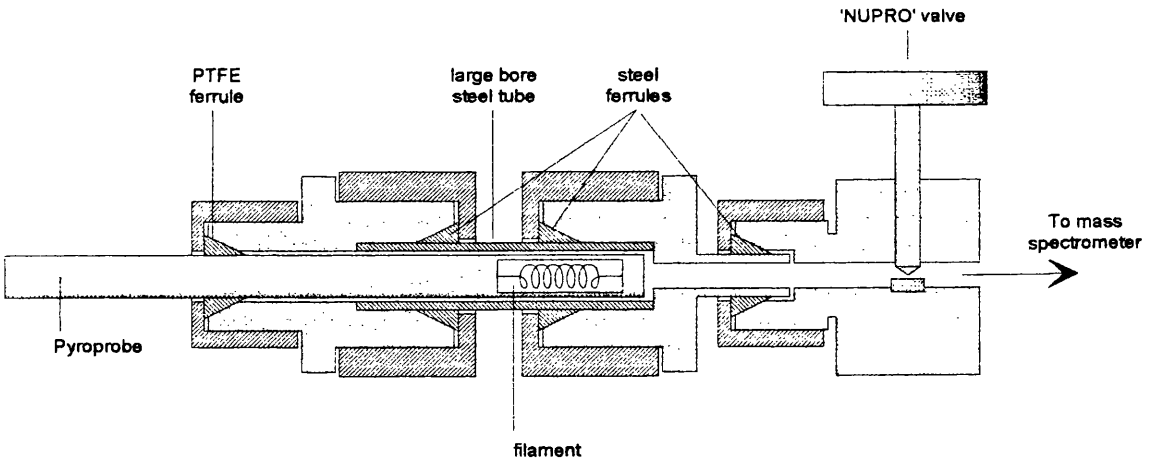

Because the Pyroprobe was connected directly to the mass spectrometer, tiny samples had to be used - very much less than 1mg. Initially these were placed inside a quartz tube that was inserted into the coiled filament but it was discovered that the tube heated unevenly, being much longer than the coil. Instead, the sample was deposited directly onto the filament from chloroform solution by evaporation. Once a sample was inserted, all joints were checked with helium and the chamber left to pump out overnight.

The probe was programmed for a ramped heating rate of 10°C/ min from 50 to 350°C and the spectra collected using the RGA Windows software.

When the data is reconstructed, the results give a trace very similar to that observed in TVA apparatus. The trace shows a single broad hump but with a pronounced peak in the initial stage. In addition, it can be seen that the polymer retains some solvent (chloroform), even though it has been exposed to an extremely high vacuum overnight. This can be seen as a sharp initial peak giving ions at 85, 87 etc.

At first glance, it would appear to be a fair assumption to say that, after loss of trapped solvent(Figure 2.15), crotonic acid is the main product throughout the degradation as the mass spectra obtained consist mainly of ions associated with crotonic acid, but, by plotting the abundance of the various ions throughout the temperature ramp it can be seen that their relative abundance varies dramatically(Figure 2.14).

The pronounced peak gives spectra with ions and intensities that would be expected for pure crotonic acid(Figure 2.16), but in the later stages it can be observed that this changes significantly(Figure 2.17), indicating that a different species of degradation product is being evolved. To aid the identification of this product(s) the averaged spectrum of the first peak (2-5mins) was subtracted, from the average of the second (15-30mins). The subtraction was carried out using a scaling factor such that the abundance of the 86 ion was cancelled out to zero in the resulting spectrum(Figure 2.18).

Figure 2.14 Relative abundance of selected ions against time during pyroprobe heating program (50 - 300°C at 10°C/min)

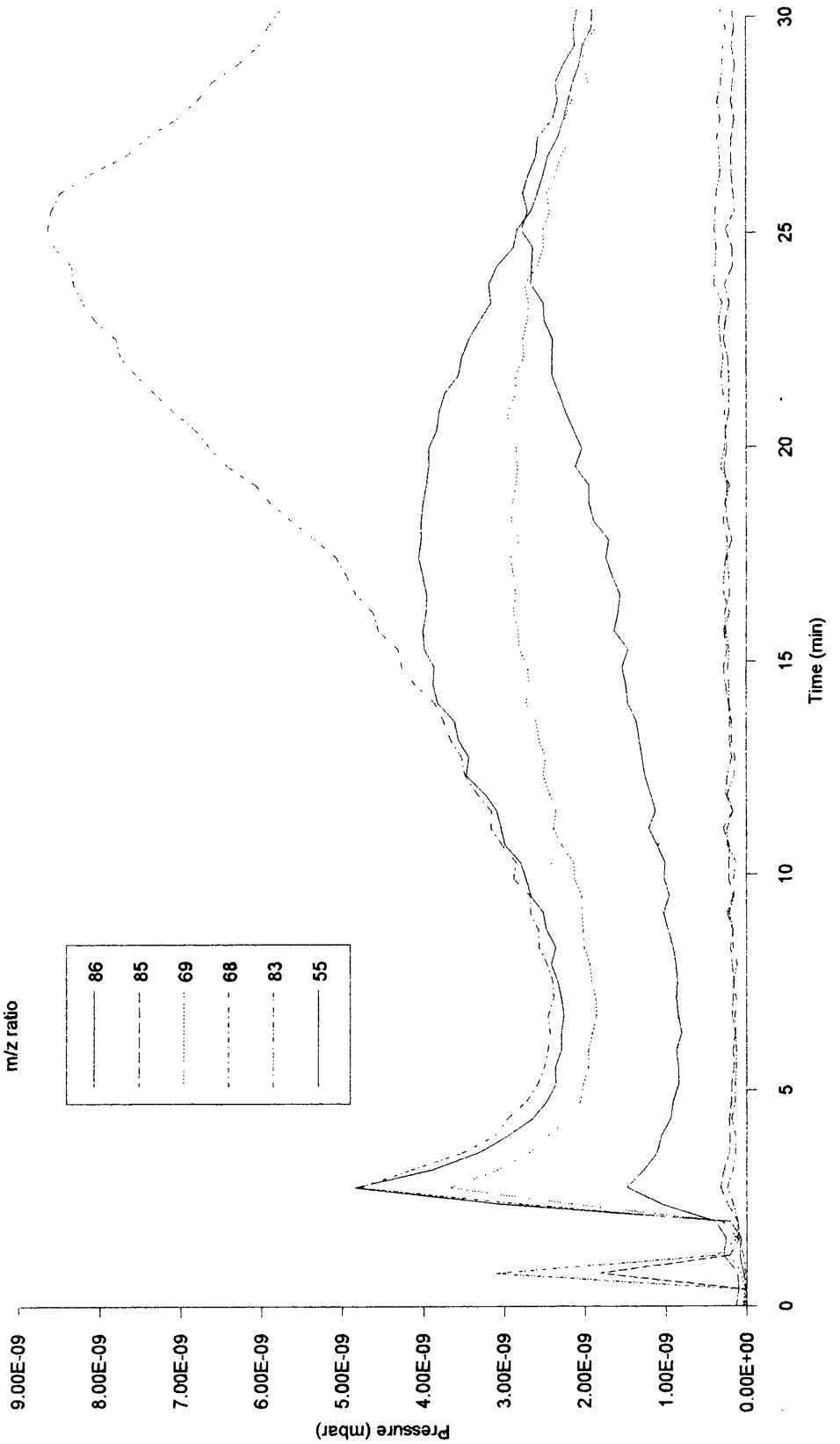

Figure 2.15 Mass spectrum of peak 1 (scan no.3) chloroform

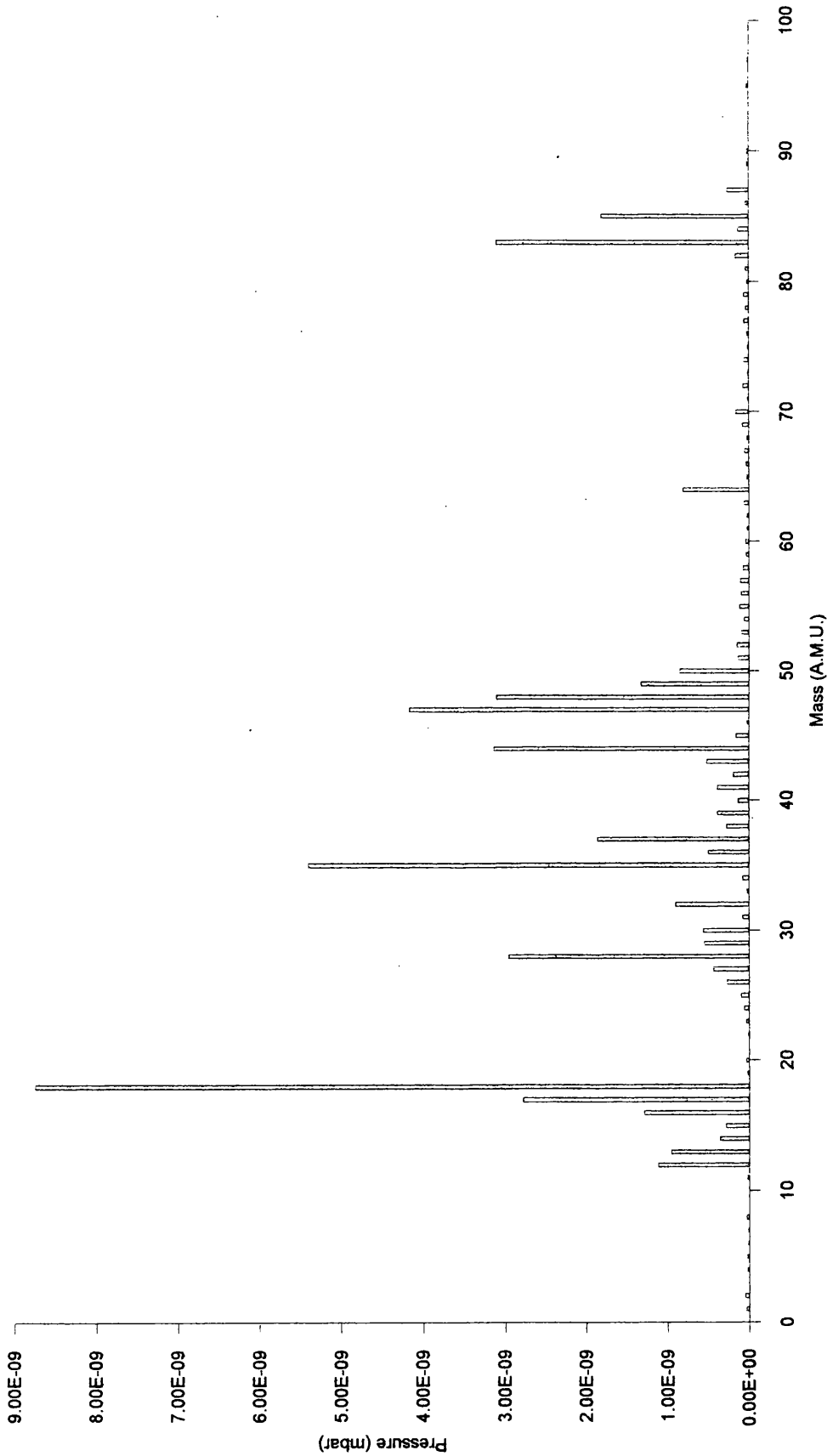

Figure 2.16 Mass spectrum of peak 2 (scan no.7) - crotonic acid

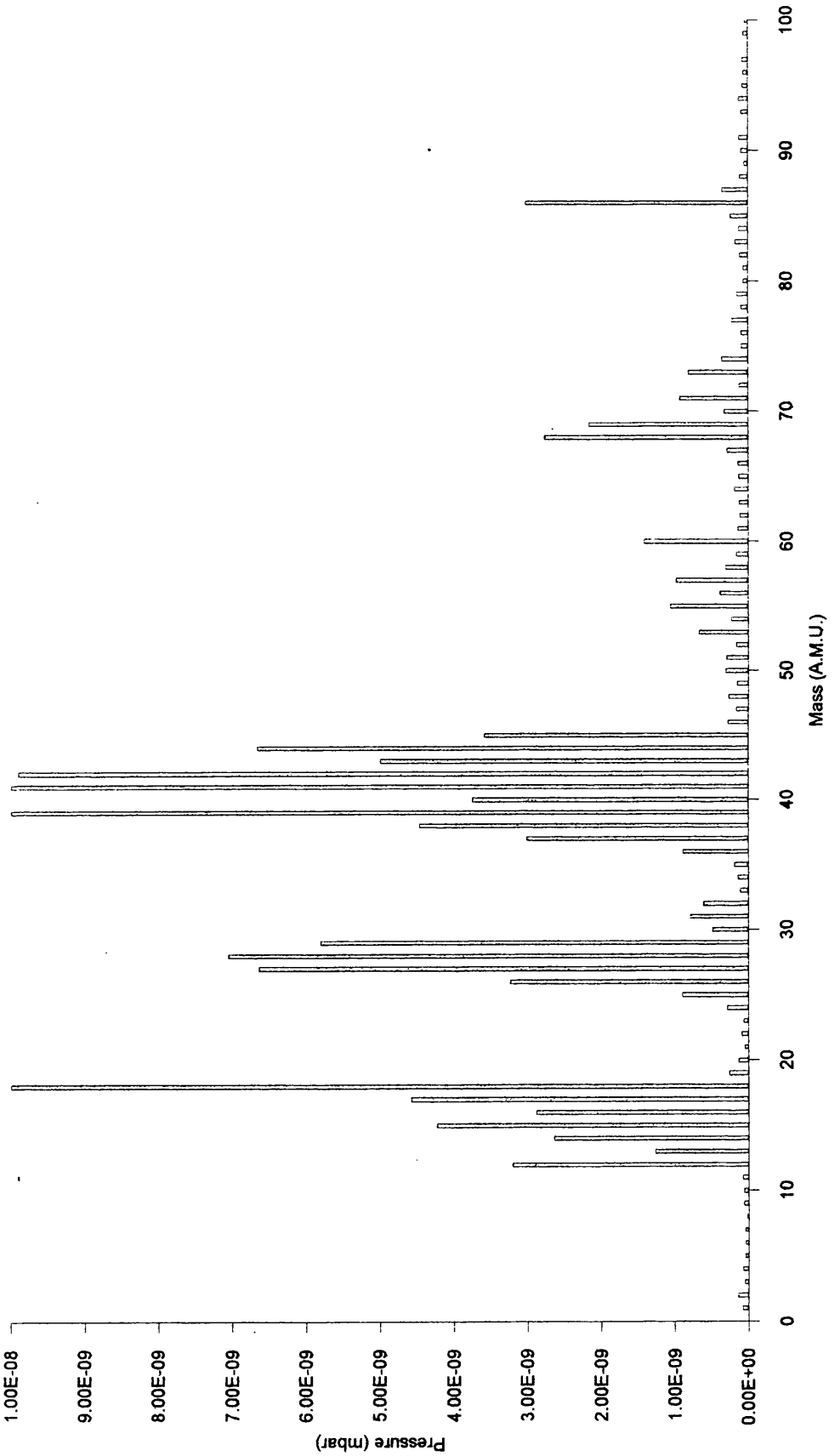

Figure 2.17 Mass spectrum of peak 3 (scan no.66) - ooligomers of crotonic acid

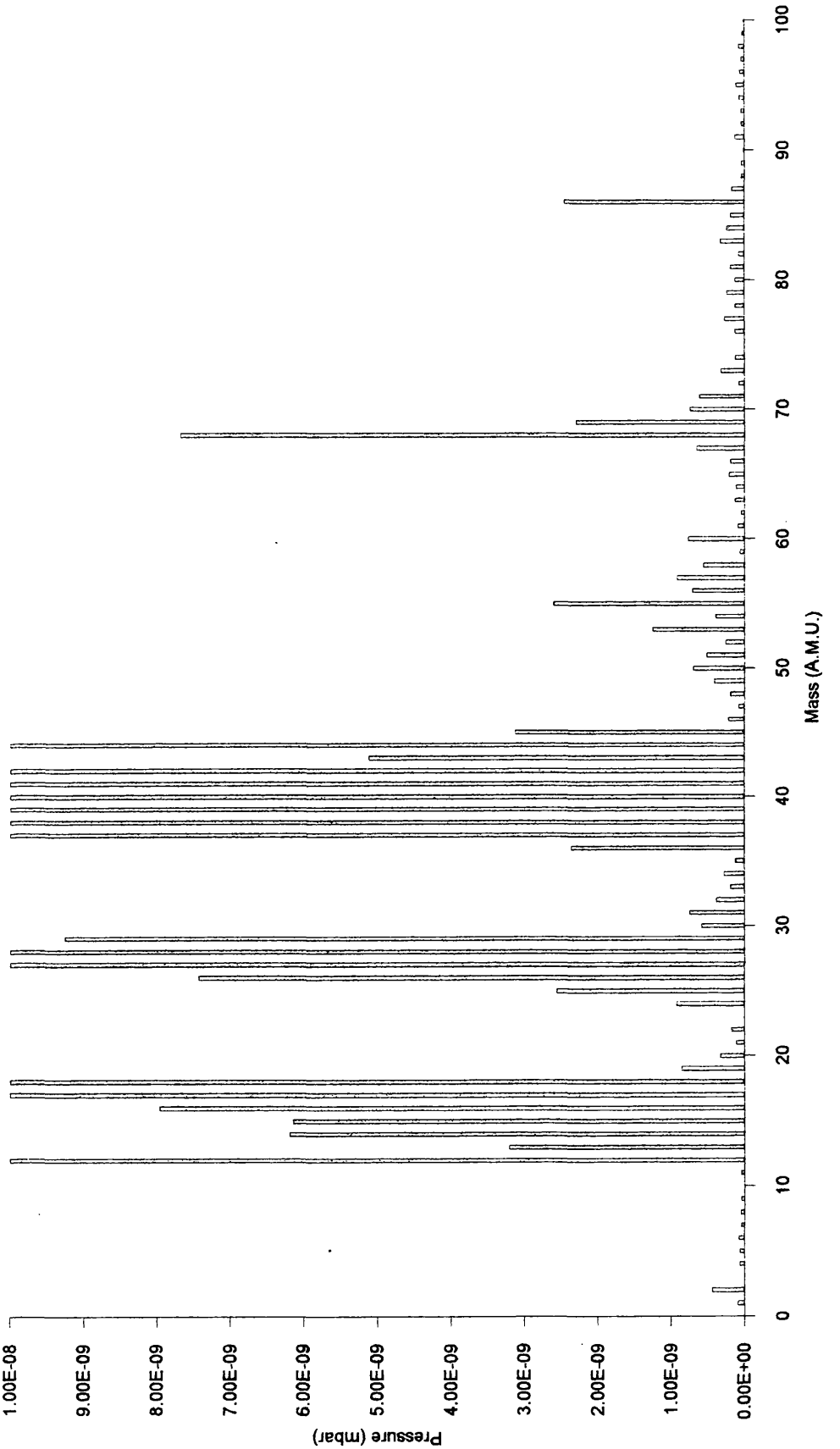

Figure 2.18 Difference spectrum of peak 2 and peak 3 (figure 2.17 - figure 2.16)

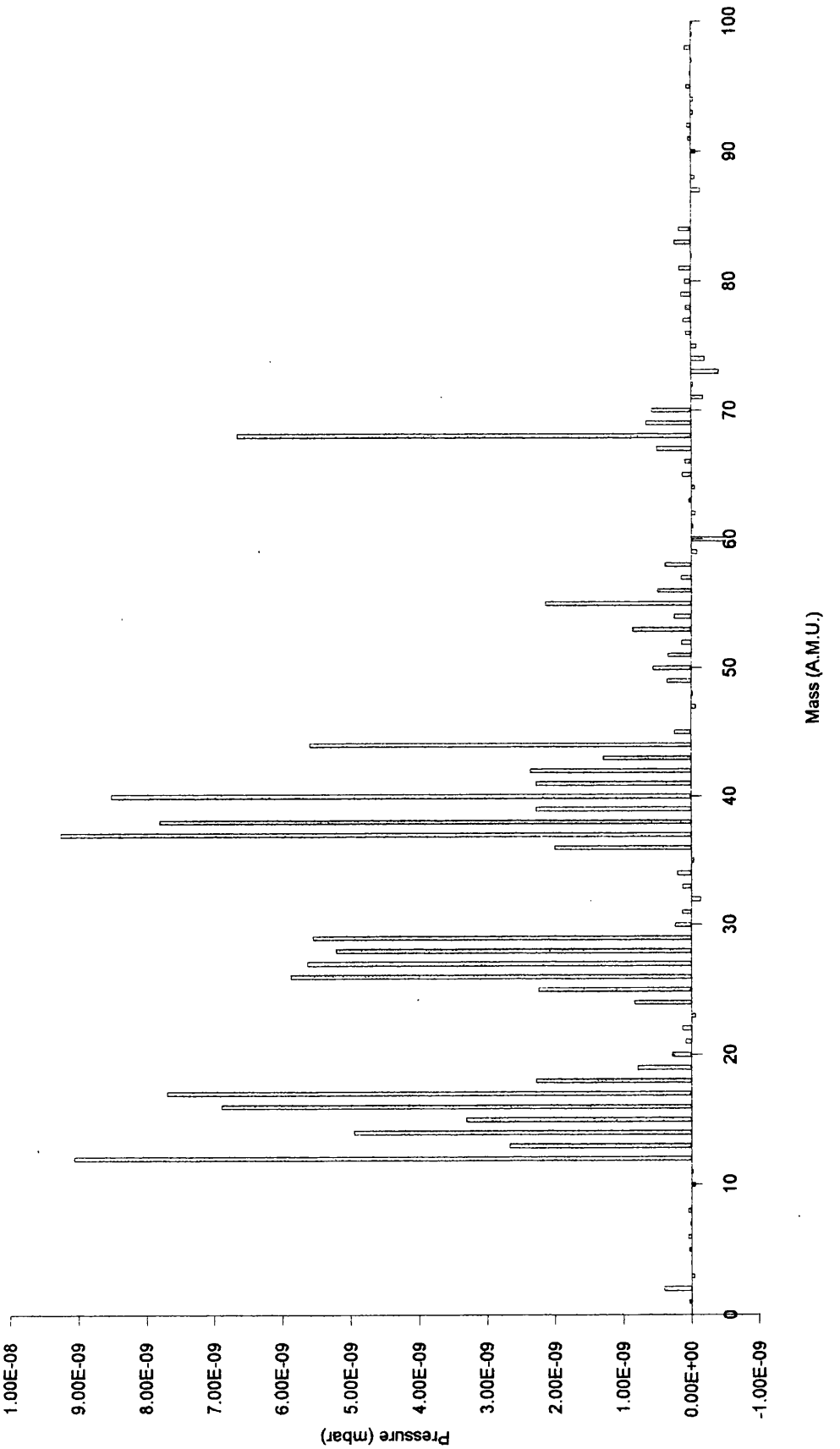

The main peaks associated with the fragmentation ions of crotonic acid (86, 69,71,60 and 57) have subtracted very well, but those remaining (most notably 68 and 55) can also be attributed to crotonic acid fragmentation. The differing relative abundance could be explained by the presence of oligomeric material in the sample which would have a different fragmentation pattern and would lead to the observed abundances at higher temperatures.

This agrees with the TVA experiments in which the internal thermocouple was used (*see p30*). Not only does the Pirani trace match that of the total ion count, but the internal thermocouples show that cold ring formation, the larger oligomers, takes place in the latter part of the peak after formation of the relatively more volatile crotonic acid.

Unfortunately, the temperature program for the Pyroprobe suggests that the temperature for the degradation is very much lower than the accepted value for PHB, and clearly much lower than that recorded in the comparable TVA experiments. However, the degradation pattern is so similar to that of TVA experiments that the data cannot be ignored. Hence it is proposed that the temperature calibration for the Pyroprobe filament is very inaccurate at the relatively low temperatures used in this case, and that the actual temperature of the sample is much higher than the nominal programmed value. A solution to confirm this would be to use a thermocouple-feedback pyrolysis filament[48], instead of the Pyroprobe, for which the absolute temperature can be accurately controlled.

It is known that the commercial polymer samples used do not contain large quantities of crotonic acid as an impurity, certainly not in the quantities observed in this experiment. It is also clear that the polymer does not show this two stage style of degradation under isothermal heating - where a single weight loss or volatilisation step is observed.

It is postulated that under ramped heating, degradation (and hence crotonic acid formation) begins at a relatively low temperature and the products remain trapped within the solid polymer matrix where they may undergo secondary

reactions. However, upon melting, these trapped products are released suddenly causing the pronounced peak. The dominance of crotonic acid under this peak may be due to it being the most volatile component at that temperature, but more likely, that it is the major product from overall degradation mechanism of the polymer and the trapped degradation products. This initial peak is then followed by more typical degradation of the melt from which the products, including the larger oligomers, can volatilise.

Quantitative FT-IR spectrometry using a heated gas cell

This piece of equipment is primarily for use to examine the infrared spectra of volatile substances in the gas phase. The unit consists of a heated chamber with NaCl windows at each end and is placed in the beam path of the spectrometer(Figure 2.19). It can be evacuated and held at constant temperature up to 240°C. As PHB degrades at temperatures below 200°C this makes it an ideal tool to study the evolution of volatile products from this polymer under heating conditions. The gas cell enables not only identification of the degradation products but quantitative measurements are also possible as the gas cell is of fixed volume. In addition, by collecting a series of spectra at regular intervals it is possible to build a more complete picture of the degradation pattern and associated kinetics.

To establish the effectiveness and sensitivity of this technique, experiments were performed using crotonic acid: the major degradation product of PHB.

Figure 2.19 Schematic diagram of heated gas cell

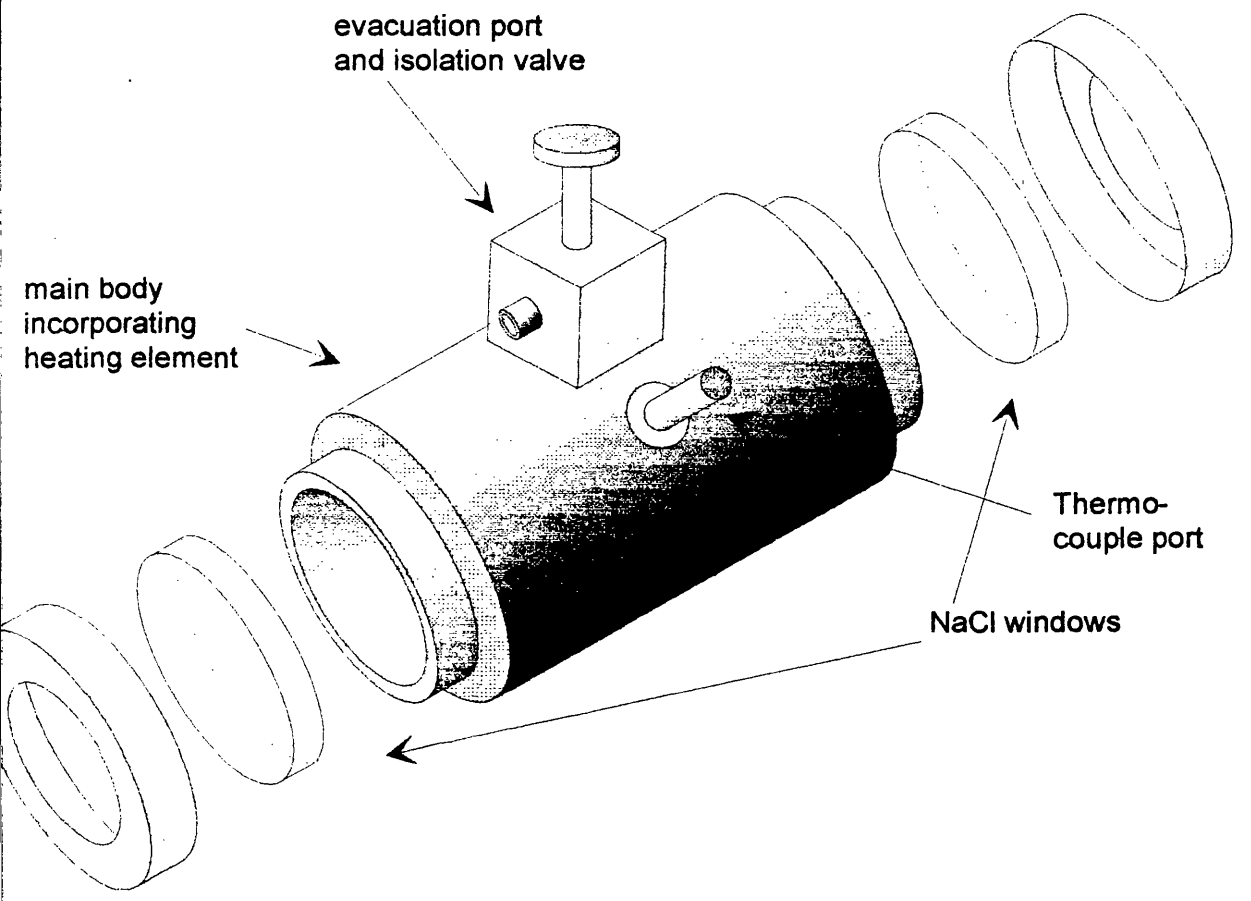

Quantification of crotonic acid in the heated gas cell

Quantitative analysis is based on the application of two fundamental principles: Lambert's law and Beer's law. Lambert's Law gives the quantitative relationship between energy transmitted at a given frequency and the thickness of the sample[49].

$T=I/I_0=\exp(-kl)$

or $A=\log_{10} I/T=\log_{10} I_0/I=kl$

T=Transmitted radiation or fractional transmission I/I_0

A=Absorbency (or optical density) $\log_{10} I_0/I$

I=Transmitted radiation

I_0=Incident Radiation

l=Sample thickness (cm)

k=Absorption coefficient

Beer's Law, a modification of Lambert's Law, replaces the thickness of material by the concentration of a substance in solution.

The two laws can be combined

$A=\log_{10} I/T=\log_{10} I_0/I=\varepsilon cl$

c=concentration in mol/l

l=path length in cm

ε=extinction coefficient

Clearly, this can be also applied to the partial pressure of a compound in the gas phase.

However, departure from Beer's Law can be encountered in certain systems where hydrogen bonding or intermolecular association can occur. Problems can also arise from the spectrometer: the spectral slit width can be large

compared with the band width giving marked curvature to Beer-Lambert calibration curves[50].

Also, for gases and vapours the extinction coefficient may be a function of the total pressure of the sample. This occurs most significantly with light gases such as CO, CO_2, SO_2, CH_4, N_2O, HCl, etc also giving curvature to the calibration curve[51].

Molecules may also be absorbed onto surfaces of the gas cell, thus removing sample from the radiation path giving a low measurement.

To calibrate the response of the spectrometer, samples of crotonic acid were accurately weighed onto a dimpled planchette and placed in the gas cell. The gas cell was evacuated for thirty seconds using a rotary oil pump. The solid sublimes extremely rapidly in vacuum so this evacuation method was standardised to minimise error. The gas cell was then heated to 200°C and the system allowed to stabilise before taking any measurements. The FT-IR spectrometer is a single beam instrument, requiring collection of a background spectrum prior to that of the sample. If the background spectrum is not collected in similar conditions to the sample spectrum then differences in the concentration of water vapour and carbon dioxide can obscure detail in the desired sample spectrum. This is particularly true with the presence of the hot cell within the instrument. The effects of the background spectra could be minimised by using a background collected with the empty, hot, evacuated gas cell present when the purging gas had created a stable atmosphere within the whole spectrometer unit. Thus the CO_2 and H_2O levels remained relatively low and uniform throughout the experiment. However, a method has been developed to reduce this effect even further.(*see Three dimensional representation of data* p55)

The spectrum of gaseous crotonic acid is very different to that in the solid state(Figure 2.20). The major differences are due to the intermolecular hydrogen bonding that takes place in the solid state resulting in the gaseous spectrum having a major peak at 3585cm^{-1} due to unbonded acid OH, a lack of

the broad bonded OH peak 2500 - 3500cm^{-1} and a shift of C=O stretch region from 1700cm^{-1}(bonded) to 1760cm^{-1}(unbonded).

An extinction coefficient *(ε)* is only valid for the particular frequency, or wavenumber, at which it was determined, and cannot be applied to other parts of the spectrum. Hence, when measuring absorbency it is important to chose the wavenumber with care. It is best to use a strong peak, for good sensitivity, that does not overlap with neighbouring peaks, as this can lead to error through poor estimation of the baseline (which would represent zero absorbance).

For the above reasons the measurements were taken for the free OH band (3591cm^{-1}) the carbonyl bands (1770cm^{-1} and 1759cm^{-1}) and a trans olefinic hydrogen bend (970cm^{-1}). The 970cm^{-1} band proved to be unsuitable in later experiments as it overlapped with a neighbouring peak making precise measurements impossible.

Figure 2.20 Comparison of infra-red spectra of solid and gaseous state crotonic acid.

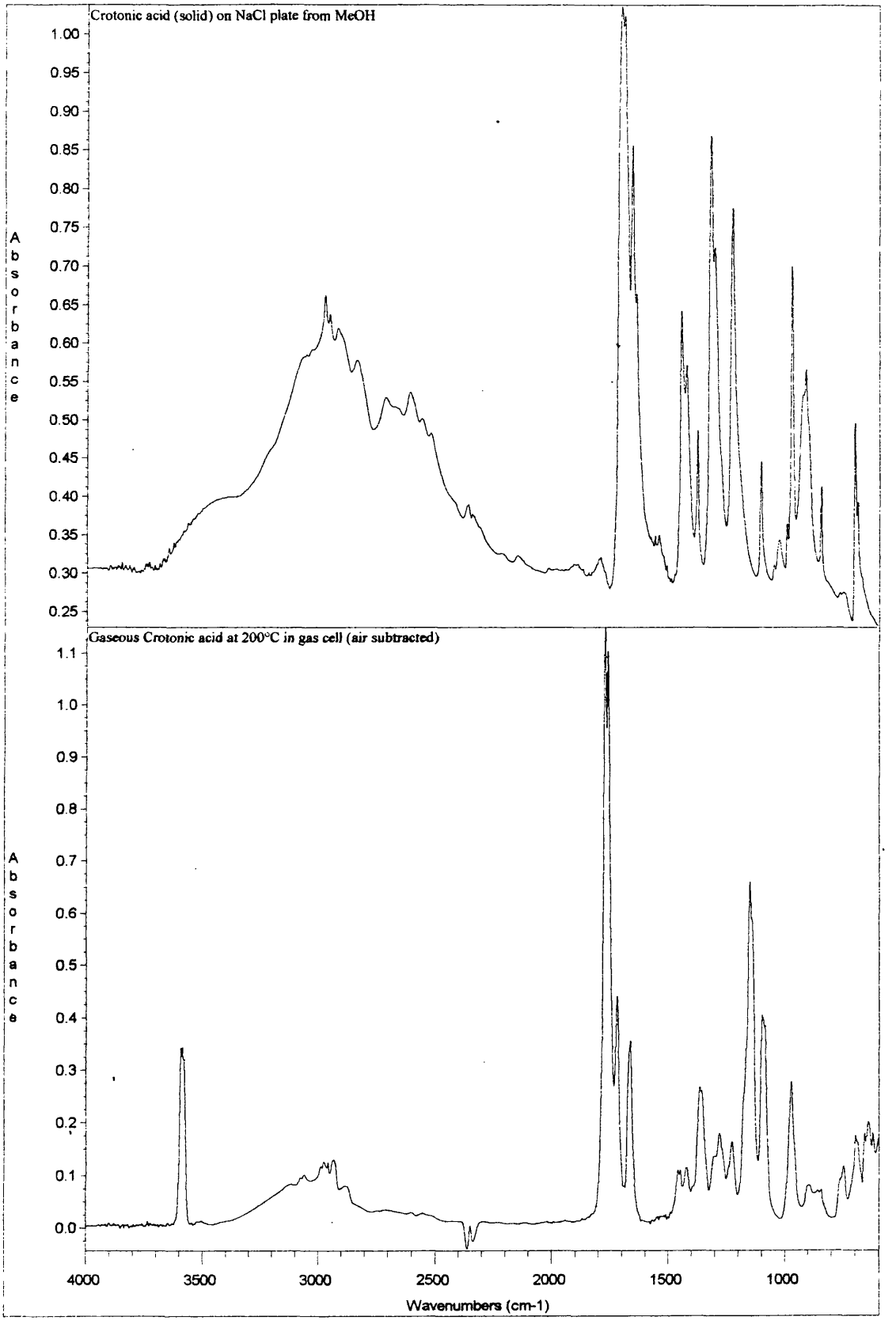

Table 2.1 *Absorbances at various wavenumbers of gaseous crotonic acid at 200°C for mass calibration.*

	Absorbance			
Mass used (g)	970cm^{-1}	1759cm^{-1}	1770cm^{-1}	3591cm^{-1}
0.0015	0.054	0.236	0.254	0.075
0.0029	0.104	0.451	0.502	0.143
0.0043	0.154	0.705	0.730	0.221
0.0053	0.203	0.920	0.955	0.289
0.0061	0.321	1.456	1.516	0.460
0.0079	0.322	1.458	1.522	0.463
0.0099	0.506			0.750

The graph of these values(Figure 2.21) shows the results to be reasonably linear, with the best fit straight lines passing through the origin calculated by least squares. This confirms that Beers' law is perfectly adequate for our purposes.

What is also apparent from these experiments is that the method is extremely sensitive: with less than 1mg of crotonic acid being easily detectable.

Figure 2.21 *Calibration curves for gaseous crotonic acid at 200°C using various wavenumbers*

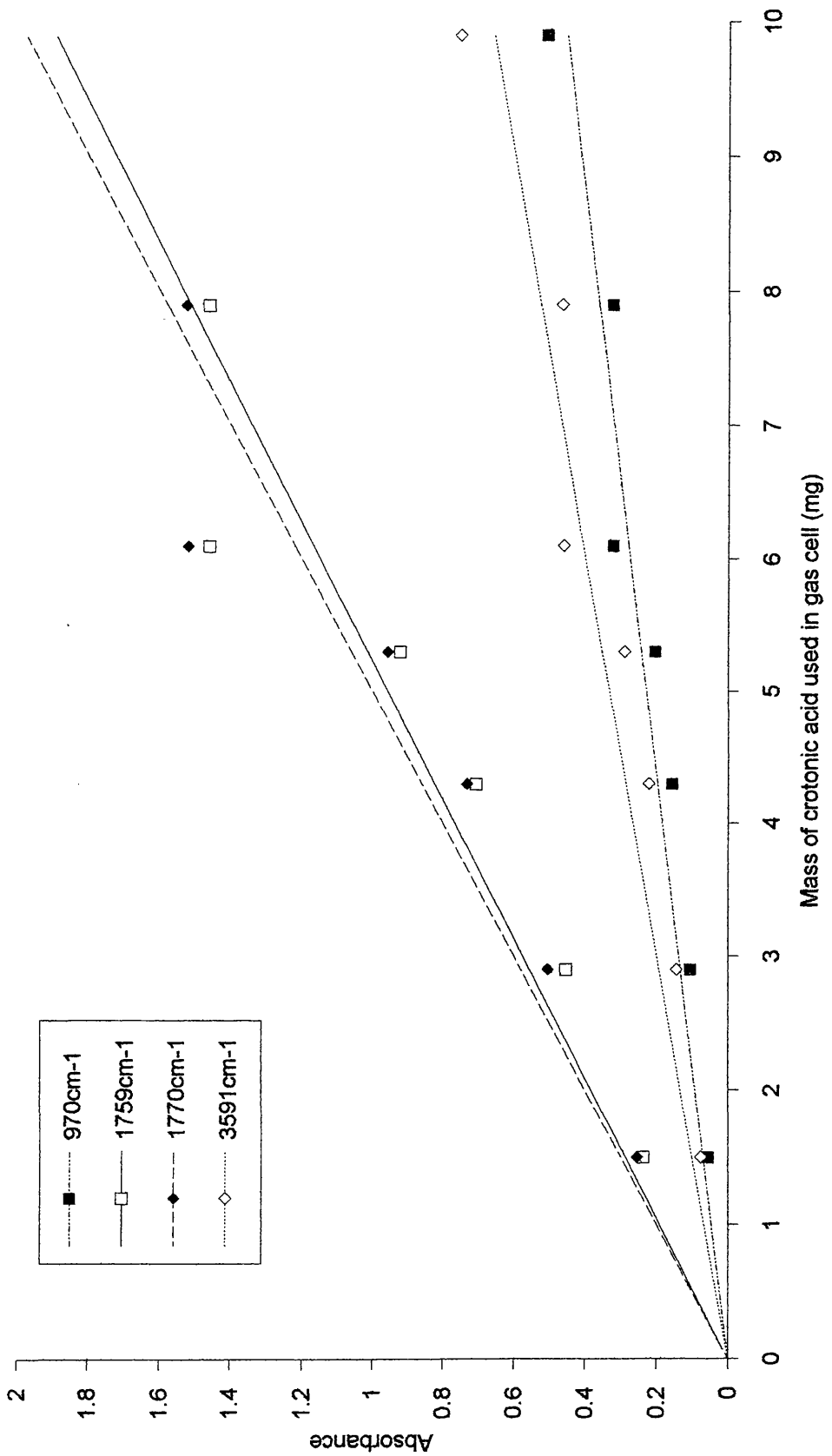

Degradation of PHB in heated gas cell

A film of technical grade PHB (G044) was cast onto a dimpled planchette from a solution of chloroform and this was sealed inside the gas cell. A planchette was used to avoid contaminating the gas cell with residue and also to enable easy measurement of the sample size. The gas cell was evacuated, warmed to 50°C and allowed to stabilise. The thermostat was then turned up to 240°C and a program was started that collected a spectrum every five minutes. The temperature was noted periodically during heating to give some indication of the heating curve. An internal temperature was measured using the thermocouple supplied with the temperature controller, positioned as close to the sample as possible, and was discovered to be approximately 230°C when the dial on the controller was set at 240°C.

On completion of the experiment the planchette was removed and reweighed to establish the mass of polymer that had volatilised.

mass of dimpled dish	0.3724g	
mass of dish + polymer	0.3779g	
mass of dish + residue	0.3727g	
mass of polymer used	0.0055g	5.5mg
mass remaining after degradation	0.0003g	0.3mg
mass decomposed		5.2mg

The mass deficit compares very favourably with the crotonic acid calibration. Taking measurements from the graph for absorbencies at 3599, 1770, 1756 and 970cm^{-1} on the gas cell spectra of 2 hours we get 4.65, 4.55, 4.6 and 4.35mg respectively.

This was repeated with a smaller sample of 3.6mg .and again shows reasonable correlation with the calibration curve giving 4.1, 4.1, 4.2 and 3.5mg of crotonic acid at 3599, 1770, 1756 and 970cm^{-1} respectively.

Three dimensional representation of data

To assist in the visualisation of the data the spectra collected are collated and plotted on a single three dimensional graph.

The x and y axes remain the same representing wavenumber and absorbancy respectively. The additional z-axis, a time axis, allows the change in absorbance with time to be plotted. In effect, the resulting graph is each spectrum stacked, one behind the other, with the first from time zero on the front and the last from the end of the experiment at the back.

The three dimensional plot was drawn using Excel after converting the spectral data to a suitable format. The 'Omnic' spectrometer software is able to store the spectral data as a comma separated variable (CSV) file, which consists of a list of x and y values, written in ASCII, separated with commas. A program was written, using a FORTRAN compiler, to read in each of these spectrum files, perform any required modifications and then write a single CSV file containing all the modified spectra. This file can then be loaded into Excel, or any other suitable graphics package, to plot the graph.

However, the Nicolet FT-IR spectrometer has a number of limitations. Since the instrument is single beamed, the computer has to store a background spectrum from which it determines the sample spectrum allowing for the sensitivity of the detector across its spectral range. This means that changing environmental conditions such as humidity and temperature can affect the resulting spectra in two ways: the baseline for the spectra is not always on the axis and can be seen to shift; and the varying humidity shows up as a water vapour spectrum added to the sample spectrum which can obscure fine details.

It is possible to remove these discrepancies from the final plot using relatively simple techniques that were incorporated into the data format conversion program.

Baseline correction

The user selects the region of interest and two points on the spectrum, between which the baseline is to be drawn.. The equation for this line *(y = mx + c)* is determined and then used to subtract the appropriate *y* value for each data point, lowering or raising the spectrum appropriately.

Water vapour correction

This is done simply by subtracting a pure water vapour spectrum, with appropriate scaling, from the offending sample spectrum. The scaling factor is determined by comparing the height of a single water vapour peak on the reference and sample spectra, this factor is then applied to the whole reference spectrum which is then subtracted. Appropriate baseline corrections are also made.

The plot(Figures 2.22 and 2.23) centres on the carbonyl region alongside the unsaturated carbon region and shows that volatile material is detectable at 15 mins and the concentration of gases rises sharply between 20 - 70 minutes.

Figure 2.22 Three dimensional plot for carbonyl region of infra red spectra of PHB heated in the heated gas cell - (uncorrected)

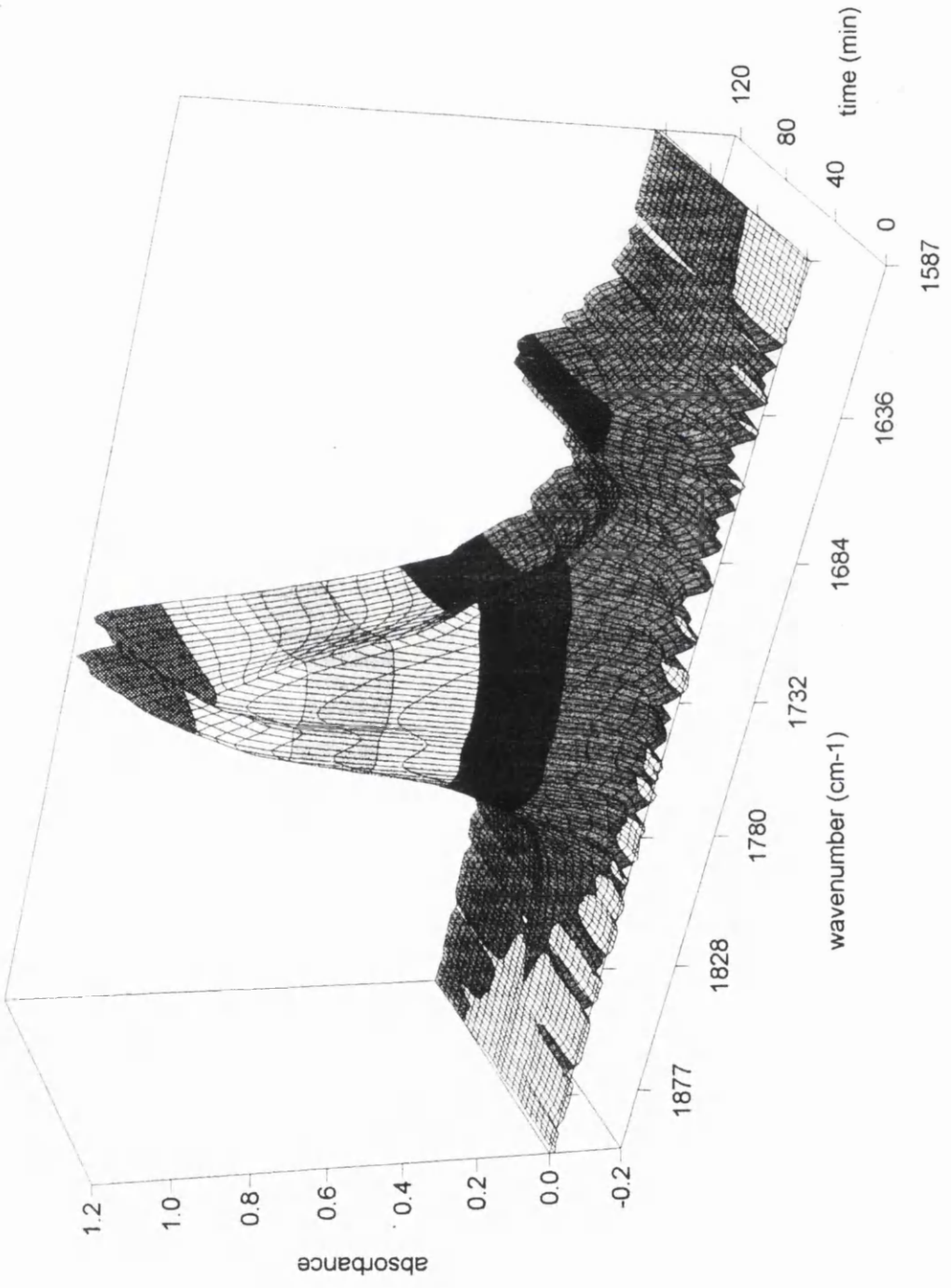

Figure 2.23 *Three dimensional plot for carbonyl region of infra red spectra of PHB heated in the heated gas cell - with baseline and water vapour corrections*

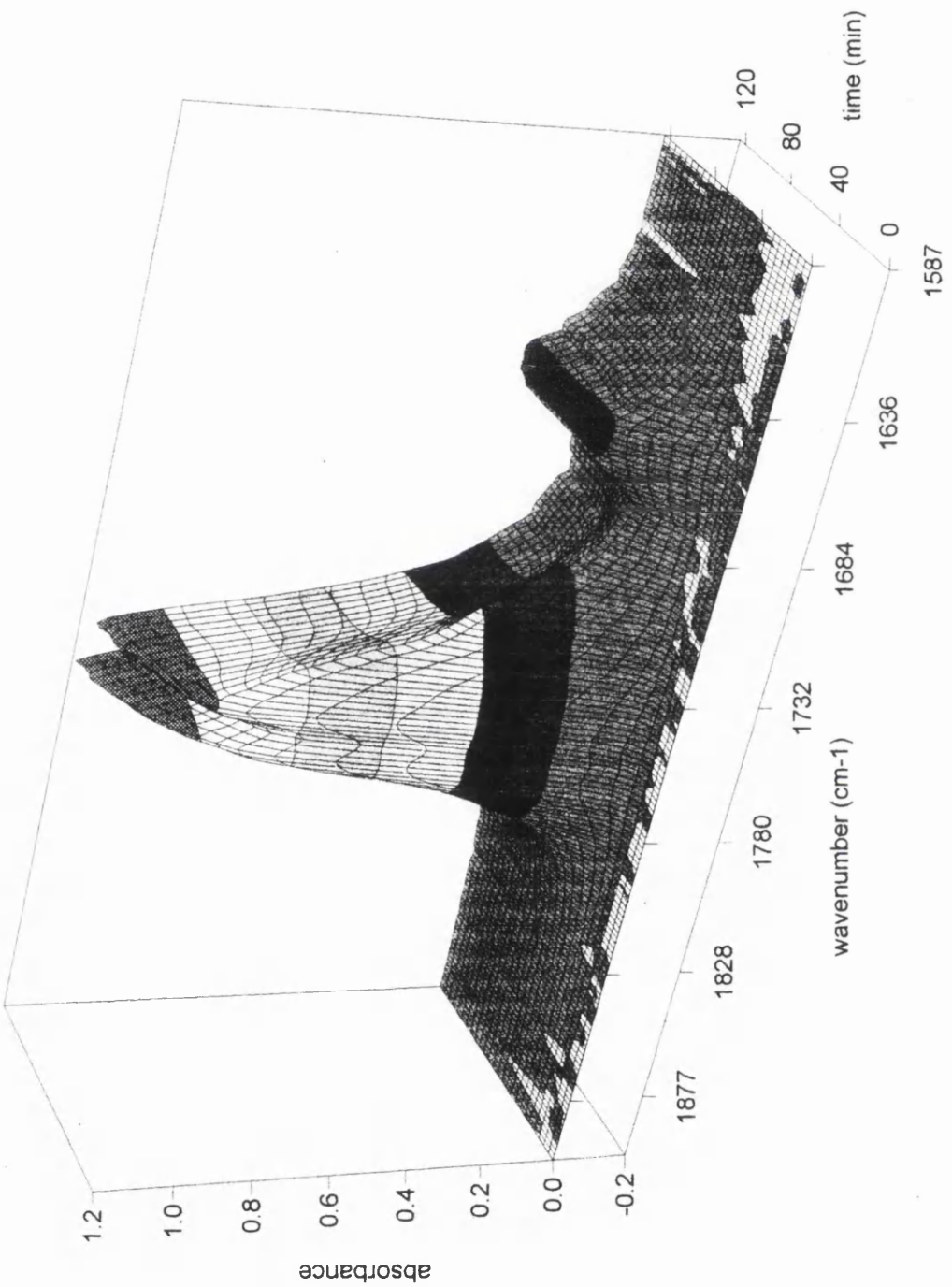

In the final stages the spectrum is very like that of gaseous crotonic acid but in the early stages the carbonyl peak is very broad. This suggests that a volatile product is formed that later decomposes. A 'clean' spectrum of this compound was obtained by subtracting a spectrum of crotonic acid from a spectrum showing this broad carbonyl peak (specifically the spectrum of 13:16:41 was subtracted from that of 11:43:16) The subtraction was scaled using a factor that reduced the free OH band to zero. The IR spectra database was then compared with the resultant spectrum giving the following results.

Table 2.2 *Results from database search for the spectrum of the primary degradation product.*

library index	percentage match	compound name
10442	69.63	poly(vinylbutyrate)
4592	66.69	ethyl butyrate
4595	65.69	methyl butyrate
4726	65.49	allyl butyrate
10447	63.87	poly(ethyl adipate)
5081	63.36	ethyl DL mandelate
10441	63.02	poly(vinylpropionate)
5064	61.49	2-phenylpropylbutyrate
4650	61.46	diethyl adipate
4822	60.89	ethyl(+/-)-2-scholar-3-hydroxypropionate

The matches were extremely good, but the abundance of esters and butyrates leads us to believe that oligomers of two or more units are the cause of the spectra. Subtracting crotonic acid will have led to the elimination of free OH and C=C bands, which would be present in such oligomers, hence leaving only the ester and butyl absorption bands.

Kinetics

The data gathered using the heated gas cell provides the ideal opportunity to examine the kinetics of the degradation as quantitative measurements versus time are made(Figure 2.24). For the calculations to be successful, Beer's law *(A = εcl)* must hold true. In this case, it has been demonstrated that the absorbance vs. concentration plot is sufficiently linear.(see *Quantification of crotonic acid in the heated gas cell* p48)

Figure 2.24 Absorption intensity for C=O band (1770cm^{-1}) for PHB in heated gas cell at 240°C.

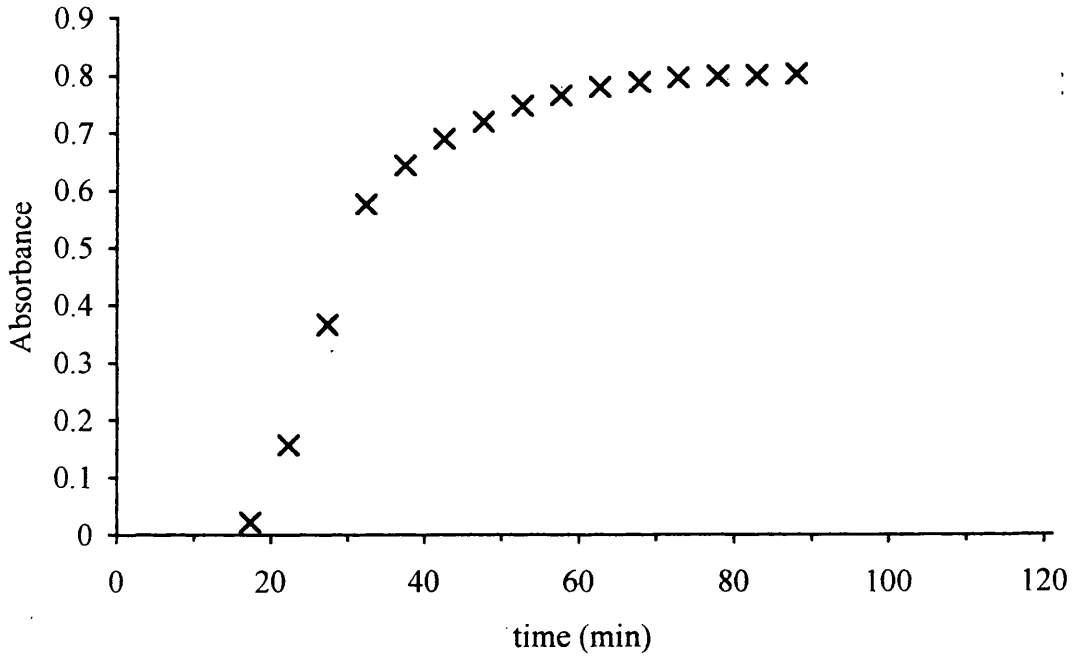

First and second order plots(Figures 2.25 and 2.26) were drawn for this data to establish the order of the reaction and some idea of the rate constant.

First order plot

For a first order reaction

$$\frac{-d[A]}{dt} = k[A]$$

i.e. the rate of change of concentration of reactant, $[A]$, is proportional to the concentration of the reactant.

therefore $$\ln\frac{[A]}{[A_0]} = -kt$$

The concentration of products, $[P]$, can also be used as a measurement of reaction

$$\ln\frac{[P_\infty]-[P]}{[P_\infty]-[P_0]} = -kt$$

where $[P]$ is the concentration of product at time t, $[P_0]$ the concentration at the start of timing and $[P_\infty]$ the expected concentration on completion of the reaction.

Since absorbance is directly proportional to concentration,

$$\ln\frac{Abs_\infty - Abs}{Abs_\infty - Abs_0} = -kt$$

Hence a graph of $\ln(Abs_\infty - Abs)$ versus t gives a straight line with slope $-k$.

Second order plot

For a second order plot

$$\frac{-d[A]}{dt} = k[A]^2$$

i.e. the rate of decrease of concentration of reactants is proportional to the square of the concentration of the reactant.

Integration gives $$\frac{1}{[A_t]} - \frac{1}{[A_0]} = kt$$

or $$\frac{1}{Abs_\infty - Abs} - \frac{1}{Abs_\infty - Abs_0} = kt$$

Thus a graph of $(Abs_\infty - Abs)^{-1}$ will yield a straight line with slope k.

These plots for the absorption data show that, in the later stages, volatilisation is predominantly first order - this curve being most linear. However, it still shows significant curvature. This is probably due to poor estimation of the endpoint of the curve. So, a method was used, attributed to Kedzy and Swinbourne[52], by which the rate constant can be calculated directly from the curve without need for the final end value. This was used in preference to the more familiar Guggenheim method as it also allows determination of the true endpoint, which can then be used in a first order plot to check the calculated rate value.

Figure 2.25 First order plot for absorption intensity of C=O band (1770cm^{-1}) for PHB in heated gas cell at 240°C

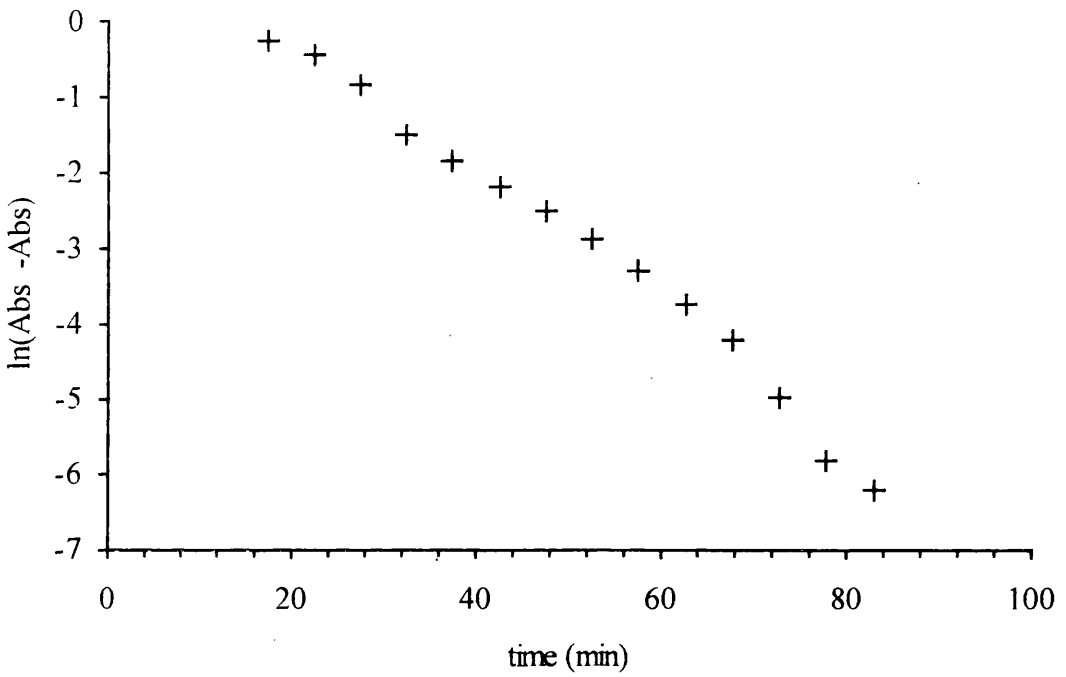

Figure 2.26 Second order plot for absorption intensity of C=O band (1770cm^{-1}) for PHB in heated gas cell at 240°C

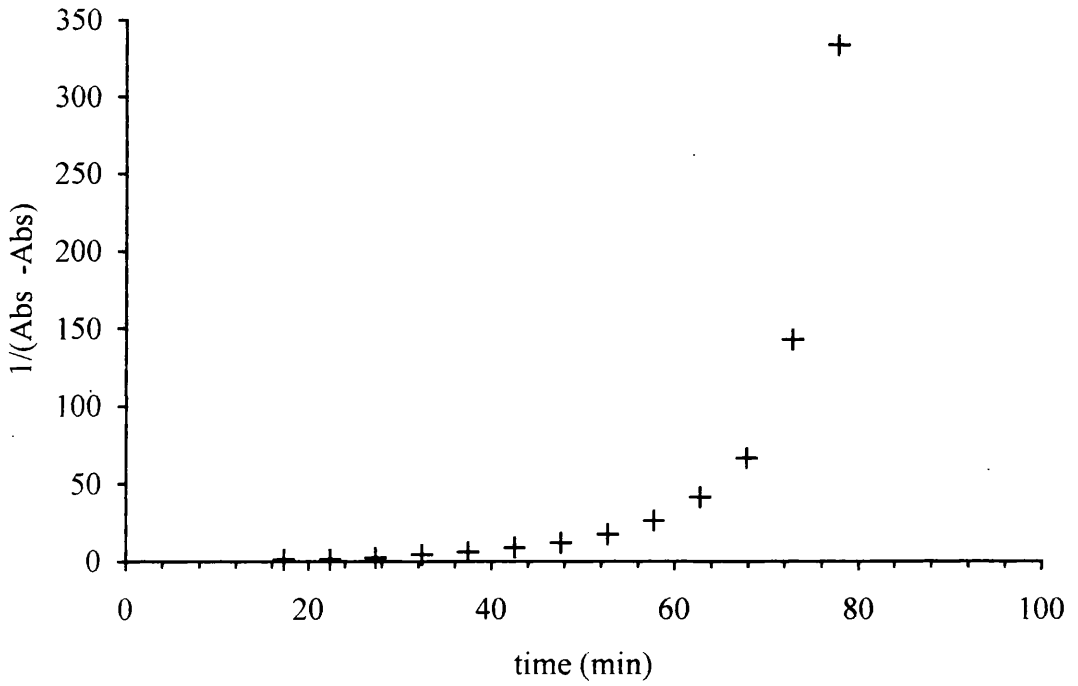

Kedzy-Swinbourne method

This method for determining the rate constant of a first order curve is based on the following expression which considers the first order kinetic data at time t and at a time τ later

$$\frac{P_t - P_\infty}{P_{t+\tau} - P_\infty} = \exp(k\tau)$$

$$P_t = P_\infty\left[\exp(k\tau) - 1\right] + P_{t+\tau}\exp(k\tau)$$

Hence, a plot of P_t versus $P_{t+\tau}$ will be linear with a slope of $\exp(k\tau)$.

So the rate constant can then be calculated from

$$k = \frac{\ln(slope)}{\tau}$$

In addition, at the endpoint $P_t = P_{t+\tau} = P_\infty$ so the intersection of the line with the 45° line gives the value of P_∞.

This was done for the absorbance data(Figure 2.27) and it was found that relatively reliable rate constants could be calculated.

Figure 2.27 Kedzy Swinbourne plot for absorption intensity of C O band (1770cm^{-1}) for PHB in heated gas cell at 240°C

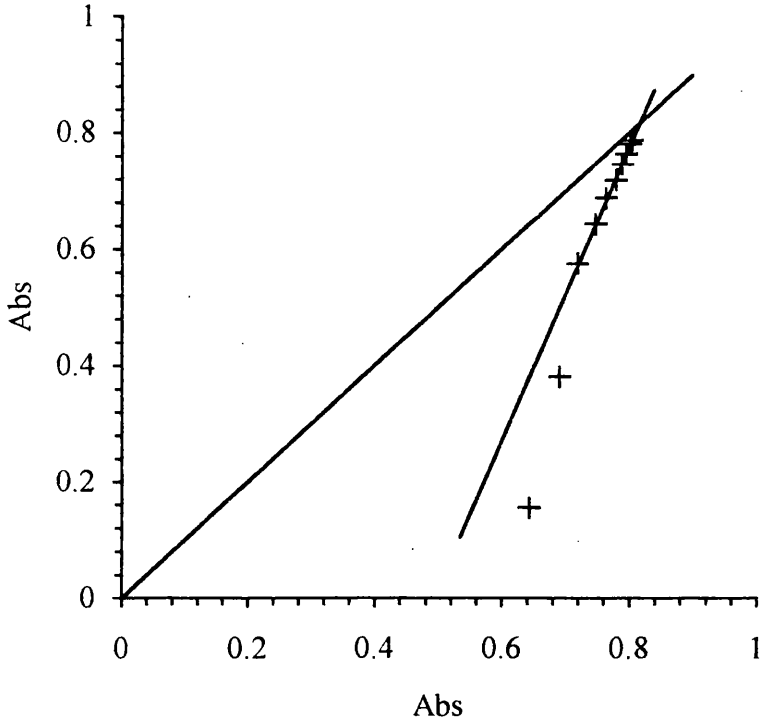

t(min)	22.5	27.5	32.5	37.5	42.5	47.5	52.5	57.5	62.5	67.5
Abs_t	0.157	0.380	0.575	0.645	0.690	0.720	0.747	0.765	0.780	0.790
$Abs_{t+\tau}$	0.645	0.690	0.720	0.747	0.765	0.780	0.790	0.797	0.802	0.805

$$\text{slope} = \frac{0.238 - 0.040}{0.238 - 0.152} = 2.30$$

$$k = \frac{\ln(2.30)}{15}$$

$$= 5.56 \times 10^{-2}\ \text{min}^{-1}$$

$$= 0.927 \times 10^{-3}\ \text{s}^{-1}$$

Comparison of random chain scission expression with experimental data for the formation of crotonic acid in the heated gas cell.

The above measurements from the heated gas cell can also be used to examine if the mechanism of PHB degradation is that of random scission. The experimental data can be fitted to and compared with theoretical production of monomer (*see Kinetics of random scission p14*).

However, before this can be accomplished a satisfactory method for determining the rate constant for a random scission curve must be determined. The experimental data suggests that the latter part of the curve can be approximated by a first order expression, so it would seem logical to fit a first order expression to that of the model to see the correlation between curves of the same rate constant.

The expression for monomer (i.e. $n=1$) production by random chain scission is

$$Z_1 = N\alpha^2 \qquad \text{from (2)}$$

$$= N(1 - \exp\{-kt\})^2$$

$$= N(1 - 2\exp\{-kt\} + \exp\{-2kt\})$$

as the endpoint is reached $\exp\{-2kt\}$ will tend to 0

so $$Z_1 = N - 2N\exp\{-kt\} \qquad (6)$$

The expression for a first order curve is

$$\ln A/A_0 = -kt$$

where A_0 is the initial quantity of reactant and A is the quantity of reactant at time t

This can be expressed in terms of the products:

$$(P_\infty - P)/(P_\infty - P_0) = \exp\{-kt\}$$

where P_0 is the initial quantity of products, P_∞ the final quantity of products and P the quantity of products at time t.

rearranging, we get:

$$P_\infty - P = (P_\infty - P_0) \exp\{-kt\}$$

$$P = P_\infty - (P_\infty - P_0) \exp\{-kt\}$$

To give this the same form as (6) let $P_\infty = N$ i.e. the final quantity of products be the same as the initial quantity of reactant and let $P_0 = 0$ i.e. the is no monomer present at time 0

$$P = N - N \exp\{-kt\}$$

To make the curves fit we shall move this curve laterally along the time axis a displacement d

$$P = N - N \exp\{-k(t+d)\}$$

$$= N - N \exp\{-kt\} \exp\{-kd\} \qquad (7)$$

If the graphs fit then (6)=(7)

i.e. $Z_1 = P$

$$N - 2N \exp\{-kt\} = N - N \exp\{-kt\} \exp\{-kd\}$$

$$2N \exp\{-kt\} = N \exp\{-kt\} \exp\{-kd\}$$

$$2 = \exp\{-kd\}$$

$$(\ln 2)/k = -d$$

We now have the correlation to overlay the curves.

Figure 2.28 Comparison of random chain scission expression for monomer production with first order expression

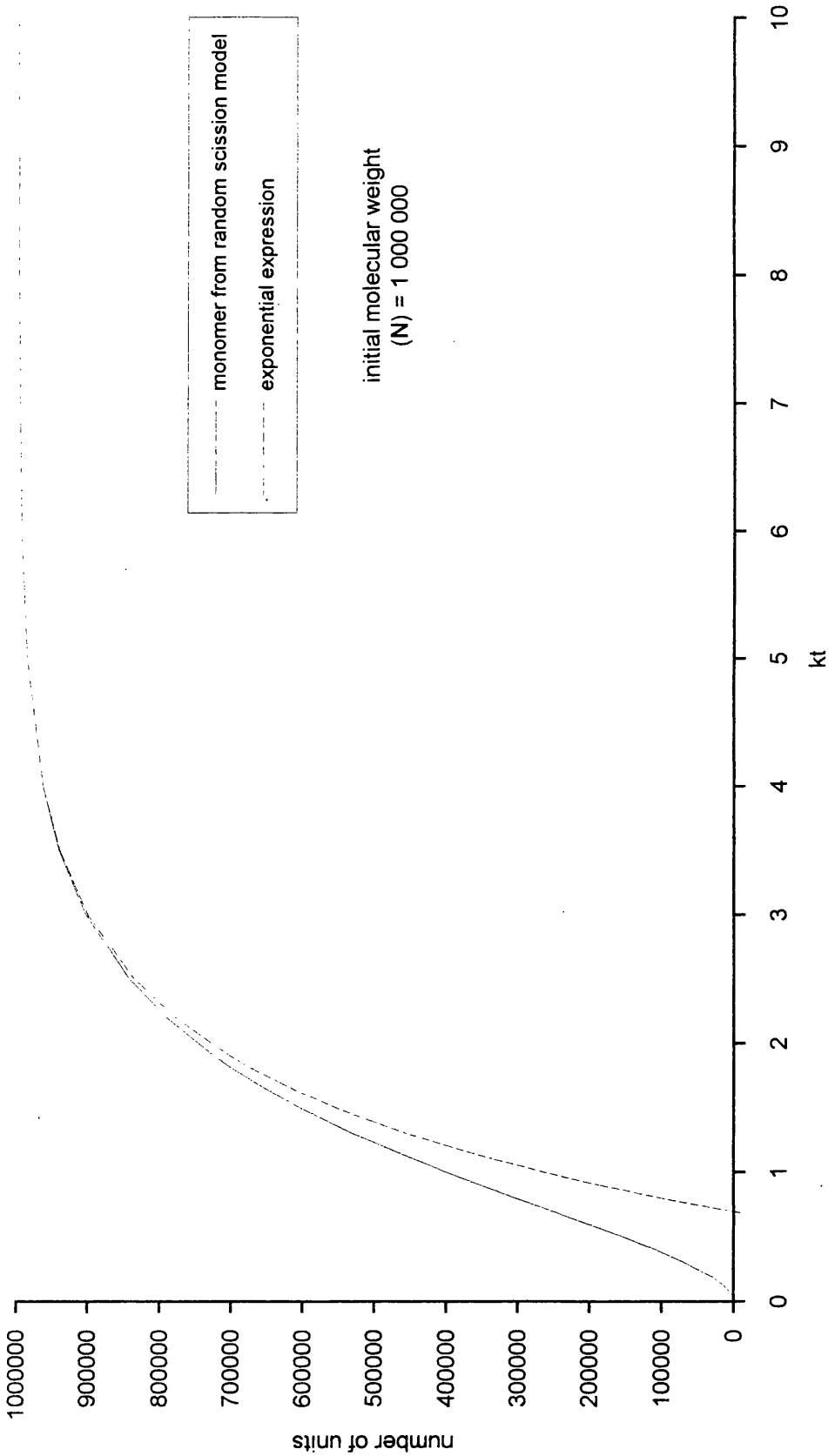

As can be seen from the graph (Figure 2.28) the first order approximation is very close to the random scission model in the later stages. Hence any rate constant calculated by this method will be reasonably accurate as long as the measurements are taken from that later part of the curve.

By applying the Kedzy Swinbourne method to experimental data, the rate constant for volatilisation of products can be determined from the latter part of the curve, allowing comparison with the random scission model.

The rate constant was determined for a carbonyl band at 1770cm^{-1} for PHB in a heated gas cell at 240°C, and substituted into the expression for the model with the chain length also chosen to reflect the maximum absorbance measured (the experimental data also had to be scaled to match the random chain model and allowed to have a lateral shift to allow for the warm up to degradation temperature.)

Although the curves match in the later stages(Figure 2.29), the two sets of data deviate significantly early on. The induction period would appear to be longer for the experimental data and the maximum rate of increase is both later and steeper.

It is clear that the model is not ideal, indicating that random scission is not the only reaction taking place, but the similar shape does suggest that it is of importance in the overall degradation process.

Figure 2.29 *Comparison of random scission model expression for monomer production with experimental data for the absorbance at 1770cm^{-1} for PHB in the heated gas cell at 240°C*

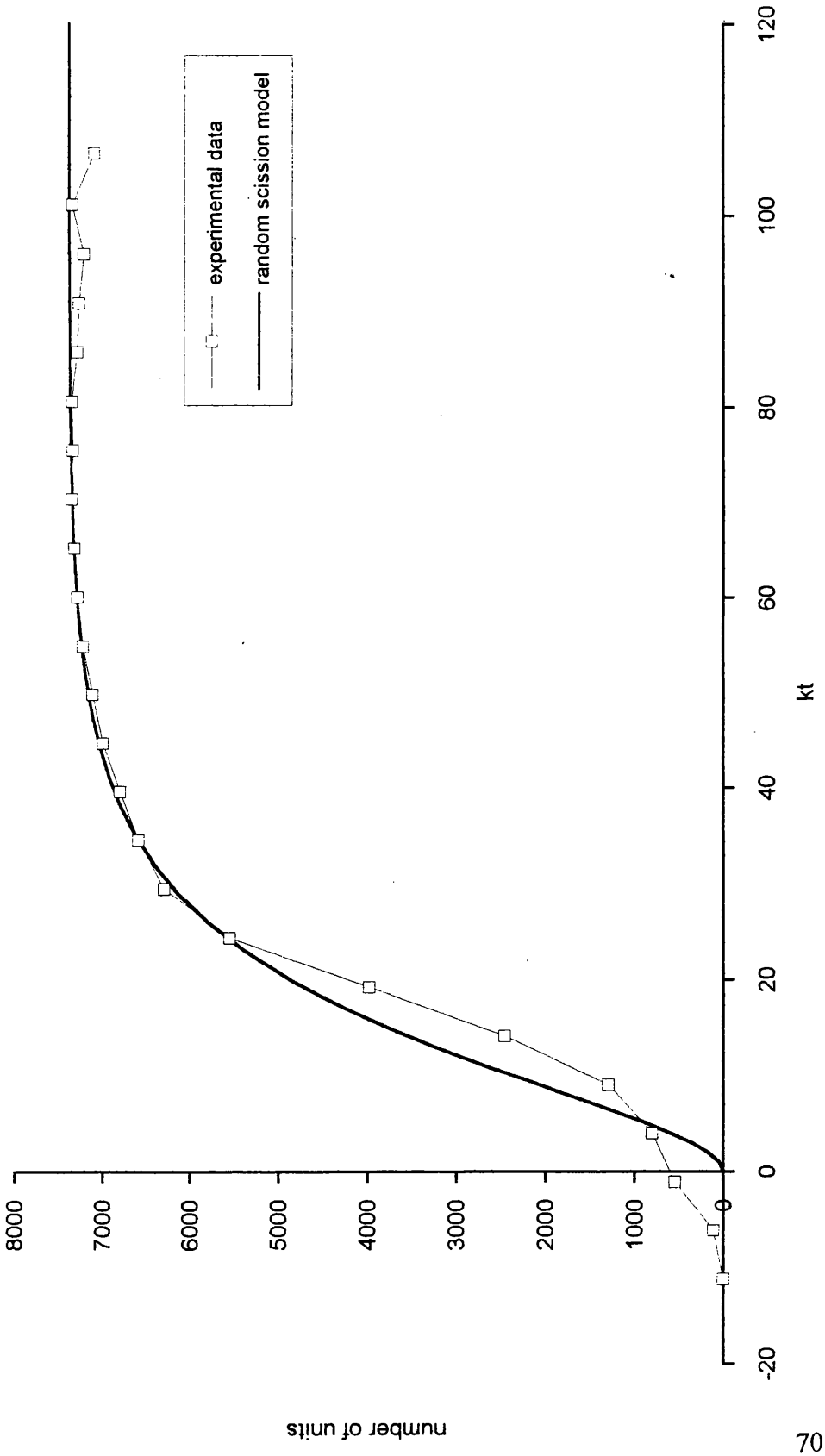

Analysis of degradation products by GC

Analysis of the degradation products by gas chromatography has been attempted previously with little success(see *TVA and PHB p20*). Generally, the peaks are very broad, reflecting the large sample size needed. When they are this shape, quantitative measurements are difficult, small peaks cannot be distinguished from the baseline and the sample size affects the retention time of the peak maxima. To obtain good resolution specialised columns and detectors must be used, but even these have their limitations.

The difficulty arises from the acidic end groups on the degradation products, which adhere strongly to surfaces and makes the boiling point of the compounds relatively high.

By converting these acidic groups to esters the resulting compounds are much more volatile and easier to analyse by GC.

Two methods were used to achieve this: base catalysed esterification and treatment with diazomethane.

The GC analysis was carried out on Hewlett Packard FID (flame ionisation detection) and MS (mass spectrometry) instruments each fitted with a CPsil 5CB fused silica capillary column (25m × 0.32mm × 0.12μm) and Grob-type injector (split injection 50:1). The gas flow was 2ml/min He carrier with 25ml/min makeup gas. The temperature program was: 50°C for 2 min, ramped at 5°C/min to 270°C and held at 270°C for 5min. The injector and detector temperature was 260°C.

Base catalysed esterification

The sample to be esterified was dissolved in methanol and treated with methoxide ions. i.e. a solution of NaOH in methanol. The resulting solution was then evaporated to dryness by blowing gently with nitrogen. The residue was dissolved in diethyl ether and excess OH ions were removed by washing with distilled water.

By this method it was clear that the crotonic acid had been converted to the methyl ester, as can be seen as a very sharp peak on the GC trace at 2.10min(Figure 2.30), but this appeared to be the only product. It had been hoped that the larger oligomers would be apparent but they had been lost, either through the evaporation process, extraction process or most probably by hydrolysis of the ester linkages in the fragments to form the constituent monomer.

Esterification with diazomethane

The sample to be esterified was dissolved in diethyl ether, which was subsequently treated with an excess of diazomethane in diethyl ether. The solution was left for a few minutes to allow the reaction to go to completion before excess diazomethane was 'killed' by addition of a small excess of acetic acid.

This method has a number of drawbacks in that diazomethane is very unstable, and has to be prepared[53] prior to the experiment, stored in darkness, kept under refrigeration and must be handled carefully. The glassware used must not contain ground glass joints and must be free of sharp edges and scratches which provide nuclei for crystallisation. These crystals are very unstable and are likely to cause an explosion. For similar reasons the excess diazomethane is 'killed' with acetic acid prior to GC analysis. However, this results in the incorporation of acetic acid and methyl acetate as impurities.

This method was much more successful than the base catalysed esterification, with many of the oligomers being apparent in the resulting GC trace.

To obtain an accurate picture of the degradation products, a sample of G044 was degraded under vacuum in a sealed tube at 200°C for 4 hrs. The tube was heated in an oilbath, controlled by a thermostatic hot plate. The reaction tube was allowed to cool and diethyl ether was introduced immediately upon opening. The reaction products were then treated as above and subjected to GC analysis.

The GC-FID trace (Figure 2.31) shows a range of products of which the main peaks (2.11, 12.05, 23.36, 32.13 and 39.37 mins) are assumed to be the methyl esters of small oligomers of 1 to 5 units. The smaller peaks (11.38, 22.83 and 31.75min) are expected to be the *cis* isomers of the neighbouring main *trans* isomer peak.

The total ion count (TIC) trace (Figure 2.32) from the GC-MS shows a similar pattern although only four main product peaks are observed (acetic acid and methyl acetate are also present as impurities). The fragmentation pattern for each peak is very similar (typical example Figure 2.33) which is what would be expected for oligomeric species.

Figure 2.30 GC-FID trace of methylated ester prepared by base esterification

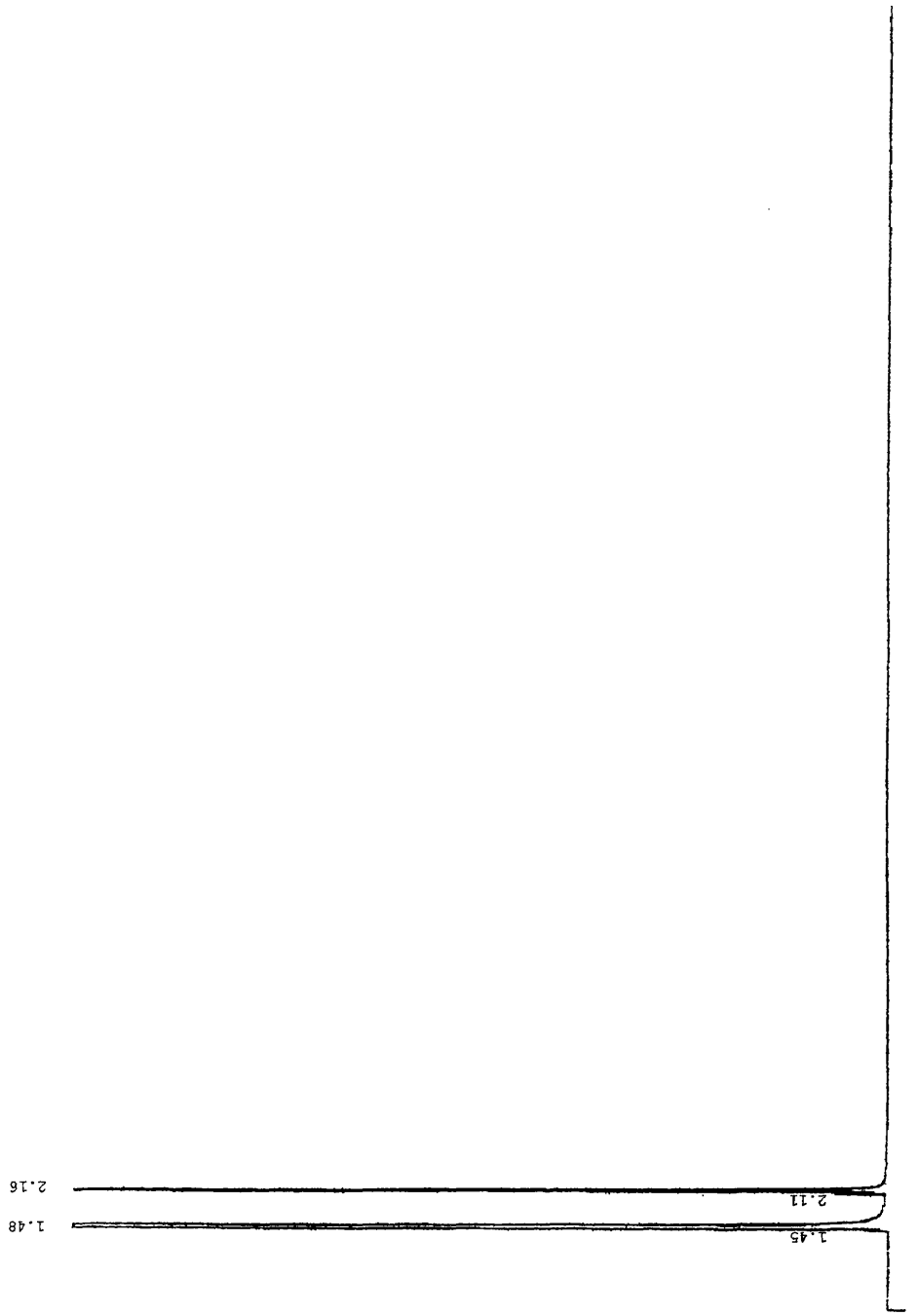

Figure 2.31 GC FID trace of esterified degradation products prepared by diazomethane treatment

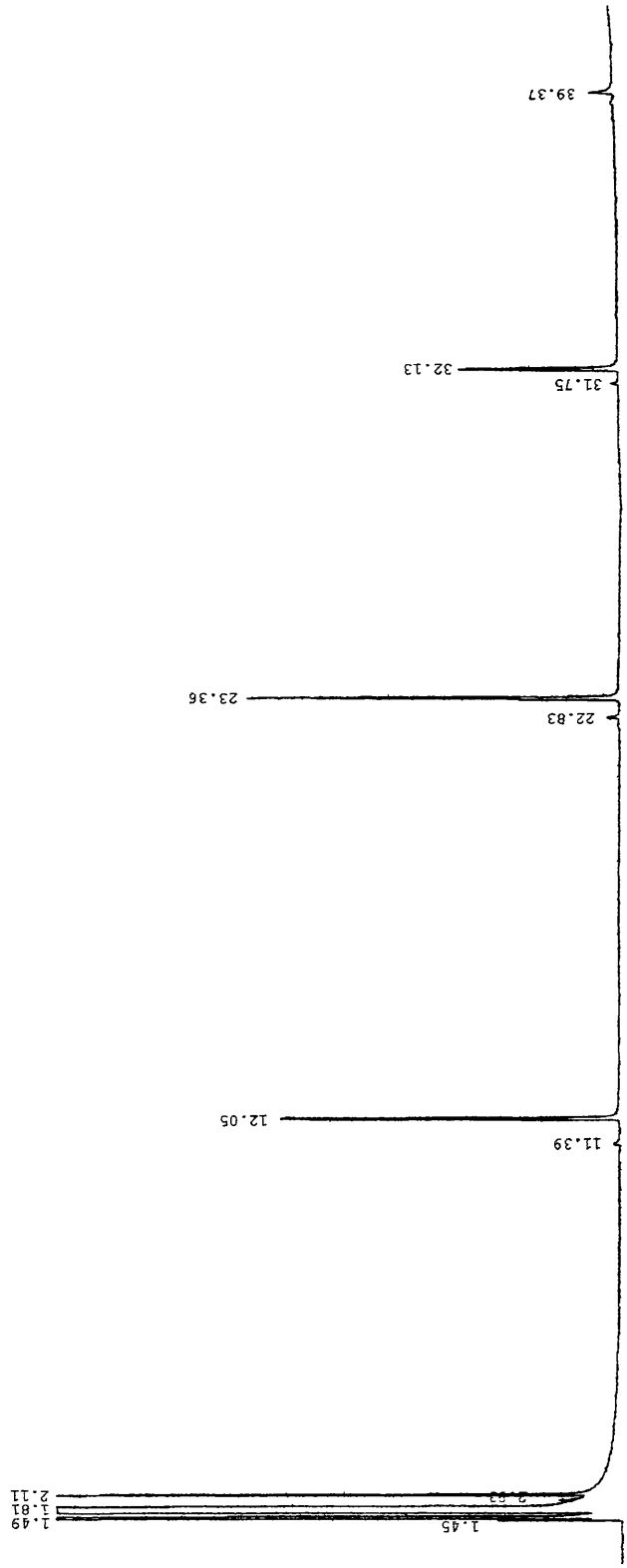

Figure 2.32 GC- TIC trace of esterified degradation products prepared by diazomethane treatment

Figure 2.33 Example of MS fragmentation pattern for each peak on GC trace of esterified degradation products

```
File:           C:\CHEMPC\DATA\STUICN7.D
Operator:       WJC
Date Acquired:  24 Aug 95    3:48 pm
Method File:    DEFAULT.M
Sample Name:                      CROTONIC ACID ME ESTERS/DIAZ. NEW DEGR.
Misc Info:
ALS vial:       1
```

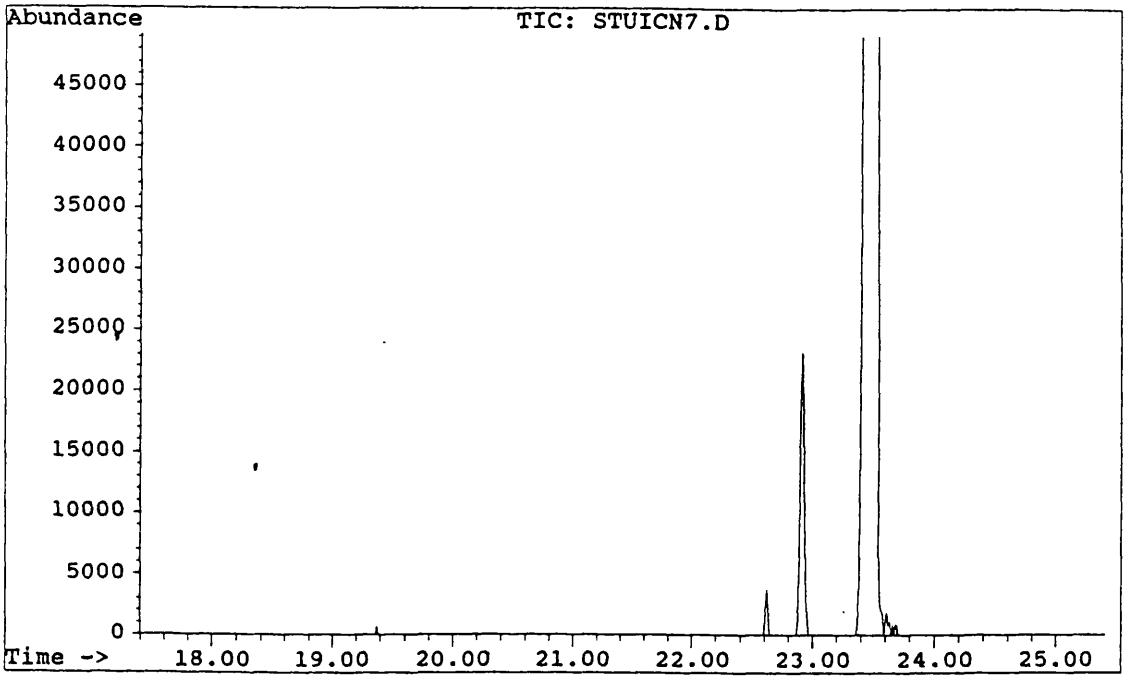

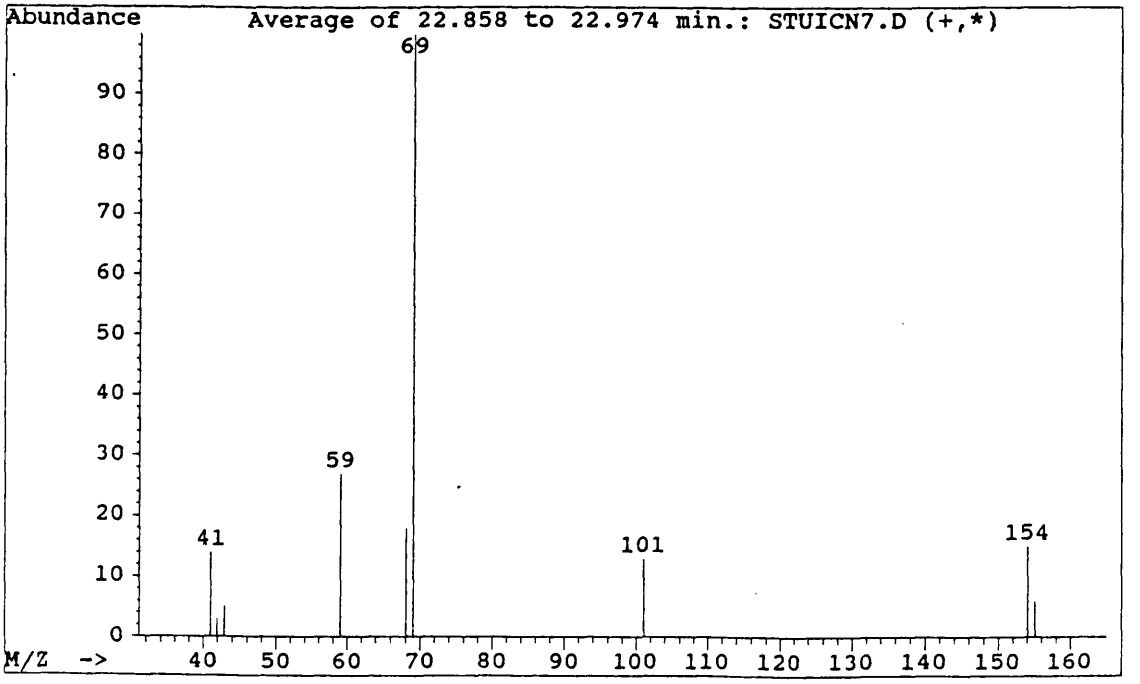

Kovats Index

To be certain that crotonic acid and its oligomers are indeed the observed products, the Kovats Index (*I*) for each compound was determined and compared. The Kovats Index is a method for determining the retention time for compounds on comparable equipment[54] In effect, the column is 'calibrated' in terms of the number of carbon atoms contained in linear aliphatic hydrocarbons. The retention times for these hydrocarbons are noted(Figure 2.34) and the graph of retention time vs. Kovats index (number of carbons × 1000) drawn(Figure 2.35). For any particular compound the retention time, measured as Kovats index, is constant when it is examined on equipment fitted with a similar column under the same heating conditions.

The Kovats Index also implies that there is a relationship between molecular weight and retention time for compounds of similar structure.

The GC trace of the degradation products was converted to Kovats index for each of the peaks and the difference between adjacent peaks was then calculated.

Figure 2.34 GC trace of aliphatic hydrocarbons for determination of Kovats Index

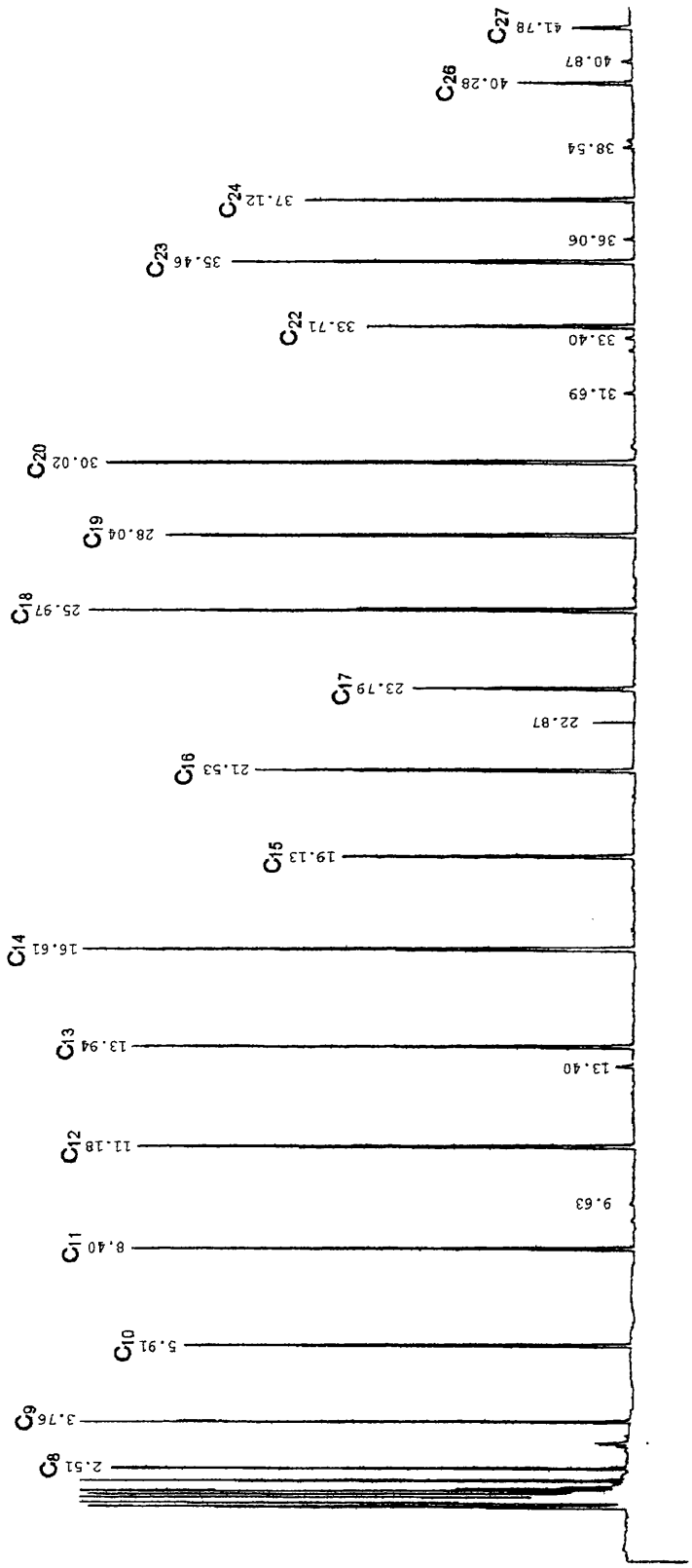

Figure 2.35 Kovats Index calibration graph:-
retentiontime vs. no. of carbons × 1000

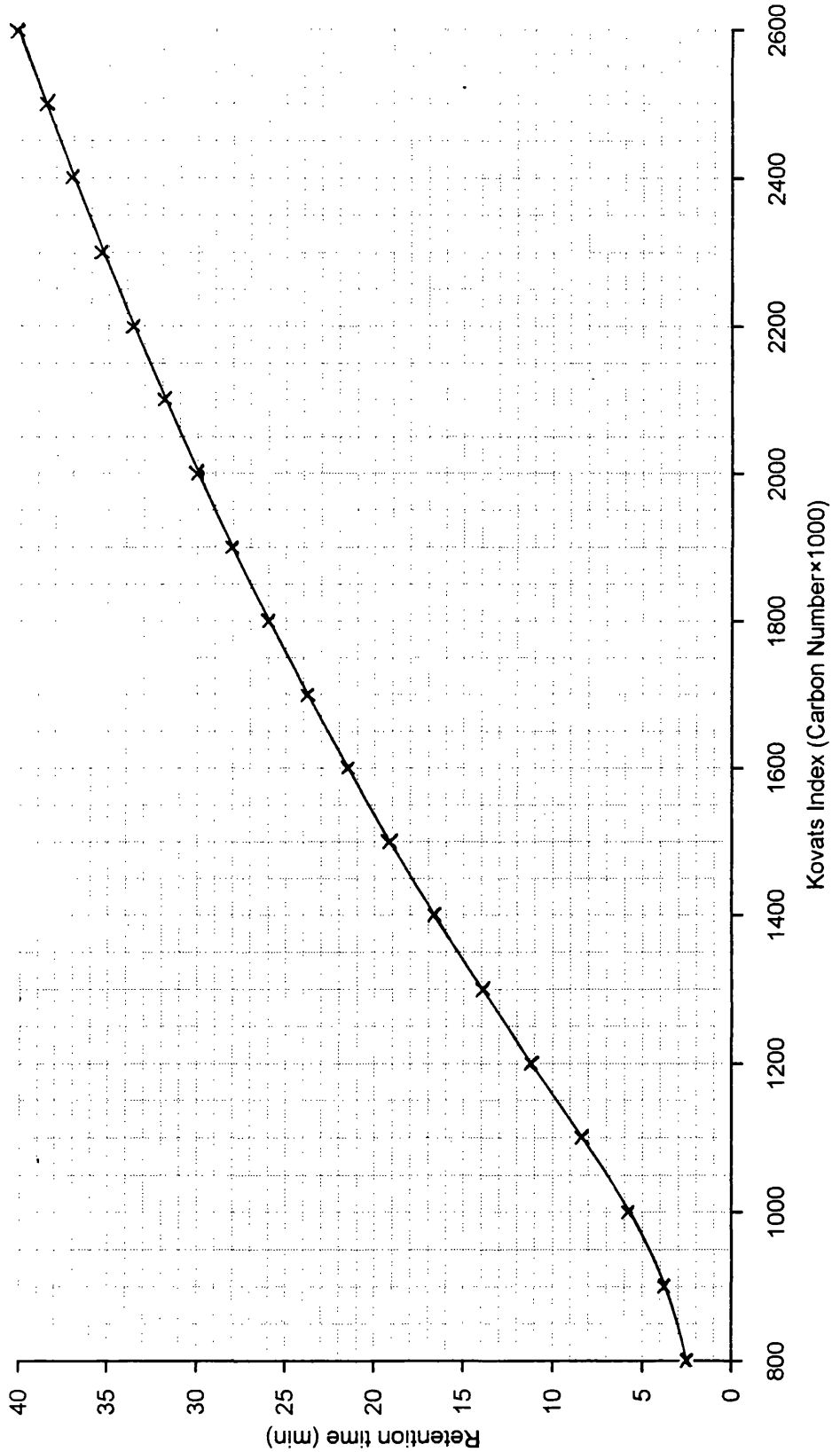

Table 2.3 *Retention time of esterified degradation productsof PHB prepared by diazomethane treatment measured as Kovats Index.*

Peak	Retention time (min)	Kovats Index *(I)*
1	2.11	780
2	12.05	1233
3	23.36	1683
4	32.13	2113
5	39.37	2547

Table 2.4 *Difference in retention time (measured in Kovats Index units) between adjacent esterified degradation products of PHB.*

peak numbers	ΔI
1-2	453
2-3	430
3-4	430
4-5	434

It can be seen that the differences are remarkably similar, demonstrating that there is the same structural difference between each of the compounds. Hence the value of 434 must be the increment for the addition of $C_5H_8O_2$ and the observed peaks are the expected oligomeric products.

Section 3: comparison of stabilisers

The main aspect of the project was to identify additives that will improve the thermal stability of PHB. To do this a method had to be developed to determine the relative stability of samples and hence the effectiveness of additives. It had to be accurate, reliable and rapid so that many additives could be tested in the short space of time.

The first problem to be addressed was to determine the extent of degradation a sample had undergone after exposure to temperature. Degradation takes the form of chain scission and hence produces carboxylic acid end groups. These acidic groups can be quantified by titration with alkali, using phenolphthalein as an indicator, and the average molecular weight can be determined. However, this method proved to be unwieldy to be used on a regular basis because of the relatively low concentration of end groups, the dissolution of the sample and the requirement for fresh sodium hydroxide/ethanol solution. IR-spectroscopy was also used to examine the formation of these end groups, but this did not have the required sensitivity to be practicable. A much more satisfactory method for determining molecular weight is to use gel permeation chromatography (GPC). Unfortunately, this equipment was not readily available and so was used only at the later stages to verify other experimental results. The simplest method used relies on the assumption that the polymer degrades via a random chain scission (see *Thermal Degradation of PHB, p11*). By this mechanism volatile products are evolved from the onset and throughout heating ultimately giving complete weight loss of the sample. Thus, there is weight loss throughout the degradation process which can be used as a measure of the extent of degradation although this is not a linear relationship with time. Being the most straightforward method, this was used as the primary measurement for the majority of experiments.

Generating reproducible experimental heating conditions is exceedingly difficult as a very slight change of temperature affects the rate of degradation of PHB significantly. This is particularly true in isothermal experiments. As a result, many experimental procedures had to be discounted as they proved to

be unreliable. These included isothermal TGA, dynamic air TVA and static nitrogen TVA. Melt flow index apparatus (MFI) also suffers from this problem, particularly in timing the exposure period, and little useful information was gained despite an extensive number of experiments.

Programmed heating eliminates the need for accurate temperature control, as all temperatures in the program will be achieved at some point regardless of the ambient temperature. However, these methods also proved to be of little use as the effects of the additives were not easily discernible. Again TG was discounted but TVA proved slightly more successful. However, running samples singly meant that the method was very labour intensive, particularly when the amount of information yielded is taken into consideration.

The most successful method to maintain experimental conditions for a range of additive/polymer mixtures was to compare them in a single experiment. Exposing many samples to the same heating source simultaneously eliminates the effect of many external influences and sources of error, which improves the comparison significantly. It took a number of attempts to create a working system, which consisted of a silicone oil bath, heated by a thermostatically controlled hot plate, in which narrow sample tubes were suspended. After heating for the chosen time at the required temperature, the tubes could be weighed to determine weight loss from the samples and so establish the relative effectiveness of additives. By this method a vast number of additives were screened and successful stabilisers were identified for further study.

GPC was used to determine and compare the effects of the selected stabilisers in the early stages of degradation and molecular weight loss curves were drawn. Some of these additives were also examined on a new apparatus that was constructed to record IR spectra of molten polymer. This demonstrated clearly that the additives have a major effect on the overall structure of the polymer and affect the degradation mechanism significantly.

TVA

On degrading PHB in a TVA experiment the Pirani trace produces a response between 180 - 250°C on which there is an initial pronounced peak. For similar samples this trace is remarkably consistent with the position of the peak being very constant with respect to the oven temperature. It should be possible to use this reading as a measure of polymer stability and use it to compare samples of PHB with and without additives. More stable polymer mixtures would have the peak maximum at a higher temperature than less stable mixtures.

The precision of this technique was confirmed by statistical analysis and it was used on samples of varying purity, with some success. But the technique is laborious for the information it yields, hence other methods were used in preference.

Statistical analysis of TVA results

The internal thermocouple trials (see *Viability of an internal thermocouple as a detector of CRF formation, p30*) provided an excellent opportunity to examine the statistical relevance of the TVA data with the same sample being run repeatedly under the same conditions. This would give us a better picture of the distribution of the measurements and their associated error.

A TVA experiment with PHB produces a Pirani trace on which there is a distinctive peak which can be measured relative to the oven thermocouple trace as an integer from the analogue to digital converter.

Thus, for each of the internal thermocouple runs we have the temperature at which the Pirani trace gives a maximum (measured in digital units).

1727	1756	1744	1745	1736	1738	1711
1731	1728	1719	1743	1751	1715	

Number of samples (N) = 13

Mean (x) = 1734.15

Sample Standard deviation $$s = \sqrt{\frac{\sum_{i=1}^{N}\left(x_i - \bar{x}\right)^2}{N-1}} = 13.855$$

Standard error of mean $$s_m = \frac{s}{\sqrt{N}} = \frac{13.855}{\sqrt{13}} = 3.84$$

This distribution can be applied to any single result, using that result as the mean value. By performing a student t-test using two of these sample distributions, the probability of overlap between the distributions and hence the significance of any difference can be determined.

$$t = \frac{\overline{x_1} - \overline{x_2}}{\sqrt{{s_{m1}}^2 + {s_{m2}}^2}} = \frac{\overline{x_1} - \overline{x_2}}{\sqrt{3.84^2 + 3.84^2}} = \frac{\overline{x_1} - \overline{x_2}}{5.43}$$

Number of degrees of freedom = (N_1-1) + (N_2-1) = (13-1) + (13-1) = 24

The probability of overlap between two sample distributions is obtained from lookup tables using the t value and the number of degrees of freedom.

It is considered that if the probability falls within certain values the following can be derived

for P > 0.05 then the difference between the results is insignificant

0.05 > P > 0.01 then the difference is significant

and if P < 0.01 then the difference is highly significant

Alternatively, the difference (x_1-x_2) can be determined for a given probability and number of degrees of freedom.

So, in this case, a probability of 0.01 is obtained with a difference of 15.18 digital units and a probability of 0.05 with a difference of 11.21 digital units

By using the appropriate conversion factor (see *Oven Thermocouple Calibration, p27*) this corresponds 2.3°C and 1.7°C respectively.

Thus it would appear that the TVA apparatus can be used for determining relative breakdown temperature with surprising precision as the experiment is reproducible within quite narrow limits i.e. ±2.3°C which is sensitive enough to allow small changes in stability to be differentiated.

TVA comparison of impure samples from each stage of the production process

These are samples of PHB, supplied by Zeneca, that were taken from the same batch at various stages in the production process. After the main fermentation process, the product undergoes a number of purification procedures to remove unwanted bacterial cell content. By examining these samples it could be ascertained if any of the processes involved had a detrimental effect upon the final product. The samples are as follows:-

(A) pre heat-shock
(B) post heat-shock
(C) post enzyme
(D) post detergent
(E) pre peroxide
(F) post peroxide

Table 3.1 *Temperature at which the Pirani trace is at its maximum in a TVA experiment at a heating rate of 5°C/min*

Sample	A	B	C	D	E	F
Temp (ADC units)	1916	1912	1852	1862	1880	1817
Temp (°C)	239.5	238.8	229.7	231.3	234.0	224.4

According to the statistical analysis there is little difference between samples (A) and (B) and samples (C) and (D). All other differences are significant. It

can be seen that samples (A) and (B) are the most stable presumably because of the large proportion of bacterial fragments present which is thought to contain compounds that act as stabilisers. (C) and (D) possibly contain prodegradant material which is washed out in the detergent step giving (E) greater stability.

It has been demonstrated that TVA could be used as a measure of stability, but it can be seen that the differences between samples are small and on the limits of the resolution possible. The method is very time consuming and uses many resources so a cheaper method was sought.

Simple weight loss methods

In order to readily compare the effect of additives on PHB, the most simple and convenient method was to measure the weight loss from degraded samples. This method relies on the assumption that volatile products are evolved from the onset of degradation and throughout heating. This relationship is not linear with respect to time but is still adequate for use as a measure of extent of degradation.

The main difficulty with this approach is obtaining uniform conditions for experiments to allow accurate comparison of samples. Simply placing samples in an oven for a pre-determined temperature and duration or subjecting it to a temperature program did not produce satisfactory results.

Attempts were made to control the atmosphere to which the sample was exposed. High vacuum was employed using isothermal TVA experiments (see *TVA and PHB, p20*), a static atmospheric pressure nitrogen atmosphere system was also used[55] and the effect of dynamic airflow was examined using apparatus designed by G. Seeley[56]. However, none of this equipment showed any significant improvement of results.

A different approach was to run a series of samples simultaneously, with a control, such that each sample would experience the same experimental conditions.

A simple experiment demonstrated that the ovens available possessed very uneven heating patterns, and that if there were many samples inside the oven they would not experience the same temperature, but it was felt that by using a liquid bath a more even temperature would be obtained. Initially it was thought that Wood's metal would be the ideal liquid: a good conductor of heat and, unlike oil, would not stick to the glass sample tubes. However, a Wood's metal bath is very difficult to control and can leave traces of oxidised metal baked onto the surfaces of sample containers. It was finally decided to use a silicone fluid bath which can be used at temperatures up to 250°C. Traces of

silicone fluid would then be washed off the sample bottles with dichloromethane.

A special rack had to be constructed to support the samples in the silicone fluid bath, with a second design producing acceptably consistent results. After tests to determine the effect of various sources of error the weight loss method was used with great success to identify many possible stabilisers and examine how they affected the shape of the weight loss curve. The same heating method was also used to prepare comparable samples for GPC analysis.

Oil bath work

The general experimental method was as follows: A one litre beaker containing 250ml of silicone oil was heated to 200°C on a heating plate and was stirred using a magnetic stirrer. Into this were placed a number of open sample tubes which were mounted in a specially constructed rack. These were left for four hours at constant temperature. After this period the tubes were removed from the bath, the oil washed off with dichloromethane, and the sample bottles re-weighed..

In the original design(Figure 3.1), it was apparent that there was not an even temperature throughout the bath, demonstrated by different weight losses from the samples(Figure 3.2). This rack was supported by three legs, situated on the periphery, which produce eddies in the flow of the stirred oil, resulting in warm and cold areas within the bath.

Consequently, a second more successful rack was designed to be hung in the bath by a single central support(Figure 3.3). It was also thought that the thermometer, being of different profile to a sample tube, would also cause similar eddies in the fluid, so the bulb of the thermometer was positioned within a sample tube filled with oil to provide good thermal contact. In this case, the sample tubes were supported by an o-ring stretched around each sample bottle which was then sandwiched between two plates. This design produced much more satisfactory results, specifically, the deviation of results within each run (Table 3.2) is of an acceptable level, and the spread of error

appears to be totally random so any heat distribution effect seems to have been eliminated. To reduce experimental error further, each sample was used in triplicate in each run. This limited the number of different samples tested to 6 per run rather than 18 but it still remained a relatively quick and easy method for screening a large number of samples containing different additives.

Figure 3.1 *Original sample rack for oilbath*

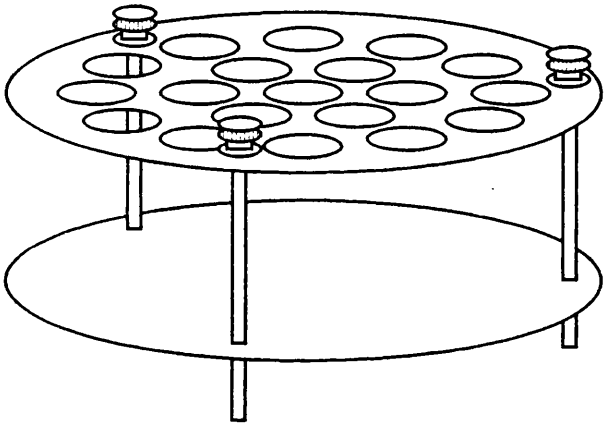

Figure 3.2 *Map of percentage weight loss from identical samples in an oil bath experiment*

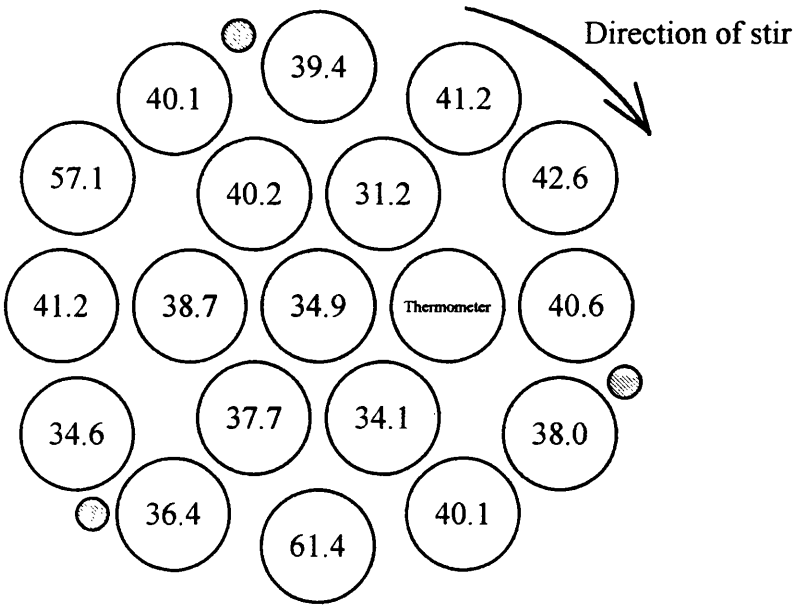

Figure 3.3 *Adopted design of sample rack for oil bath*

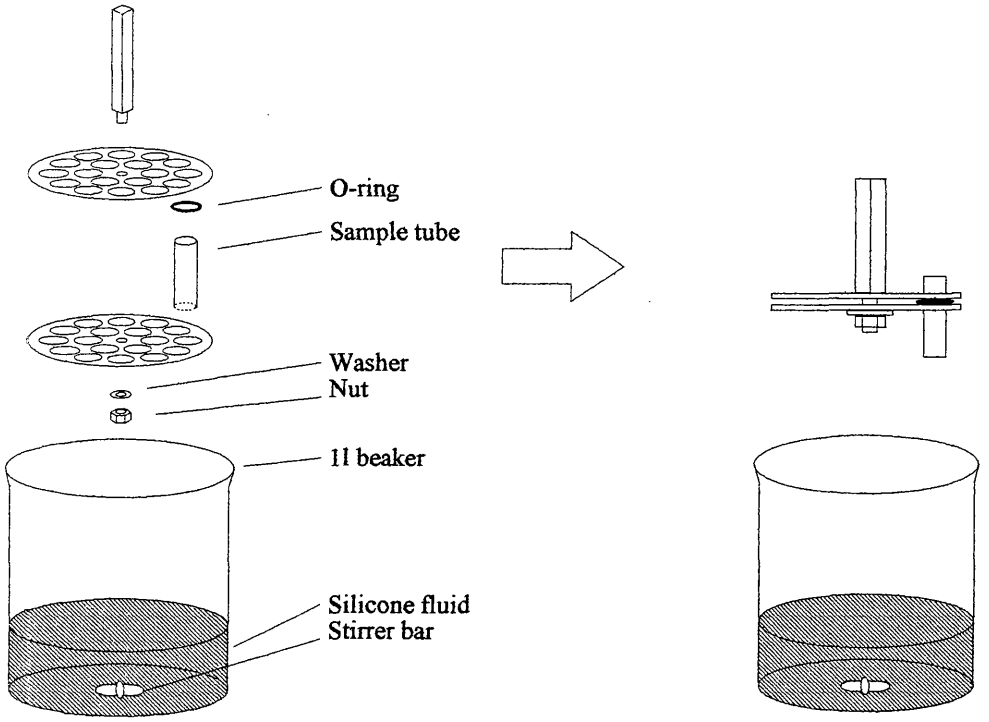

Table 3.2 *Measurements from oil bath experiment with the same pure PHB sample in each tube*

tube no.	sample size (mg)	weight loss (mg)	% weight loss
1	103.2	56.2	54.5
2	97.4	48.3	49.6
3	101.2	55.0	54.4
4	96.4	50.9	52.8
5	99.3	48.1	48.4
6	97.3	50.6	52.0
7	100.4	47.6	47.4
8	100.8	46.8	46.4
9	98.4	50.1	50.9
10	98.3	53.7	54.6
11	95.5	50.9	53.3
12	97.0	52.3	53.9
13	104.9	60.6	57.8
14	105.0	57.3	54.6
15	102.4	54.7	53.4
16	98.2	54.2	55.2
17	97.5	56.5	57.9
18	Thermometer		
		Mean	52.8
		Standard Deviation	3.3.

Effect of Sample Size

It was important to establish if the sample size had any significant effect upon the degradation of samples and what magnitude of error would be incurred through variations in the precision of weighing. To investigate this an oil bath experiment was set up with a different quantity of sample in each tube, ranging from 30 to 200 milligrams which were subjected to the usual experimental conditions i.e. heated for four hours in an oilbath at 200°C.

Table 3.3 Data from sample size experiment.

tube no.	sample size (mg)	weight loss (mg)	% weight loss
1	30.2	17.9	59.3
2	51.0	30.7	60.2
3	71.1	42.8	60.2
4	92.0	57.2	62.2
5	100.5	68.5	68.2
6	109.1	64.8	59.4
7	128.9	84.1	65.2
8	149.0	134.6	90.3
9	169.7	119.4	70.4
10	181.0	123.3	68.1
11	191.9	128.0	66.7
12	197.8	139.2	70.4
13	162.3	117.3	72.3
14	137.2	96.5	70.3
15	82.4	54.1	65.7
16	59.1	36.2	61.3
17	39.8	25.5	64.1
18	Thermometer		

When a graph is drawn of weight loss versus sample size, with appropriate error bars(Figure 3.4), the best fit shows a gradual increase in weight loss with sample size. The data shows that for the expected precision in weighing (100±5mg) there will be negligible effect upon the percentage weight loss.

Figure 3.4 *Comparison of weight loss with sample size after heating in an oil bath for four hours at 200°C*

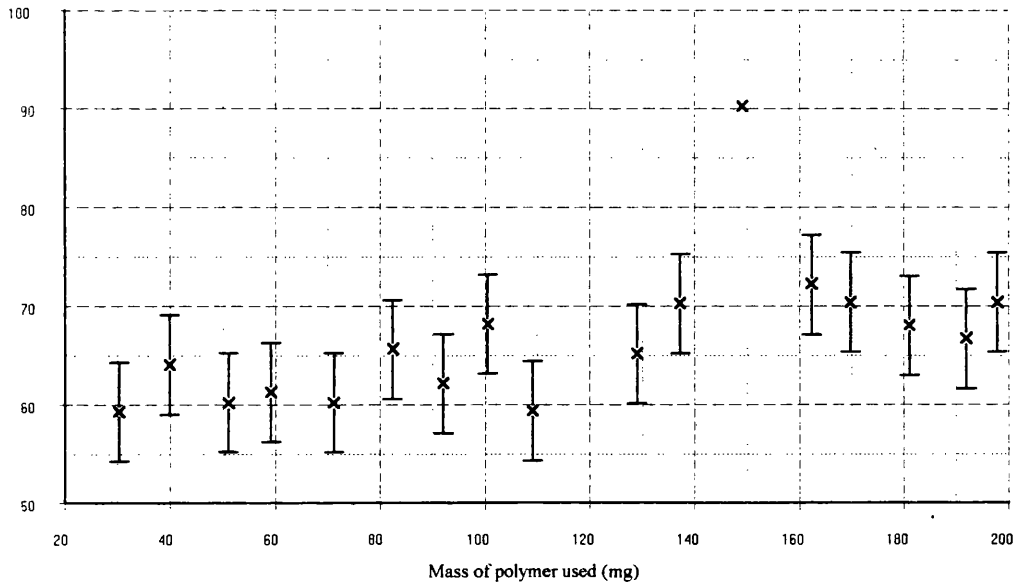

Grinding and Mixing Tests

A series of samples were made up to test the effect of mixing additive with the polymer. The additive used was pyromellitic anhydride which was known to have a significant stabilising effect[57]. These samples were then subjected to normal oil bath experimental conditions. i.e. 100mg weighed into sample tubes which were then placed into an oil bath at 200°C for four hours. They would then be removed, allowed to cool, the oil would be removed from the outside with tissue paper, and the tubes reweighed.

The samples were prepared by placing around 2g of PHB into a mortar followed by about 10mg of pyromellitic anhydride to give a concentration of 5000ppm. This was then stirred for 1 minute with a nickel spatula. A sample was then taken from this mixture and stored for later use. The mixture was then ground using a pestle for a further minute and a sample from this mixture was also taken and stored. The grinding was then repeated for further 2, 2 and 5 minute periods, with samples taken after each period of grinding.

After four hours in the oil bath, the samples with additive had all undergone a similar weight loss within the expected distribution (Table 3.4). This shows that the grinding has little effect upon the weight loss though common sense tells us that the additive must be evenly dispersed throughout the polymer to obtain consistent results. Stirring for one minute achieved this for pyromellitic anhydride, which was in fine powder form, though this will not be enough for crystalline or liquid additives. For these types of samples the grinding is necessary and so the standardised procedure for mixing, five minutes of grinding in the mortar and pestle, appears to be adequate.

Table 3.4 *Measurements taken from oil bath experiments (Grinding test 4hrs at 200°C)*

Sample	Mass of sample Used (g)	Mass lost (g)	Mass lost (%)
A	94.9	29.4	31.0
stirred for 1min	97.8	36.7	37.5
	104.7	39.8	38.0
B	92.7	31.7	34.2
ground for 1 min	92.7	24.7	26.6
	100.3	33.9	33.8
C	100.3	29.0	28.9
ground for 3 min	97.6	28.2	28.9
	65.0	24.9	38.9
D	101.6	29.5	29.0
ground for 5 min	106.0	33.0	31.1
	96.8	30.0	31.0
E	103.7	32.8	31.6
ground for 10 min	96.0	27.1	28.2
	100.0	29.4	29.4
F	98.5	83.5	85.0
control	99.6	90.5	91.0

Figure 3.5 *Weight losses from grinding test samples in oil bath experiment (5hrs at 200°C)*

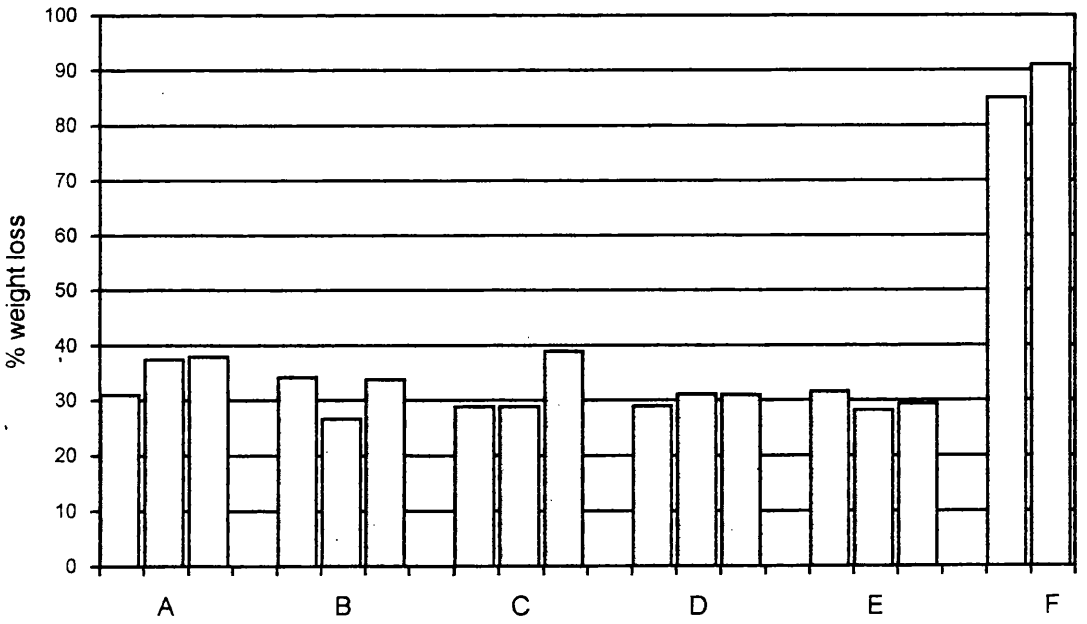

Mixing

Using a mortar and pestle to grind the additive with the polymer only mixes on a particulate level, i.e. the mix would be made up of relatively large particles of polymer and additive. It would be expected that at this particulate level there will be poor contact between polymer and additive and that a much improved effect would be be observed if they could be dispersed at a much finer level.. This improved dispersion could be achieved by mixing the two components as solutions and evaporating the solvent.

This experiment consisted of two sets of samples: powder and solution. In each set there was control, Weston TLTTP an oxalic acid samples. The powder samples were prepared in the usual way: 10mg of additive to 2g polymer ground in a mortar and pestle for five minutes. The samples in solution were prepared by first dissolving the polymer in chloroform which was then concentrated using Buchii apparatus to reach a concentration of around 50mg/ml. The actual concentration of the solution was determined by measuring the mass of polymer remaining after evaporation of solvent from a 1ml sample. The additive solutions were made up to around 0.5mg/ml. The Weston TLTTP was dissolved in chloroform whilst the oxalic acid had to be dissolved in a mixture of acetone and chloroform. 1ml of the additive solution was pipetted into a sample tube, of which the mass had been recorded earlier, followed by the polymer solution, the sample tubes were then shaken and left in the fumehood until the solvent had evaporated. The oil bath experiment was then carried out as normal with the required number of samples.

Table 3.5 Measurements taken for oil bath experiment - comparison of mixing

Sample	Conc (ppm)	Mass of sample used (g)	Mass lost (g)	Mass lost (%)	Average Mass Lost (%)
Powders					
Control	-	85.2 98.3	72.8 87.2	85.4 88.7	87.1
Weston TLTTP	6096	102.1 90.5 87.2	18.4 15.8 14.3	18.0 17.5 16.4	17.3
Oxalic acid	4999	95.8 96.2 88.2	20.4 19.4 16.6	21.3 20.2 18.8	20.1
Solutions					
Control	-	81.4 81.2 83.0	77.9 76.7 78.7	95.7 94.5 93.9	94.7
Weston TLTTP	~5920	87.2 85.2 86.0	17.5 16.1 15.8	20.1 18.9 18.4	19.1
Oxalic acid	~5930	87.6 87.3	27.9 28.1	31.8 32.2	32.0

The solution mixed samples showed a consistently higher decomposition than the powder samples, but this was thought to be due to degradation caused by heating during the dissolution and evaporation of the polymer solution, and it was felt that, in practice, there is little significant difference between the powder and solution samples indicating that the additives must disperse fully when the polymer melts.

Concentration Tests

Six samples were made up with differing concentrations of pyromellitic anhydride to investigate how the concentration of additive in the polymer affects the decomposition.

The samples varied in concentration from no additive to 10,000ppm.

At around 5000ppm, which is used for most experimental runs, ±1000ppm produced a difference in weight loss of only ±4% which is less than the observed experimental error. Again, it can be seen that small variances in the concentration of additive that may occur by operator error, produced only a small deviation form the expected value

Table 3.6 *Measurements taken from concentration test samples in oil bath experiment (4hrs at 200°C)*

Additive concentration (ppm)	Mass of sample used (g)	Mass Lost (g)	Mass Lost (%)
0	100.1	82.1	82.0
	98.2	83.4	85.0
2170	103.7	49.9	48.1
	95.9	47.7	49.7
	95.1	45.4	47.7
4308	104.2	37.7	36.2
	96.4	33.1	34.3
5424	98.8	30.6	31.0
	96.4	28.3	29.4
	96.8	28.0	28.9
6105	95.6	28.2	29.5
	97.5	27.4	28.1
	99.3	32.7	32.9
10,409	96.9	24.7	25.5
	100.2	19.6	19.6
	100.8	24.5	24.3

Figure 3.6 *Effect of concentration of pyromellitic anhydride upon weight loss from PHB sample in oil bath experiment (4hrs at 200°C)*

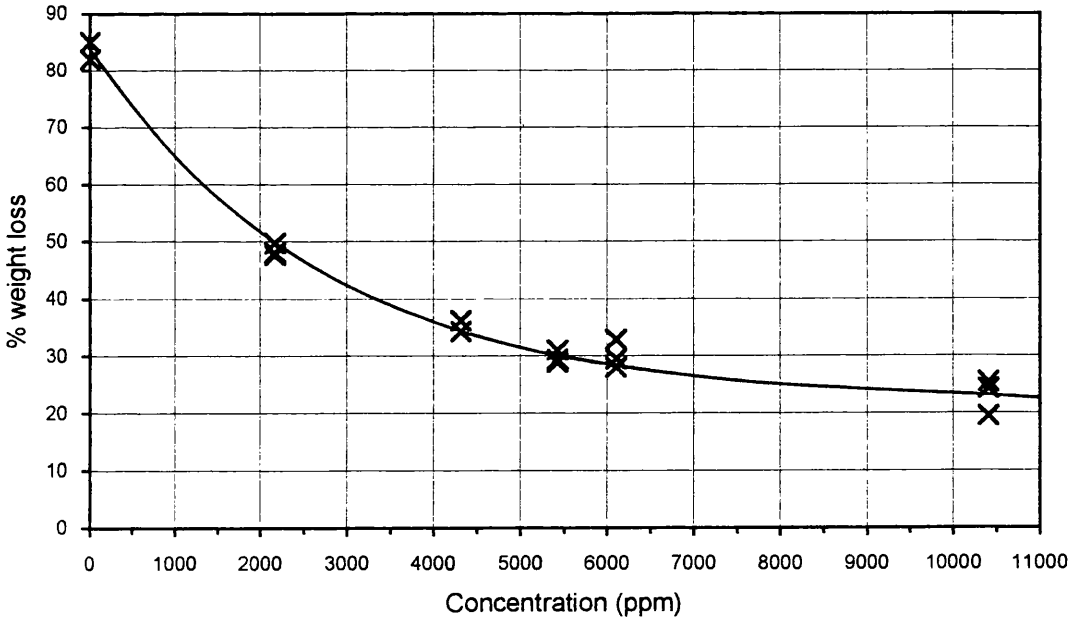

Additives

The oil bath technique proved to be consistent, reliable, and simple to use. It allowed direct comparison of up to five additives (each in triplicate to reduce uncertainty) in a single experiment by measuring the weight lost from each sample versus that of a control. This gives a measure of its stabilising (or destabilising) effect.

However, the results cannot be extrapolated with much accuracy to compare additives from different experiments as the weight loss versus time curve cannot be taken into account which is unlikely to be similar for the many different stabilisers under test.

A wide range of additives were examined. Initially a number of commercial stabilisers including antioxidants, peroxide decomposers and radical traps were tested. Most of these had severe prodegradant effects or no effect at all, apart from a 'Weston' phosphite based compound, which had a significant stabilising effect. This led to the use of other phosphite compounds of which a few had an apparently larger stabilising effects than pyromellitic dianhydride (already known to have a significant stabilising effect). Compounds related to pyromellitic dianhydride , such as phthalic anhydride, succinic anhydride, led to the use of succinic acid, and later to aromatic carboxylic acids. It had been observed that highly purified polymer was more stable than more crude forms, which contain baterial remnants from the production process, so all of the naturally occurring amino acids were also tried. The amino acids contained many different functional groups, but more importantly, they indicated that the structure of the additives is important. This was confirmed by study of a range of aromatic carboxylic acids and an experiment for various chain length aliphatic dicarboxylic acids. PHB is unusual in that each monomeric unit is the same enantiomer, making the polymer optically active. It was shown in an experiment comparing various forms of tartaric acid that not only the structure of the additives is important but also the stereochemistry. Other types of additive examined included inorganics and food grade antioxidants

Although only an indication of additive performance, a stabilisation (or destabilisation) factor has been calculated to give an overall picture for the additives. The factor is taken as the ratio of the percentage weight loss for the control sample to the percentage weight loss from the sample with additive, or its reciprocal, whichever gives a value greater than one. This factor gives a rough quantitative measure of the comparative effect of different additives - the larger the value, the bigger the effect of stabilisation or destabilisation. For convenience, a stabilising factor is denoted as a positive number and a destabilising factor as a negative number. Also, for comparative reasons, it can be seen that some of the more interesting additives have been used in more than one experiment.

Table 3.7 *Comparison of stabilisation and destabilisation factors, determined by oil bath technique, for additives in PHB*

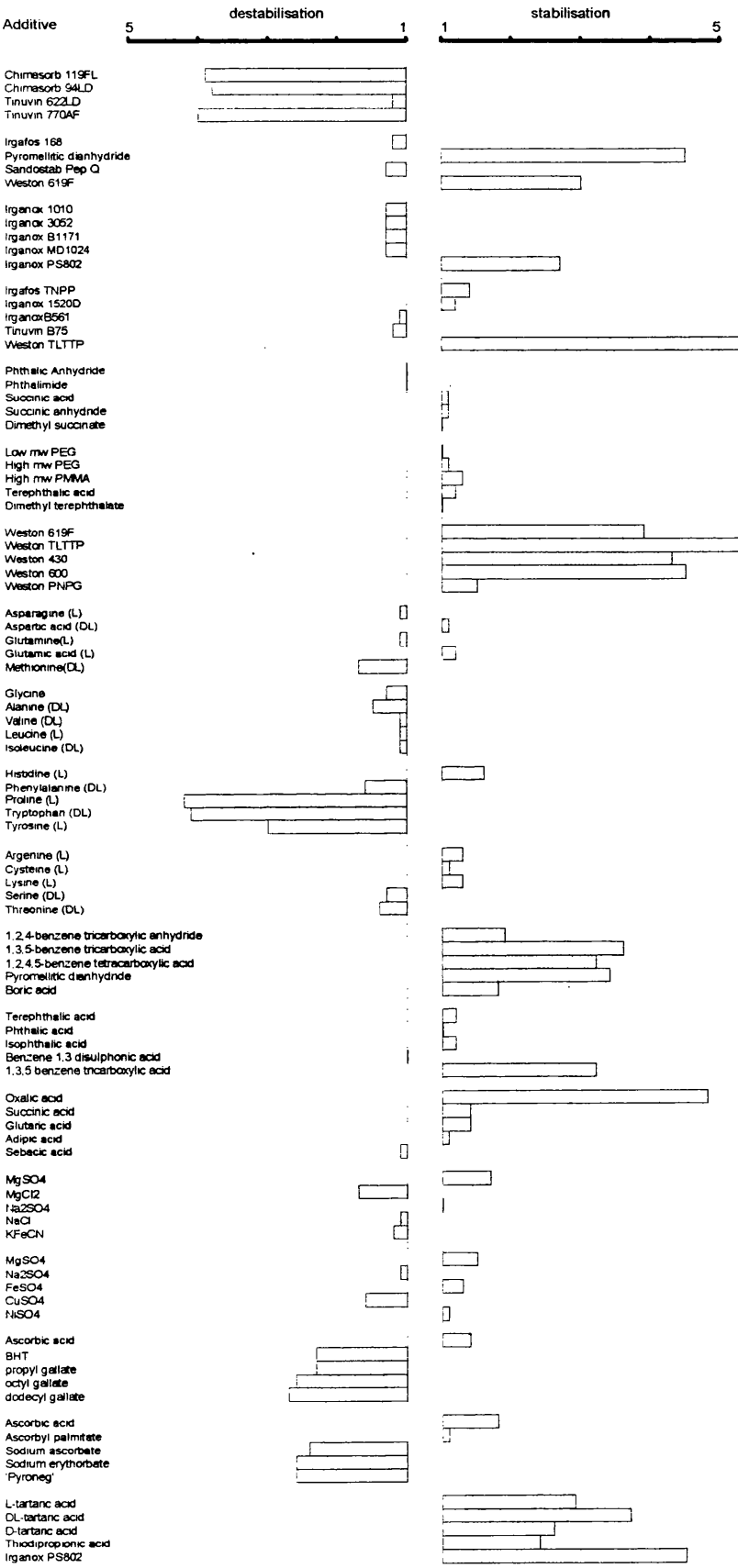

Hindered amine additives

Sample	Conc (ppm)	Mass of sample (g)	Mass lost (g)	Mass lost (%)	Average loss (%)	Stability factor
Chimasorb 119FL	5303	106.6 97.6 109.8 103.7	102.6 92.9 105.4 98.9	96.2 95.2 96.0 95.4	95.7	-3.91
Chimasorb 944LD	6497	87.5 97.6 98.3	80.3 91.1 90.7	91.8 93.3 92.3	92.5	-3.78
Tinuvin 622LD	5395	103.6 98.4 98.9	39.1 27.7 40.1	37.7 28.2 40.5	30.5	-1.24
Tinuvin 770AF	5382	98.8 97.3 98.5	96.1 94.7 95.7	97.3 97.3 97.2	97.3	-3.97
Control	-	96.7 97.5 106.2 101.9	19.1 25.9 28.1 25.6	19.8 26.6 26.5 25.1	24.5	

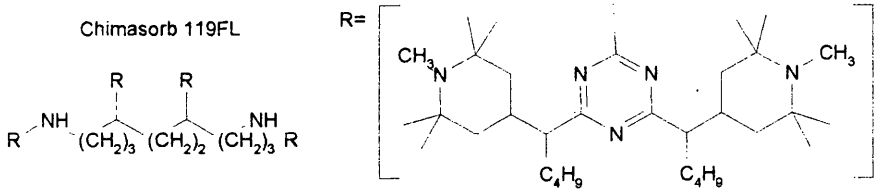

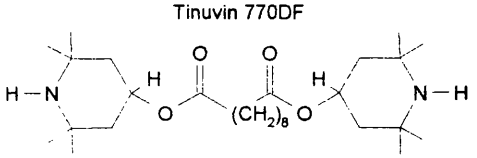

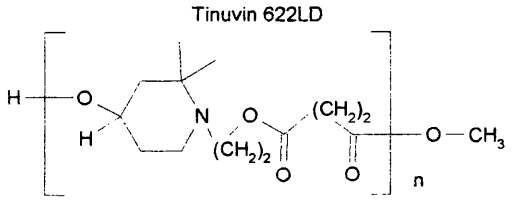

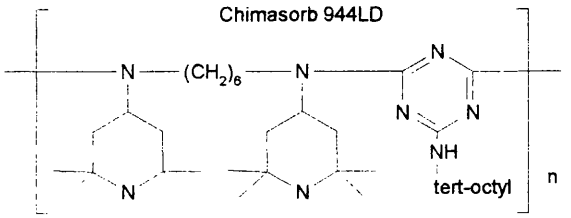

Commercial additives (I)

Sample	Conc (ppm)	Mass of sample (g)	Mass lost (g)	Mass lost (%)	Average loss (%)	Stability factor
Irgafos 168	4917	101.1 101.5 91.0	35.0 32.8 39.8	34.6 32.3 43.7	36.9	-1.25
Pyromellitic Ahydride	5424	98.7 104.2 99.9	7.2 5.7 6.6	7.3 5.5 6.6	6.5	4.53
Sandostab PEP Q	5271	102.0 97.4 99.5	38.4 34.9 42.7	37.6 35.8 42.9	38.7	-1.31
Weston 619F	6361	100.4 101.3	9.6 9.9	9.6 9.8	9.7	3.04
Control	-	100.8 100.2 101.9	29.2 29.4 30.8	29.0 29.3 30.2	29.5	

Pyromellitic Anhydride

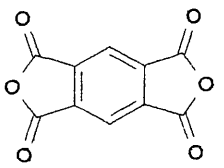

Irgafos 168

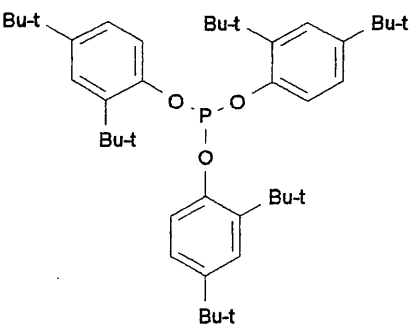

Sandostab P-EPQ

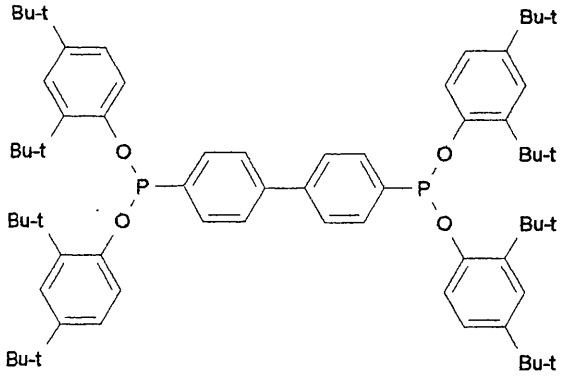

Weston 619F

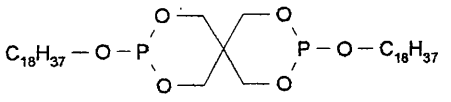

Commercial stabilisers (II)

Sample	Conc (ppm)	Mass of sample (g)	Mass lost (g)	Mass lost (%)	Average loss (%)	Stability factor
Irganox 1010	5973	102.9 96.7 103.8	98.2 92.9 101.2	95.4 96.1 97.5	96.3	-1.26
Irganox 3052	4759	96.1 102.5 103.9	93.0 92.9 100.5	96.8 96.7 96.7	96.7	-1.26
Irganox B1171	5465	99.0 103.2 100.3	95.3 99.6 96.2	96.3 96.5 95.9	96.2	-1.26
Irganox MD1024	4871	96.4 103.0 98.0	93.0 98.6 93.2	96.5 95.7 95.1	95.8	-1.25
Irganox PS802	5020	99.6 96.7 101.7	35.1 27.2 20.7	35.2 28.1 20.4	27.9	2.74
Control	-	103.0 105.6	78.2 81.3	75.9 77.0	76.5	

Irganox 1010

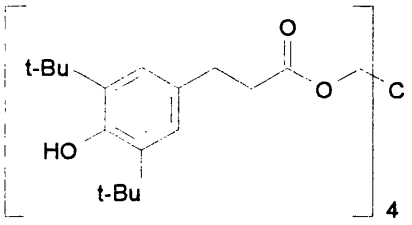

Irganox PS802

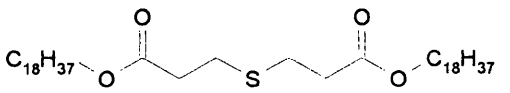

Irganox MD1024

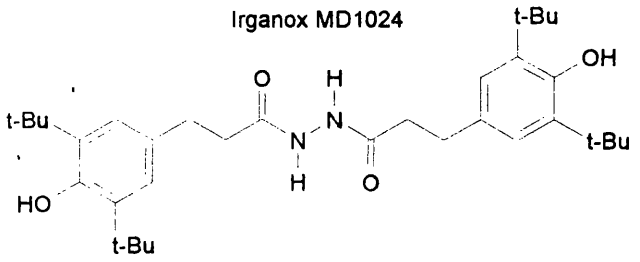

Irganox B1171

[50% Irgafos 168
50% Irganox 1098]

Irganox 3052
(unknown)

Commercial stabilisers (III)

Sample	Conc (ppm)	Mass of sample (g)	Mass lost (g)	Mass lost (%)	Average loss (%)	Stability factor
Irgafos TNPP	8791	104.7 102.5 96.4	68.5 59.1 58.2	65.4 57.7 60.4	61.2	1.37
Irganox 1520D	7200	97.4 99.7 98.2	69.3 68.7 67.9	71.1 68.9 69.1	69.7	1.21
Irganox B561	4537	99.0 99.1 101.2	94.0 92.7 93.7	94.9 93.5 92.6	93.7	-1.11
Tinuvin B75	8373	99.4 102.6 103.1	96.4 99.5 99.9	97.0 97.0 97.0	97.0	-1.15
Weston TLTTP	6096	95.6 98.2 96.8	15.3 16.7 14.2	16.0 17.0 14.7	15.9	5.29
Control	-	103.9 100.2	86.7 85.2	83.4 85.0	84.2	

Irgafos TNPP

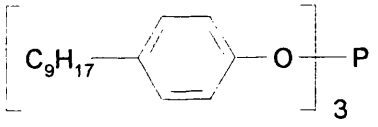

Irganox 1520D

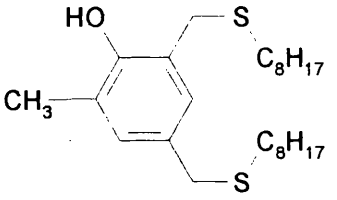

Irganox B561

80% Irgafos 168
20% Iganox 1010

Weston TLTTP

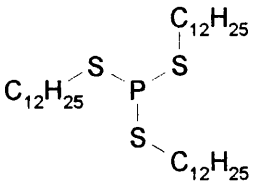

Tinuvin B75

40% Tinuvin 765
40% Tinuvin 571
20% Irganox L135

Compounds related to Pyromellitic Anhydride

Sample	Conc (ppm)	Mass of sample (g)	Mass lost (g)	Mass lost (%)	Average loss (%)	Stability factor
Phthalic Anhydride	6541	102.9 100.4 104.4	71.1 67.3 63.3	69.1 67.0 60.6	65.6	-1.03
Phthalimide	4728	96.4 105.8 96.8	62.2 68.0 62.2	64.5 64.3 64.3	64.4	-1.02
Succinic Acid	4853	105.8 96.5 99.0	62.2 53.7 52.1	58.8 55.6 54.6	56.3	1.13
Succinic Anhydride	5927	104.8 101.5 104.5	62.7 56.5 61.3	59.8 55.7 58.7	58.1	1.09
Dimethyl Succinate	7339	98.1 103.3 100.9	59.5 62.6 60.7	60.7 60.6 60.2	60.5	1.05
Control	-	103.8 95.6	67.4 59.4	64.9 62.1	63.5	

Phthalic Anhydride

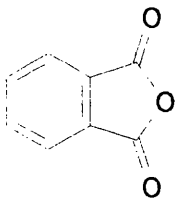

Phthalimide

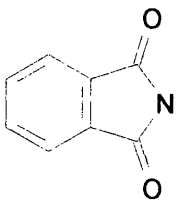

Succinic Acid

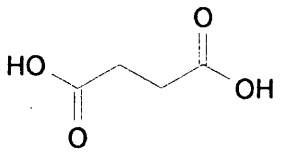

Succinic Anhydride

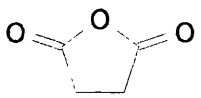

Dimethyl Succinate

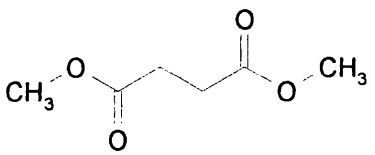

PEG, PMMA and dicarboxyl compounds

Sample	Conc (ppm)	Mass of sample (g)	Mass lost (g)	Mass lost (%)	Average loss (%)	Stability factor
Low mw PEG	6177	99.1 104.1 97.4	74.1 80.4 73.6	74.8 77.2 75.6	75.9	1.01
High mw PEG	5714	103.4 95.2 96.9	75.8 65.4 67.2	73.3 68.7 69.3	70.4	1.09
High mw PMMA	6112	97.6 105.3 97.4	73.6 73.7 66.7	75.4 70.0 68.1	71.2	1.25
Terephthalic Acid	5635	102.5 103.4 104.1	65.1 66.9 65.9	63.5 64.7 63.3	63.8	1.20
Dimethyl Terephthalate	5271	100.8 98.6 101.1	78.1 71.1 69.5	77.5 72.1 68.7	72.8	1.05
Control	-	96.3 98.7	74.9 74.5	77.8 75.5	76.7	

Polyethylene Glycol

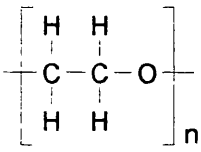

Polymethyl Methacrylate

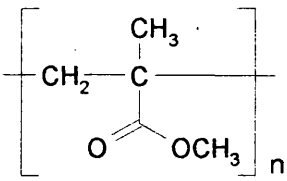

Terephthalic Acid

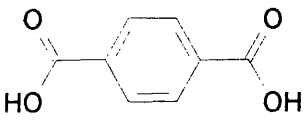

Dimethyl Terephthalate

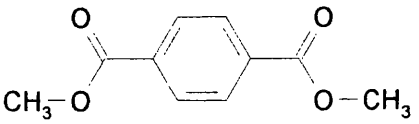

Weston additives

Sample	Conc (ppm)	Mass of sample (g)	Mass lost (g)	Mass lost (%)	Average loss (%)	Stability factor
Weston 619F	6361	97.3 99.9 104.1	23.4 19.0 22.1	24.0 19.0 21.2	21.4	3.85
Weston TLTTP	6096	100.7 94.8 102.3	14.8 13.6 13.1	14.7 14.3 12.8	13.9	5.92
Weston 430	7869	100.7 108.4 98.7	19.4 20.4 18.9	19.3 18.8 19.1	19.1	4.31
Weston 600	6260	96.7 99.2 92.6	17.9 18.3 16.7	18.5 18.4 18.0	18.3	4.50
Weston PNPG	6918	97.8 100.6 99.4	59.2 54.2 49.2	60.5 53.9 49.5	54.6	1.51
Control	-	102.1 98.3	81.6 83.3	79.9 84.7	82.3	

Weston 619F

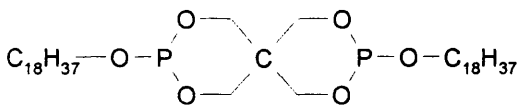

Weston PNPG

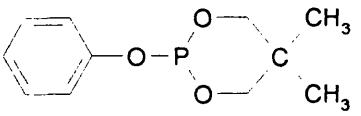

Weston 600

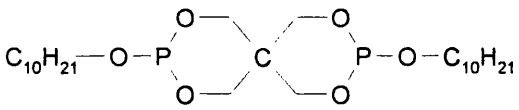

Weston TLTTP

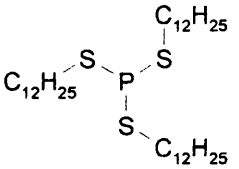

Weston 430

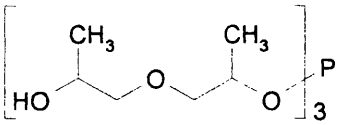

Amino Acids (I)

Sample	Conc (ppm)	Mass of sample (g)	Mass lost (g)	Mass lost (%)	Average loss (%)	Stability factor
Asparagine (L)	5530	100.2 97.8 101.7	46.6 47.4 51.7	46.5 48.5 50.8	48.6	-1.07
Aspartic Acid (DL)	4322	102.2 95.6 96.4	41.8 38.3 36.9	40.9 40.1 38.3	39.8	1.14
Glutamine (L)	4775	105.4 95.7 95.0	53.0 49.2 45.7	50.3 51.4 48.1	49.9	-1.10
Glutamic Acid (L)	5074	97.0 103.8 102.7	35.7 39.1 37.3	36.8 37.7 36.3	36.9	1.23
Methionine (DL)	5294	103.7 102.3 97.4	81.3 77.8 70.9	78.4 76.1 72.8	75.8	-1.67
Control	-	96.7 94.7	43.1 43.8	44.6 46.3	45.5	

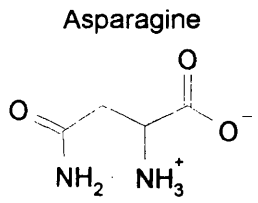

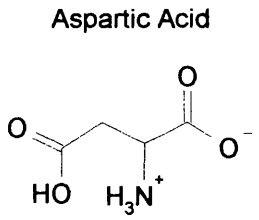

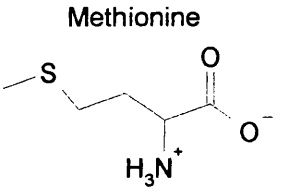

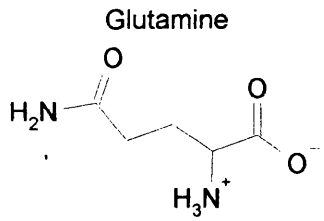

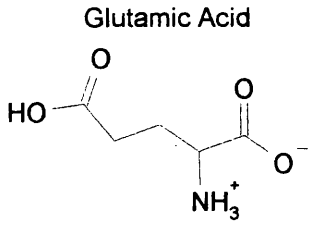

Amino Acids (II)

Sample	Conc (ppm)	Mass of sample (g)	Mass lost (g)	Mass lost (%)	Average loss (%)	Stability factor
Glycine	4893	95.4 97.7 100.2	61.7 62.5 56.3	64.7 64.0 56.2	61.6	-1.27
Alanine (DL)-α	5226	103.3 100.2 98.6	71.6 75.4 67.5	69.3 75.2 68.5	71.0	-1.47
Valine (DL)	5682	100.2 98.6 103.7	61.3 55.4 51.5	61.2 56.2 49.7	55.7	-1.15
Leucine (L)	4938	99.1 97.1	49.5 53.4	49.9 55.0	52.5	-1.08
Isoleucine (DL)	5512	100.2 100.9 98.5	53.0 50.2 51.9	52.9 49.8 52.7	51.8	-1.07
Control	-	96.2 95.5	47.0 45.7	48.9 47.9	48.4	

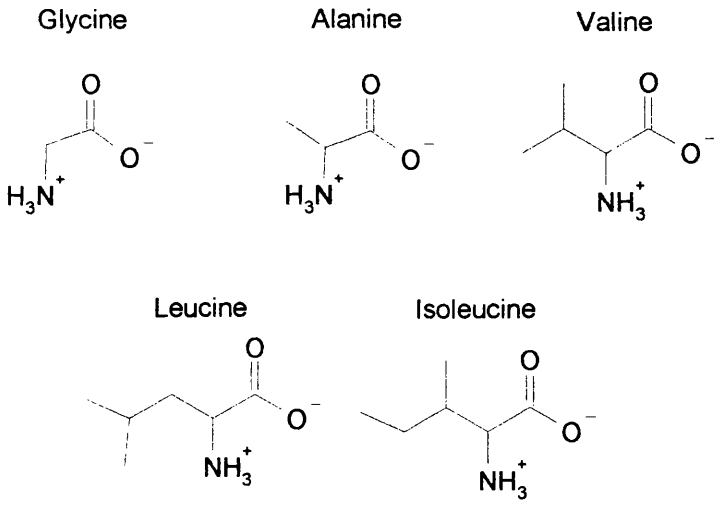

Amino Acids (III)

Sample	Conc (ppm)	Mass of sample (g)	Mass lost (g)	Mass lost (%)	Average loss (%)	Stability factor
Histidine (L) hydrochloride	6361	101.5 98.4 99.6	10.2 9.4 9.0	10.0 9.6 9.0	9.5	1.57
Phenylalanine (DL)-β	4475	98.7 103.3 100.9	24.8 24.7 21.1	25.1 23.9 20.9	23.3	-1.56
Proline (L)	6222	94.9 96.5 102.1	60.0 63.9 60.7	63.2 66.2 59.5	63.0	-4.23
Tryptophan (DL)	5068	98.9 99.1 102.1	59.9 59.7 62.0	60.6 60.2 64.8	61.9	-4.15
Tyrosine (L)	4642	97.4 97.4 105.0	44.6 45.5 45.7	45.8 46.7 43.5	45.3	-3.04
Control	-	96.8 96.0	14.2 14.4	14.7 15.0	14.9	

Histidine
mono hydrochloride

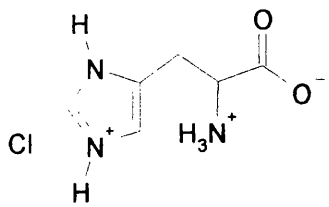

Phenylalanine

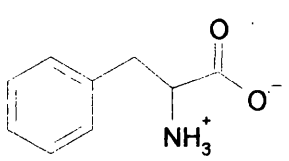

Proline

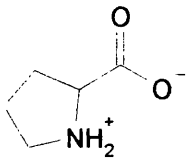

Tryptophan

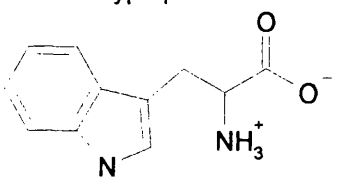

Tyrosine

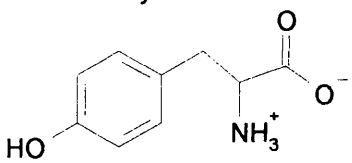

Amino Acids (IV)

Sample	Conc (ppm)	Mass of sample (g)	Mass lost (g)	Mass lost (%)	Average loss (%)	Stability factor
Argenine (L) hydrochloride	6285	100.6 96.1 101.4	49.9 49.4 50.1	49.6 51.4 49.4	50.1	1.26
Cysteine (L)	4878	96.1 101.6 102.2	58.5 57.8 54.2	60.9 56.9 53.0	56.9	1.11
Lysine (L) hydrochloride	4664	100.2 99.6 95.5	49.2 48.9 48.3	49.1 49.1 50.6	49.6	1.27
Serine (DL)	4971	97.9 98.6 96.1	82.2 84.4 77.3	84.0 85.6 80.4	83.3	-1.32
Threonine (DL)	5280	95.2 100.5 97.2	84.4 84.5 84.1	88.7 84.1 86.5	86.4	-1.36
Control	-	101.2 96.1	64.1 60.5	63.3 63.0	63.2	

Argenine
mono hydrochloride

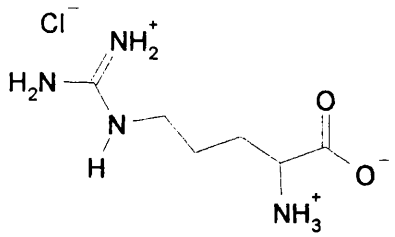

Lysine
mono hydrochloride

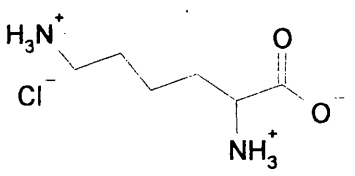

Cysteine

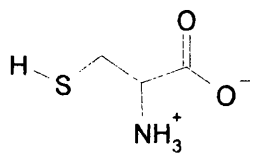

Serine

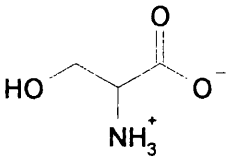

Threonine

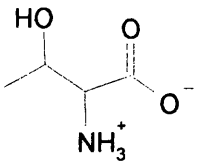

Pyromellitic anhydride type compounds

Sample	Conc (ppm)	Mass of sample (g)	Mass lost (g)	Mass lost (%)	Average loss (%)	Stability factor
1,2,4-Benzene tricarboxylic anhydride	4777	96.1 97.3 95.5	33.7 33.3 31.9	35.1 34.2 33.4	34.2	1.89
1,3,5-Benzene tricarboxylic acid	5210	99.3 95.6 99.9	18.3 17.3 18.0	18.4 18.1 18.0	18.2	3.55
1,2,4,5-Benzene tetracarboxylic acid	5964	92.9 95.8 103.5	15.2 20.1 23.3	16.4 21.0 22.5	20.0	3.23
Pyromellitic Anhydride	5424	106.7 96.0 101.5	19.0 18.7 19.3	17.8 19.5 19.0	18.8	3.43
Boric Acid	4692	96.4 99.9 97.3	33.8 33.1 35.7	35.1 33.1 36.7	35.0	1.85
Control	-	100.8 103.0	66.2 65.3	65.7 63.4	64.6	

1,3,5 Benzene tricarboxylic acid

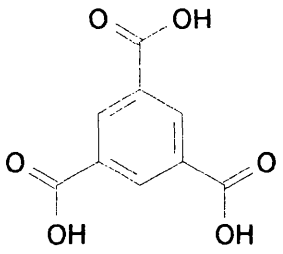

1,2,4 Benzene tricarboxylic anhydride

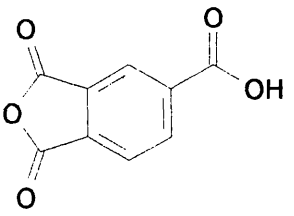

1,2,4,5 Benzene tetracarboxylic acid

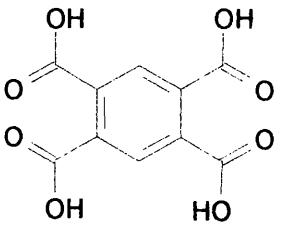

Pyromellitic anhydride

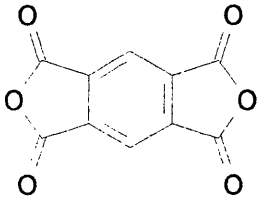

Boric acid

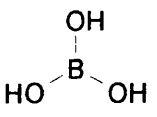

Benzene carboxylic acids

Sample	Conc (ppm)	Mass of sample (g)	Mass lost (g)	Mass lost (%)	Average loss (%)	Stability factor
Terepthalic acid	5029	94.4 102.1 104.1	48.6 52.9 55.9	51.5 51.8 53.7	52.3	1.18
Pthalic acid	5030	102.5 99.3 99.0	59.7 60.2 61.5	58.2 60.6 62.1	60.3	1.03
Isopthalic acid	4892	105.0 95.6 104.1	51.2 47.2 53.6	48.8 49.4 51.5	49.9	1.24
Benzene 1,3, disulphonic acid	7114	94.6 105.5 104.4	62.2 70.1 72.1	65.7 66.4 69.1	67.0	-1.08
1,3,5 tricarboxylic acid	5300	104.3 108.6 101.5	19.5 20.3 20.5	18.7 18.7 20.2	19.2	3.23
Control	-	95.0 99.8	57.6 63.2	60.6 63.3	62.0	

Terephthalic acid

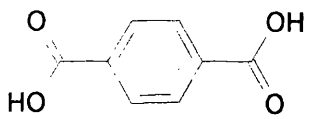

Phthalic acid

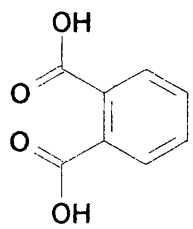

Isophthalic acid

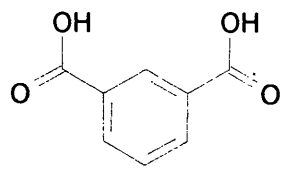

Benzene 1,3 disulphonic acid

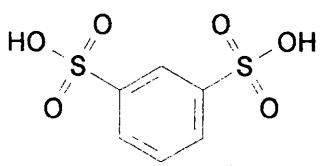

1,3,5 Benzene tricarboxylic acid

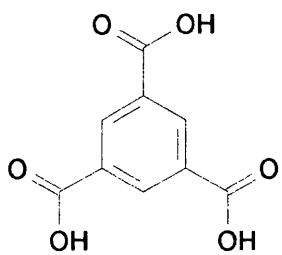

Aliphatic dicarboxylic acids

Sample	Conc (ppm)	Mass of sample (g)	Mass lost (g)	Mass lost (%)	Average loss (%)	Stability factor
Oxalic acid	4999	96.1 99.1 93.3	6.7 6.4 6.2	7.0 6.5 6.6	6.7	4.75
Succinic acid	4853	98.2 98.2 95.6	23.7 21.3 21.7	24.1 21.7 22.7	22.8	1.39
Glutaric acid	5049	99.2 99.8 98.1	21.0 23.5 23.9	21.1 23.5 25.0	23.2	1.37
Adipic acid	4575	97.0 97.8 98.1	29.9 28.6 28.6	30.8 29.2 29.2	29.7	1.07
Sebacic acid	5505	100.3 99.9 98.1	33.8 36.1 34.2	34.0 36.1 34.8	35.0	-1.10
Control	-	97.0 93.5	30.4 30.2	31.3 32.3	31.8	

Oxalic acid	HOOC-COOH
Malonic acid	$HOOC(CH_2)COOH$
Succinic acid	$HOOC(CH_2)_2COOH$
Glutaric acid	$HOOC(CH_2)_3COOH$
Adipic acid	$HOOC(CH_2)_4COOH$
Sebacic acid	$HOOC(CH_2)_8COOH$

Various inorganic salts

Sample	Conc (ppm)	Mass of sample (g)	Mass lost (g)	Mass lost (%)	Average loss (%)	Stability factor
Magnesium sulphate ($MgSO_4$)	5153	98.3 103.6 100.8	31.9 33.2 36.2	32.5 32.0 35.9	33.5	1.70
Magnesium chloride ($MgCl_2$)	5082	101.0 100.4 98.1	98.5 97.7 95.6	97.5 97.3 97.5	97.4	-1.71
Sodium sulphate (Na_2SO_4)	5314	99.2 99.9 96.7	56.2 50.5 61.2	56.7 50.6 63.3	56.9	1.00
Sodium chloride (NaCl)	5366	105.0 104.0 100.2	71.4 67.2 64.6	68.0 64.6 64.5	65.7	-1.15
Potassium ferricyanide ($K_3Fe(CN)_6$)	5405	106.2 94.5 103.8	82.0 63.3 67.0	77.2 67.0 64.5	65.8	-1.22
Control	-	94.8 102.1	53.4 58.9	56.3 57.7	57.0	

Sulphate with various cations

Sample	Conc (ppm)	Mass of sample (g)	Mass lost (g)	Mass lost (%)	Average loss (%)	Stability factor
Magnesium sulphate ($MgSO_4$)	5153	97.9 104.7 99.6	28.4 31.7 29.9	29.0 30.3 30.0	29.8	1.48
Sodium sulphate (Na_2SO_4)	5314	93.0 104.9 102.4	42.7 51.9 48.7	45.9 49.5 47.6	47.7	-1.08
Iron (II) sulphate ($FeSO_4$)	4985	101.8 101.6 98.3	34.6 36.5 34.9	34.0 35.9 35.5	35.1	1.25
Copper (II) sulphate ($CuSO_4$)	5030	102.9 103.0 94.3	72.6 71.1 67.3	70.6 69.0 71.3	70.3	-1.60
Nickel (II) sulphate ($NiSO_4$)	5018	101.9 104.5 99.4	43.0 41.2 37.6	42.2 39.4 37.8	39.8	1.11
Control	-	97.7 101.8	44.0 43.9	45.0 43.1	44.1	

Food grade antioxidants

Sample	Conc (ppm)	Mass of sample (g)	Mass lost (g)	Mass lost (%)	Average loss (%)	Stability factor
Ascorbic acid (Vitamin C)	5107	101.4 98.7 97.2	16.4 16.0 17.0	16.2 16.2 17.4	16.6	1.44
BHT	5253	97.4 100.0 102.2	47.3 56.7 64.5	48.6 56.7 63.1	56.1	-2.34
propyl gallate	4868	102.2 96.2 97.4	57.8 52.8 56.4	56.6 54.9 57.9	56.4	-2.35
octyl gallate	4909	96.3 93.7	59.6 58.4	61.9 62.3	62.1	-2.59
dodecyl gallate	4695	100.6 97.5	64.2 61.5	63.8 63.1	63.5	-2.65
Control	-	90.6 99.4	27.0 18.0	29.8 18.1	23.9	

Ascorbic acid

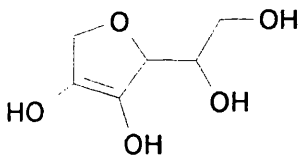

BHT

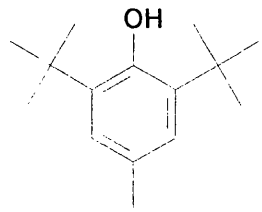

Propyl gallate

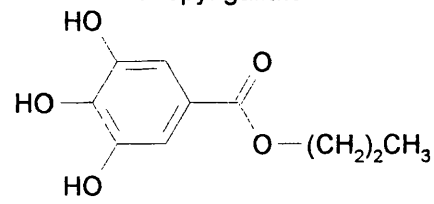

Octyl gallate

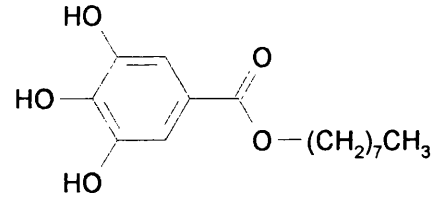

Dodecyl gallate

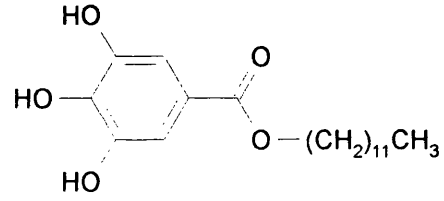

Ascorbic acid related compounds

Sample	Conc (ppm)	Mass of sample (g)	Mass lost (g)	Mass lost (%)	Average loss (%)	Stability factor
Ascorbic acid	4925	100.5 102.5 96.9	21.0 22.9 21.0	20.1 22.4 21.7	21.4	1.79
Ascorbyl palmitate	4960	93.6 103.1 103.4	27.5 37.2 36.6	29.4 36.1 35.4	33.6	1.14
Sodium ascorbate	5223	94.8 104.1	78.6 102.4	82.9 98.4	90.7	-2.36
Sodium erythorbate	5411	95.3 102.7 98.3	93.4 100.8 96.4	98.0 98.1 98.1	98.1	-2.55
'Pyroneg'	4789	104.6 97.6 100.4	102.5 95.5 98.2	98.0 97.8 97.8	97.9	-2.55
Control	-	102.4 98.2	38.8 38.1	37.9 38.8	38.4	

Ascorbic acid

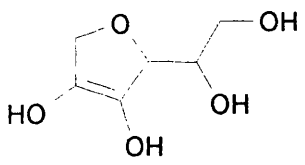

Ascorbyl palmitate

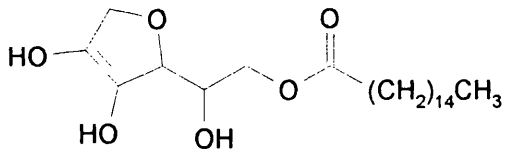

Sodium Ascorbate

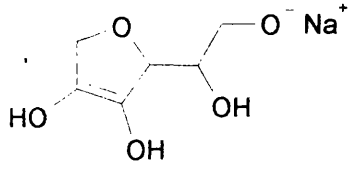

Sodium erythorbate

enantiomer of sodium ascorbate

Tartaric acid stereoisomers and another food grade additive

Sample	Conc (ppm)	Mass of sample (g)	Mass lost (g)	Mass lost (%)	Average loss (%)	Stability factor
L-Tartaric acid (natural)	5576	94.7 101.2	14.8 14.4	15.6 14.2	14.9	2.93
DL-Tartaric acid	5866	99.6 98.1 101.2	12.0 12.1 12.1	12.0 12.3 11.5	11.9	3.68
D-Tartaric acid (unnatural)	4880	96.7 96.3	17.4 14.9	18.0 15.5	16.8	2.61
Thiodipropionic acid	5741	105.3 97.7 92.7	18.7 20.2 15.2	17.8 20.6 16.4	18.3	2.39
Irganox PS802	5334	98.0 97.8 99.7	9.2 9.1 10.5	9.4 9.3 10.5	9.7	4.52
Control	-	95.1 103.0	41.7 45.1	43.8 43.8	43.8	

Tartaric acid

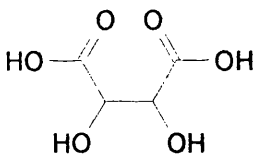

Thiodipropionic acid

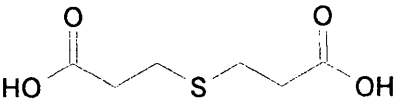

Irganox PS802

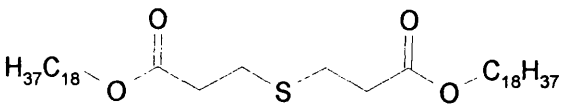

Rationalisation of structure to stabilisation efficiency

The oil bath work identified many additives that possess stabilising effects and on observation it is possible to separate the active stabilisers into materials with four main types of functional groups.

(a) phosphite type compounds
(b) carboxylate groups (carboxylic acid or ester linkages)
(c) OH or other groups with H-bonding potential
(d) ether type links

(a) Phosphite type compounds

Phosphites are used widely in PVC, polyolefins and polyaldehyde and are thought to act as peroxide decomposers. However, in the case of PHB there is little evidence to suggest that peroxides play a major role in the degradation.

It will be the case that the central phosphorus atom of the phosphite is electrophilic and may co-ordinate to the oxygen of the carbonyl groups in the main polymer system.

This may also be the case with boric acid which also displays electrophilic tendencies i.e.

$$B(OH)_3 + H_2O \rightarrow B(OH)^-_4 + H^+$$

Notably one phosphite compound demonstrated a prodegradant effect, Irgafos 168. The phosphorus atom in this compound is surrounded by aromatic and tertiary butyl groups, making the phosphorous atom very stearically hindered.

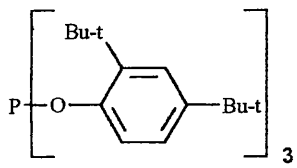

Irgafos 168

(b) Compounds containing carboxylate groups

It has been established that many compounds that contain a carboxylate type group can lead to improved stability in terms of the weight loss experiments. This group can be in the form of an ester, carboxylic acid or anhydride. e.g. succinic acid, succinic anhydride and dimethyl succinate all show stabilising properties. Here, the acid shows a greater stabilising effect than the anhydride which, in turn, shows a greater stabilising effect than the ester which has only a minimal effect.

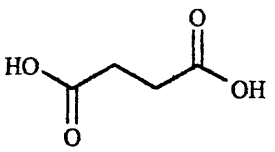

Succinic acid

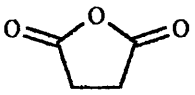

Succinic anhydride

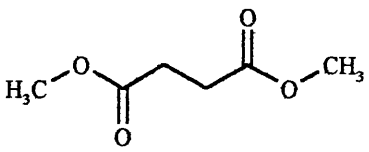

Dimethyl succinate

It is apparent that compounds with more than one carboxylate group are more effective than compounds with just one. i.e. Lauric acid ($C_{11}H_{23}COOH$) is less effective than succinic acid. Poly(acrylic acid) and poly(methyl methacrylate) which have large numbers of carboxylate groups per molecule also fall into this category.

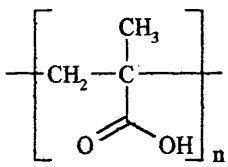

poly acrylic acid

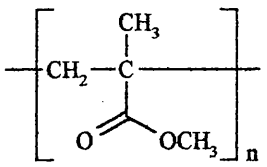

poly methyl methacrylate

It would also appear that the structure of these compounds is also very important. The orientation of the carboxylate groups has to be such that the single bonded oxygen atom of the groups are directed away from the centre of the molecule such as in Irganox PS802, but not like Irganox 1010. There are exceptions to this such as some of the Tinuvin additives which would be predicted to be stabilisers, but it is thought that there may be some

prodegradant functionality in these large molecules that offset the small stabilising functionality.

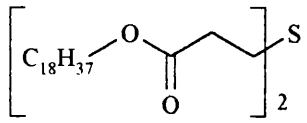

Irganox PS802

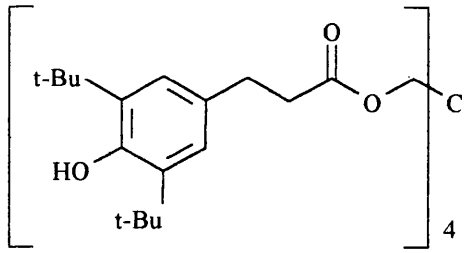

Irganox 1010

Benzene carboxylic acids

Benzene carboxylic acid compounds show large stabilising effects. A preliminary test demonstrated that the number of acid groups and their position on the benzene ring played a large role in the stabilising effect.

The effect of the positioning of the functional groups on the benzene ring was examined in an oil bath experiment using various suitable compounds. The *ortho*, *meta* and *para* isomers of benzene dicarboxylic acid were compared along with 1,3,5-benzene tricarboxylic acid and 1,3-benzene disulphonic acid.

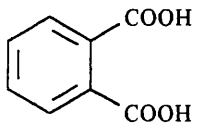

ortho
(pthalic acid)

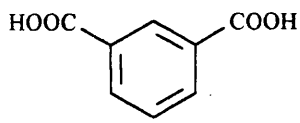

meta
(isopthalic acid)

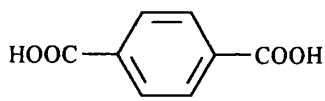

para
(terepthalic acid)

The results (*see p115*) show that the dicarboxyl compounds work best when the functional groups are in the meta position. However, the trifunctional acid was far superior and the deprotonated sulphonic acid showed no stabilising effect.

When these findings are added to the results of previous experiments a pattern begins to emerge. The meta position appears to be the most effective: the di-acid has only one such meta 'gap', the tetra-acid has two such gaps and the

tri-acid has three. Pyromellitic dianhydride may also fit into this category as it is similar to the tetra-acid with only two 'meta gaps' but it is much more effective at preventing weight loss. It is possible this may be due to the C=O groups being fixed and not free to rotate as in the acids.

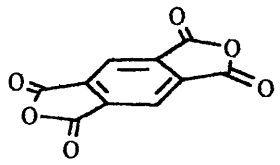

Pyromellitic dianhydride

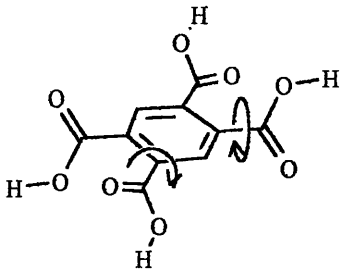

1,2,4,5 benzene tetracarboxylic acid

These experiments seem to indicate that the mechanism is very dependent upon the structure of the molecules involved suggesting that the stabilisers may be binding atoms or acting as a catalyst on the main polymer bulk.

Aliphatic dicarboxylic acids

A similar set of experiments was carried out for various chain length aliphatic dicarboxylic acids:

Oxalic acid	HOOC-COOH
Malonic acid	$HOOC(CH_2)COOH$
Succinic acid	$HOOC(CH_2)_2COOH$
Glutaric acid	$HOOC(CH_2)_3COOH$
Adipic acid	$HOOC(CH_2)_4COOH$
Sebacic acid	$HOOC(CH_2)_8COOH$

The results (*see p116*) show that oxalic acid is the most effective with the effectiveness of the additive decreasing with increasing chain length. This again indicates that the structural properties of the additives are very important.

Stereochemical effects

It has been demonstrated that not only the chemical nature of the functional groups and the structure of an additive affects its stabilising ability, but also its stereochemistry.

This was successfully demonstrated in an experiment comparing the various stereoisomers of tartaric acid.(*see p121*)

Tartaric acid is a symmetrical molecule with a chiral centre in each half. Thus it has three stereoisomers: R,R; S,S and S,R, also known as L, D and DL.

Although each showed a large stabilising effect, the DL stereoisomer was the most effective followed by L then D.

It is unsurprising that the stereoisomers have different effects as biologically produced PHB has every repeat unit configured in its R form. Hence it is clear that potential additive that is optically active must have its other stereoisomers tested also.

(c) Compounds containing OH or other H-bonding functionality

Another group of compounds that act as stabilisers also became apparent in these tests. It would appear that they have the ability to form some sort of hydrogen bond. Most notable is tartaric acid, which shows an extremely large effect, especially when compared to its dicarboxylic acid equivalent, succinic acid. Sorbitol has only OH functionality. Histidine and other amino acids that show stabilising effects also have either OH or NH groups present.

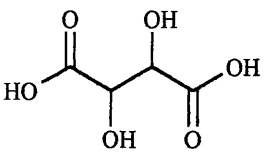

Tartaric acid

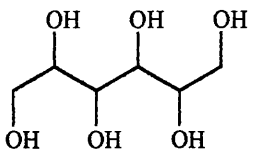

Sorbitol

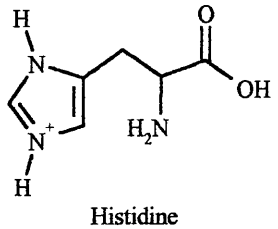

Histidine

(d) ***Compounds with ether type linkages***

It is clear that ether type functionality also has an effect as this is the only functionality present on polyethylene glycol. This type of fuctionality is also present in Irganox 1520D, Irganox PS802 and thiodipropionic acid (*see p119*).

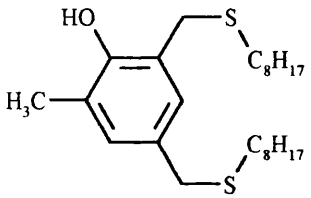

Irganox 1520D

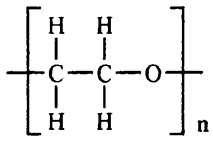

Polyethylene glycol

With the additives falling into these apparent categories, only a selection were used in further studies. For the MFI apparatus (*see p128*) a large number were used, but for further experiments these were narrowed down to five: Irganox PS802, oxalic acid, magnesium sulphate, pyromellitic dianhydride and Weston TLTTP. It was felt that these were the most effective and representative of the above chemical functionalities.

Melt Flow Index (MFI) measurements

The oil bath experiments (*see p89*) are dependant upon the weight loss of volatile products from the bulk polymer. This only happens at high degrees of degradation which may not satisfactorily represent the situation in an industrial process. The melt flow indexer (MFI) is a piece of apparatus for assessing the progress of degradation of a polymer in an environment similar to that of processing equipment. It was originally developed by ICI and accepted as a British standard[58]. A number of samples were tested using this apparatus to examine if the results from the oil bath experiments held any relevance to the performance of the additives in more realistic conditions.

The melt flow index apparatus consists of a barrel that is loaded with polymer and heated to the desired temperature. The polymer melt is then forced out through a die forming a 'lace' which is cut and weighed at regular intervals. This gives a series of weight measurements representing the quantity of polymer extruded each minute. As the experiment proceeds the polymer degrades, reducing its viscosity, hence more lace will be extruded. This decreasing viscosity gives rise to an exponential growth of the mass of polymer extruded.

Conventionally, there are two values obtained from this data: the melt flow index (MFI) and doubling time (Td). The melt flow index (MFI) is an indication of the flow rate of the polymer and is measured in grams per ten minutes. In the case of PHB it is impossible to obtain MFI values by cutting the extruded lace every ten minutes, because the polymer degrades so rapidly that most of the sample will be extruded in this time. Instead, the extruded lace is cut every minute and its weight multiplied by a factor of ten to obtain the desired units of measurement. Generally, the MFI at 5 minutes is quoted (MFI_5): to give an indication of the initial flow rate of the polymer melt. This is calculated by plotting the logarithm of the MFI values and the resulting line is extrapolated back to give the value at 5 minutes. The doubling time (Td) is the time taken for the MFI to double and is a measure of the rate of degradation. This can also be readily determined from the logarithmic graph.

The above method works on the assumption that the curve is of the form $y = A\,e^{kt}$, however, when experimental error is taken into account this is very rarely the case. If the curve for this data is adjusted by a constant, i.e. the curve is shifted vertically, then the resulting logarithmic plots will show noticable curvature, thus making the Td value inaccurate when determined from the best fit straight line. This fitted line also affects the MFI_5 value but the timing of the experiment is even more critical. The problem is actually determining the start of the experiment: the polymer is loaded into a hot piece of apparatus and it takes around 30 seconds to load the sample so clearly it is very difficult to determine the exact starting time of the experiment. This means that the MFI_5 value may not actually be the MFI value at five minutes but with a timing error of, say, ±10 seconds which can make large differences to the actual value if the graph is steep. The timing error does not affect the rate constant hence the Td values are also unaffected.

i.e. if the equation is of the form

$$y = A\,e^{kt}$$

and we include an error in determining the start of the experiment

$$y = A\,e^{k(t+d)}$$

expanding: $y = A\,e^{kt}\,e^{kd}$

e^{kd} will be constant and can be incorporated into the coefficient A, resulting in an equation of the same form as the initial one.

The MFI system is satisfactory for polymers with low flow rates and low rates of degradation where, relatively speaking, the errors encounterd are minor but it does not work well with PHB because the experiment is short making any errors relatively large.

The Kedzy Swinbourne method (*see p64*) could be used here as it will allow us to determine the rate constant for a first order curve without knowledge of the starting or endpoint values but it has been discovered that there are many

computer programs available, such as Fig.P. or Sigmaplot, that are able to calculate the parameters for any desired equation to obtain a best fit for the data. So if we assume the curve is a first order growth we can put in extra variables to compensate for any uncertainty.

Following is a comparison of the curves calculated by these various methods. It demonstates that we must be very careful when choosing the method that is used for the curve fitting. The conventional method for fitting an exponential curve, and that taken by the MFI method, is as follows:-

It is assumed the equation is of the form $y = A\,e^{kt}$

and if we take the logarithm of this equation we end up with a linear form upon which we can calculate a best fit straight line by least squares.

$$\ln(y) = \ln(A) + kt$$

When the values from this are taken and used to plot the curve against the original experimental data it can be seen that the curve deviates more from the points with larger y values than those with small y values. This is because the parameters of the curve have been determined by minimising the logarithms of the values and hence the calculated errors are proportional to the original y value. i.e. the curve has been calculated by minimising the percentage differences from the original data. This is unlike the method employed by the computer program which minimises the actual differences between the original data and the curve via a Newton-Rhapson method that varies the parameters of the desired equation. However, it can be seen that the form of the equation that allows for a y- shift in the curve produces the most acceptable line and it is felt that this will produce more accurate rate constants.

Figure 3.7 *Comparison of different curve fitting methods for control sample at 180°C in MFI apparatus*

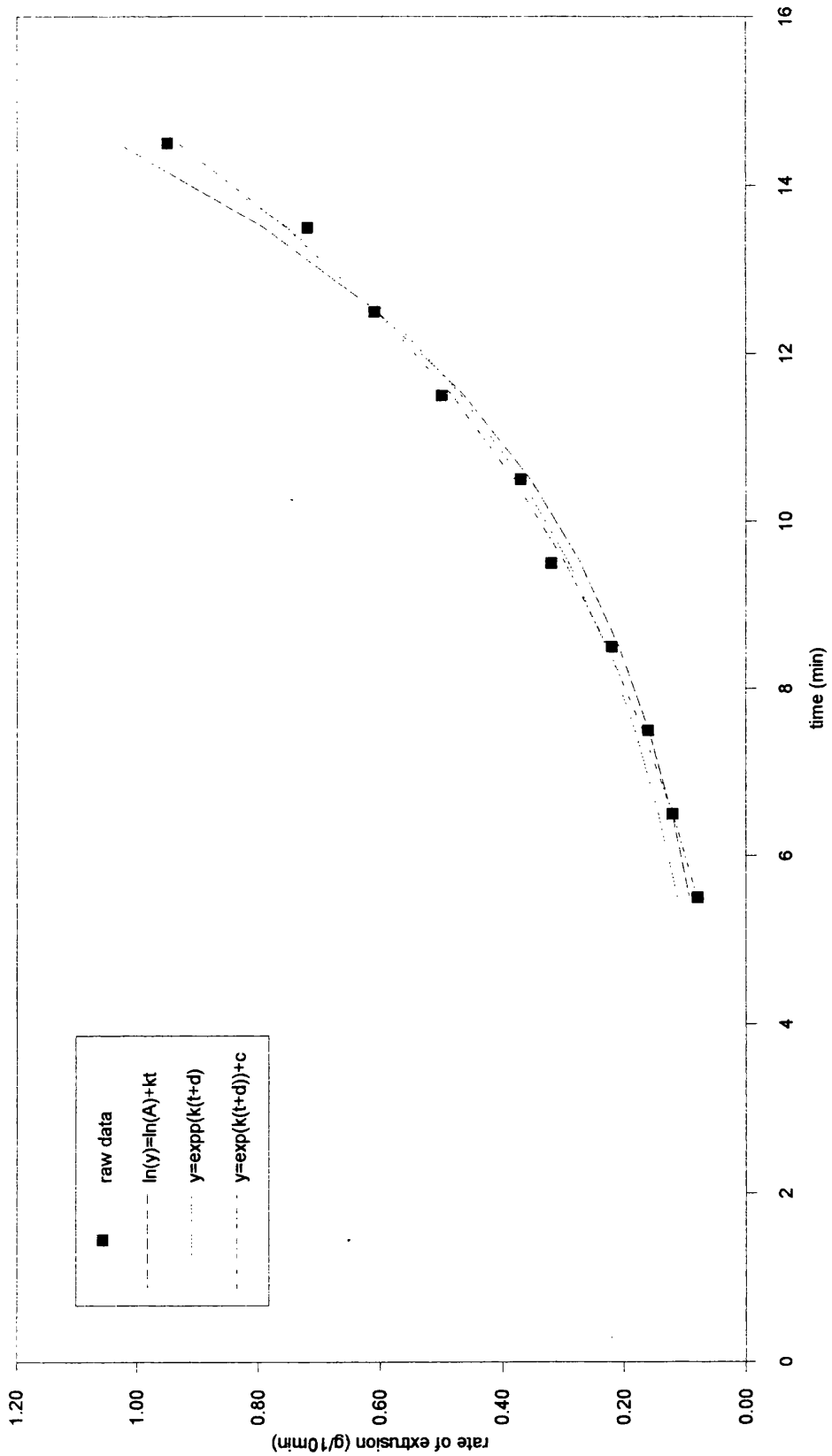

The whole procedure was carried out for a representative selection of the additives tested in the oil bath experiments in an attempt to find some correlation between the two methods. A valerate copolymer was used (PB22A) for these experiments rather than the homopolymer because it has a lower melting point and is more manageable in the MFI apparatus - it will begin to flow before any significant degradation has taken place. The nature of the copolymer is very similar to that of the homopolymer so it is unlikely that there will be significant differences in the effect of the additives upon them.

The best fit curves have been calculated for all the samples examined in the MFI apparatus (*see tables 3.10 and 3.11*) and an attempt has been made to rationalise the results from this.

On comparing the calculated rate constants with the molecular weight measurement of the five minute cut-off (*see figures 3.8 - 3.11*) there is still no apparent trend, but this is hardly surprising if the expected error for the molecular weight measurements (±50,000) are taken into account.

Plots using the stabilising factor for the oil bath experiments (*see figures 3.13 - 3.15*) would seem to be better, but again the measurement of the stabilising factor is subject to large error when comparing factors from different experiments. The results at 180°C are similar whichever method is used but the 190°C results do show some trend.

To sum up, it would seem that there is far too much uncertainty in the experimental results to obtain useful comparisons though a few general trends can be seen.

Table 3.8 Raw data from MFI experiments at 190°C

Additive	Conc.	rate of extrusion (g/min) at time t(min)													
	(ppm)	5.5	6.5	7.5	8.5	9.5	10.5	11.5	12.5	13.5	14.5	15.5	16.5	17.5	18.5
Control	0	0.41	0.72	1.18											
Control	0	0.40	0.72	1.17	1.71										
Benzene tricarboxylic acid	2500	0.24	0.41	0.65	0.94	1.39									
Benzene tricarboxylic acid	2500	0.23	0.39	0.63	0.91	1.30									
Chimasorb 119FL	2500	0.43	0.84	1.31											
Glutamic Acid (L)	2500	0.38	0.70	1.05	1.51										
Glutamine (L)	2500	0.56	1.31	2.70											
Histidine (L) mono hydrochloride	2500	0.24	0.39	0.67	1.10										
Irganox 1010	2500	0.36	0.67	1.14	1.73										
Irganox PS802	2500	0.36	0.67	1.12	1.65										
Lauric acid	2500	0.52	0.93	1.39											
Methionine (DL)	2500	1.23	2.92												
PMMA high mw	2500	0.31	0.62	1.01	1.46										
Pyromellitic dianhydride	2500	0.14	0.21	0.34	0.52	0.75	1.02	1.34							
Succinic Acid	2500	0.23	0.43	0.69	0.94	1.38									
Tartaric acid (DL)	2500	0.28	0.48	0.75	1.01	1.46									
Tinuvin 622LD	2500	0.31	0.58	0.96	1.56										
Weston 430	2500	0.30	0.56	0.95	1.40										
Weston 600	2500	0.33	0.59	1.00	1.43										
Weston 619F	2500	0.39	0.70	1.00	1.27										
Weston PNPG	2500	0.41	0.74	1.17	1.75										
Weston TLTTP	2500	0.41	0.71	1.07	1.54										
Benzene tricarboxylic acid	5000	0.30	0.51	0.83	1.15	1.57	***								
PMMA high mw	5000	0.31	0.52	0.87	1.31										
Pyromellitic dianhydride	5000	0.26	0.43	0.69	1.01	1.39									
Weston 430	5000	0.37	0.68	1.03	1.54										
Weston 600	5000	0.30	0.56	0.91	1.52										
Weston 619F	5000	0.38	0.64	1.05	1.72										
Weston TLTTP	5000	0.32	0.55	0.82	1.16										

Table 3.9 Raw data from MFI experiments at 180°C

Additive	Conc	rate of extrusion (g/min) at time t(min)													
	(ppm)	5.5	6.5	7.5	8.5	9.5	10.5	11.5	12.5	13.5	14.5	15.5	16.5	17.5	18.5
Control	0	0.08	0.12	0.16	0.22	0.32	0.37	0.50	0.61	0.72	0.95				
Benzene tricarboxylic acid	2500	0.06	0.08	0.11	0.14	0.17	0.22	0.27	0.34	0.41	0.49	0.64	0.69		
Chimasorb 119FL	2500		0.16	0.22	0.32	0.43	0.58	0.75	0.91						
Lauric acid	2500	0.08	0.11	0.16	0.23	0.32	0.44	0.56	0.71	0.98					
PMMA high mw	2500	0.08	0.10	0.14	0.19			0.45	0.57	0.71	0.91				
Pyromellitic Dianhydride	2500	0.06	0.07	0.09	0.11	0.14			0.24	0.29	0.34	0.40	0.45	0.53	0.63
Tartaric acid (DL)	2500	0.06	0.08	0.10	0.12	0.16	0.20	0.26	0.33	0.42	0.49	0.58	0.70	0.80	
Weston 600	2500	0.09	0.12	0.17	0.23	0.30	0.40	0.51	0.63	0.78	1.00				
Weston 619F	2500	0.09	0.14	0.18	0.25	0.29	0.34	0.41	0.46	0.55	0.65	0.73			
Weston TLTTP	2500	0.08	0.11	0.15	0.20	0.26	0.34	0.43	0.54	0.63	0.84	1.02			
Benzene tricarboxylic acid	5000	0.07			0.16	0.22	0.29	0.39	0.51	0.63	0.81	0.97			
PMMA high mw	5000	0.08	0.10	0.15	0.20	0.26	0.35	0.46	0.57	0.71	0.84				
Pyromellitic Dianhydride (4.85g)	5000	0.08	0.10	0.14	0.20	0.27	0.36	0.46	0.58	0.68	0.87				
Tartaric acid (DL)	5000	0.07	0.09	0.12	0.15	0.22	0.31	0.43	0.60	0.76	0.90	***			
Weston 600	5000	0.08	0.11	0.14	0.20	0.26	0.34	0.44	0.63	0.77					
Weston 619F (4.80g)	5000	0.08	0.11	0.16	0.21	0.27	0.35	0.45	0.55	0.66	0.91				

Table 3.10 Parameters calculated by Fig.P. for best fit curves for 190°C data

Additive	Conc (ppm)	Parameters calculated for curve y=exp(k(t+d)) k	d	y=exp(k(t+d))+c k	d	c
Control	0	0.517	7.17	0.394	6.63	0.2307
Control	0	0.446	7.26	0.249	4.83	0.7870
Benzene tricarboxylic acid	2500	0.407	8.67	0.319	8.06	0.1989
Benzene tricarboxylic acid	2500	0.396	8.80	0.272	7.73	0.3177
Chimasorb 119FL	2500	0.516	6.96			
Glutamic Acid (L)	2500	0.414	7.47			
Glutamine (L)	2500	0.754	6.17	0.616	5.7	0.3177
Histidine (L) mono hydrochloride	2500	0.510	8.31	0.497	8.28	0.0151
Irganox 1010	2500	0.482	7.34	0.304	5.75	0.5713
Irganox PS802	2500	0.462	7.38	0.252	4.94	0.7976
Lauric acid	2500	0.463	6.77			
Methionine (DL)	2500	0.865	5.26			
PMMA high mw	2500	0.453	7.62			
Pyromellitic dianhydride	2500	0.337	10.58	0.238	9.48	0.2685
Succinic Acid	2500	0.392	8.66	0.253	7.22	0.4081
Tartaric acid (DL)	2500	0.373	8.46	0.255	7.14	0.3700
Tinuvin 622LD	2500	0.509	7.62	0.413	7.14	0.1951
Weston 430	2500	0.468	7.74	0.253	5.59	0.6817
Weston 600	2500	0.448	7.65	0.222	4.75	0.8596
Weston 619F	2500	0.341	7.71			
Weston PNPG	2500	0.448	7.22	0.285	5.53	0.5802
Weston TLTTP	2500	0.408	7.41	0.230	4.96	0.7211
Benzene tricarboxylic acid	5000	0.367	8.21	0.188	4.81	0.8447
PMMA high mw	5000	0.461	7.89	0.339	7.15	0.2666
Pyromellitic dianhydride	5000	0.383	8.59	0.238	6.89	0.4657
Weston 430	5000	0.435	7.49	0.268	5.73	0.5638
Weston 600	5000	0.517	7.69	0.459	7.45	0.1014
Weston 619F	5000	0.497	7.41	0.478	7.32	0.0374
Weston TLTTP	5000	0.396	8.09	0.200	5.39	0.7013

Table 3.11 Parameters calculated by Fig.P. for best fit curves for 180°C data

Additive	Conc (ppm)	Parameters calculated for curve y=exp(k(t+d)) k	d	y=exp(k(t+d))+c k	d	c
Control	0	0.237	14.70	0.186	14.24	0.1166
Benzene tricarboxylic acid	2500	0.201	18.07	0.158	17.91	0.0846
Chimasorb 119FL	2500	0.268	12.72	0.167	11.32	0.2982
Lauric acid	2500	0.289	13.58	0.252	13.40	0.0596
PMMA high mw	2500	0.257	14.86	0.216	14.60	0.0696
Pyromellitic Dianhydride	2500	0.167	21.21	0.136	21.28	0.0613
Tartaric acid (DL)	2500	0.195	18.40	0.149	18.03	0.1087
Weston 600	2500	0.243	14.46	0.202	14.11	0.0904
Weston 619F	2500	0.169	17.14	0.091	14.87	0.3287
Weston TLTTP	2500	0.231	15.35	0.199	15.06	0.0706
Benzene tricarboxylic acid	5000	0.241	15.50	0.202	15.14	0.8830
PMMA high mw	5000	0.237	15.06	0.172	14.49	0.1473
Pyromellitic Dianhydride (4.85g)	5000	0.240	15.00	0.178	14.50	0.1356
Tartaric acid (DL)	5000	0.275	14.69	0.224	14.40	0.0909
Weston 600	5000	0.278	14.36	0.260	14.33	0.2330
Weston 619F (4.80g)	5000	0.245	14.96	0.222	14.85	0.0386

Table 3.12 Results from MFI apparatus at 190°C

Additive	conc. (ppm)	MFI (g/10min)	Td (min)	rate constant $y=Ae^{kt}$	rate constant $y=Ae^{kt}+c$	mw of 5min cut-off (x1000)	oil bath stabilising factor
Control	0	3.18	1.31	0.517	0.394		0
Control	0	3.31	1.43	0.446	0.249	370	0
Benzene tricarboxylic acid	2500	2.06	1.60	0.407	0.319		3.55
Benzene tricarboxylic acid	2500	1.98	1.61	0.396	0.272	348	3.55
Chimasorb 119FL	2500	3.38	1.24	0.516		388	-4.01
Glutamic Acid (L)	2500	3.25	1.53	0.414		391	1.23
Glutamine (L)	2500	3.86	0.88	0.754	0.616	360	-1.09
Histidine (L) mono hydrochloride	2500	1.84	1.36	0.510	0.497	418	1.56
Irganox 1010	2500	2.91	1.32	0.482	0.304	386	-1.26
Irganox PS802	2500	2.96	1.36	0.462	0.252	408	2.74
Lauric acid	2500	4.19	1.41	0.463		369	1.13
Methionine (DL)	2500	7.98	0.80	0.865		313	1.67
PMMA high mw	2500	2.61	1.35	0.453		383	1.25
Pyromellitic dianhydride	2500	1.24	1.81	0.337	0.238	392	3.44
Succinic Acid	2500	2.07	1.59	0.392	0.253	358	1.13
Tartaric acid (DL)	2500	2.48	1.71	0.373	0.255	417	2.27
Tinuvin 622LD	2500	2.47	1.30	0.509	0.413	413	-1.49
Weston 430	2500	2.45	1.35	0.468	0.253	417	4.31
Weston 600	2500	2.71	1.41	0.448	0.222	384	4.50
Weston 619F	2500	3.52	1.78	0.341		439	3.85
Weston PNPG	2500	3.39	1.44	0.448	0.285	389	1.51
Weston TLTTP	2500	3.47	1.58	0.408	0.230	373	5.91
Benzene tricarboxylic acid	5000	2.66	1.68	0.367	0.188	348	3.55
PMMA high mw	5000	2.49	1.43	0.461	0.339	406	1.25
Pyromellitic dianhydride	5000	2.24	1.65	0.383	0.238	379	3.44
Weston 430	5000	3.11	1.48	0.435	0.268	382	4.31
Weston 600	5000	2.38	1.29	0.517	0.459	406	4.50
Weston 619F	5000	2.98	1.38	0.497	0.478	378	3.85
Weston TLTTP	5000	2.73	1.63	0.396	0.200	372	5.91

Table 3.13 Results from MFI apparatus at 180°C

Additive	conc. (ppm)	MFI (g/10min)	Td (min)	rate constant $y=Ae^{kt}$	rate constant $y=Ae^{kt}+c$	mw of 5min cutoff (x1000)	oil bath stabilising factor
Control	0	0.82	2.59	0.237	0.186	478	0.00
Benzene tricarboxylic acid	2500	0.61	3.11	0.201	0.158	526	3.55
Chimasorb 119FL	2500	1.08	2.35	0.268	0.167	472	-4.01
Lauric acid	2500	0.73	2.22	0.289	0.252	501	1.13
PMMA high mw	2500	0.70	2.51	0.257	0.216	520	1.25
Pyromellitic Dianhydride	2500	0.57	3.80	0.167	0.136	503	3.44
Tartaric acid (DL)	2500	0.58	3.15	0.195	0.149	539	2.27
Weston 600	2500	0.85	2.60	0.243	0.202	489	4.50
Weston 619F	2500	1.06	3.54	0.169	0.091	462	3.85
Weston TLTTP	2500	0.79	2.76	0.231	0.199	505	5.91
Benzene tricarboxylic acid	5000	0.65	2.60	0.241	0.202	532	3.55
PMMA high mw	5000	0.74	2.58	0.237	0.172	488	1.25
Pyromellitic Dianhydride (4.85g)	5000	0.73	2.55	0.240	0.178	516	3.44
Tartaric acid (DL)	5000	0.58	2.31	0.275	0.224	534	2.27
Weston 600	5000	0.71	2.43	0.278	0.260	506	4.50
Weston 619F (4.80g)	5000	0.78	2.65	0.245	0.222	528	3.85

Figure 3.8 *Molecular weight of the 5 minute cut-off vs. rate constant calculated by Fig.P. using $y=e^{k(t+d)}$ for 180°C data*

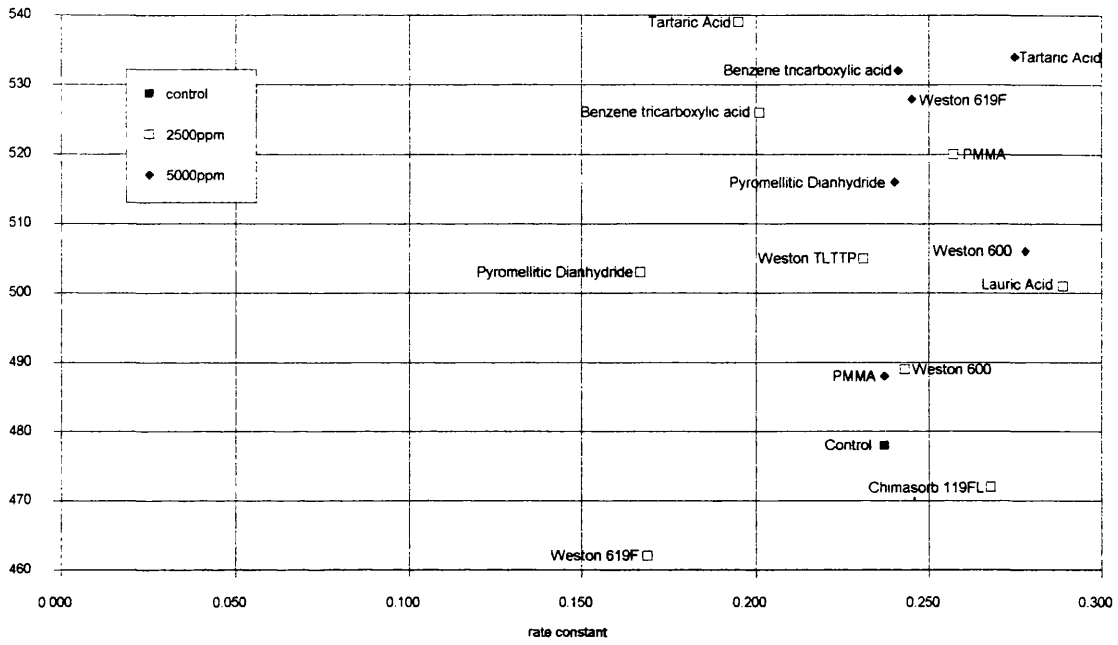

Figure 3.9 *Molecular weight of the 5 minute cut-off vs. rate constant calculated by Fig.P. using $y=e^{k(t+d)}+c$ for 180°C data*

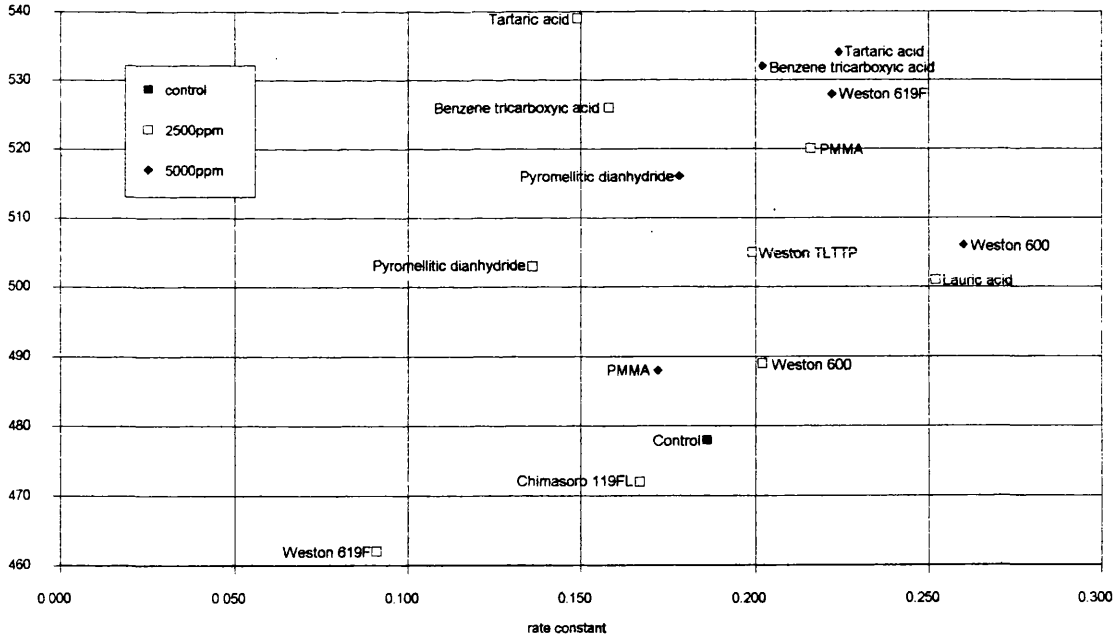

Figure 3.10 Molecular weight of 5minute cut-off vs. rate constant calculated by Fig.P. using $y=e^{k(t+d)}$ for 190°C data

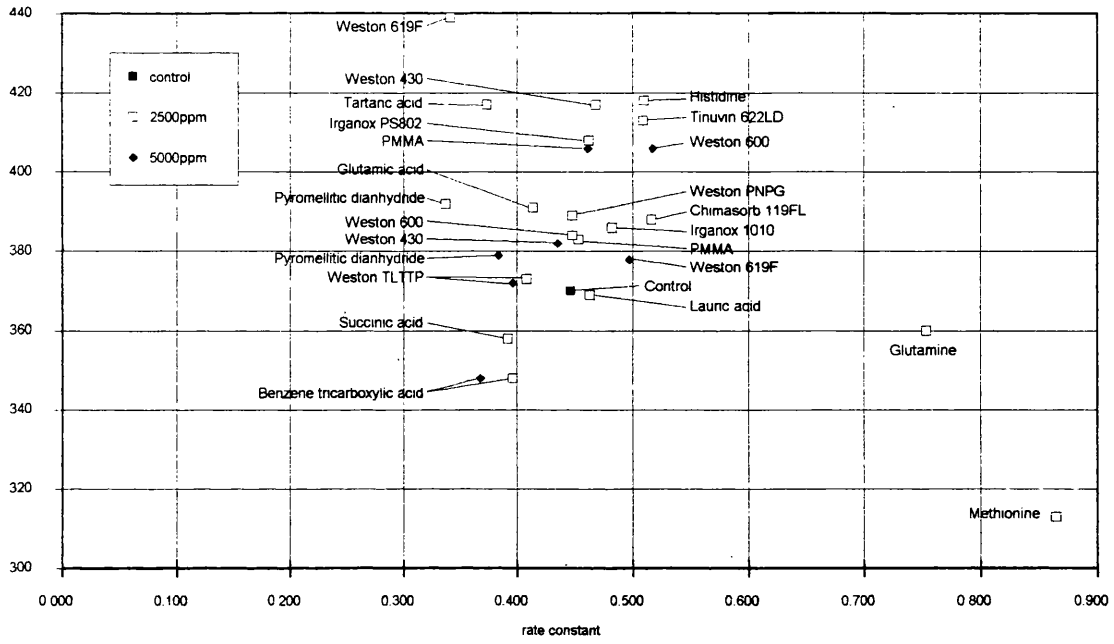

Figure 3.11 Molecular weight of 5minute cut-off vs. rate constant calculated by Fig.P. using $y=e^{k(t+d)}+c$ for 190°C data

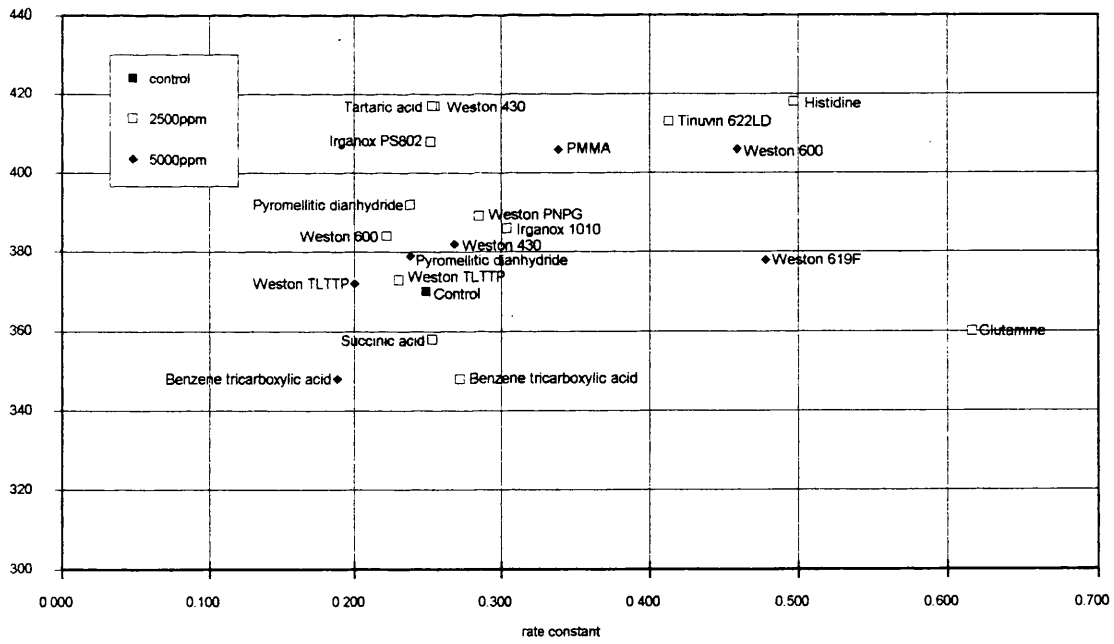

Figure 3.12 Oil bath stabilising factor vs. rate constant calculated by Fig.P. using $y=e^{k(t+d)}$ for 180°C data

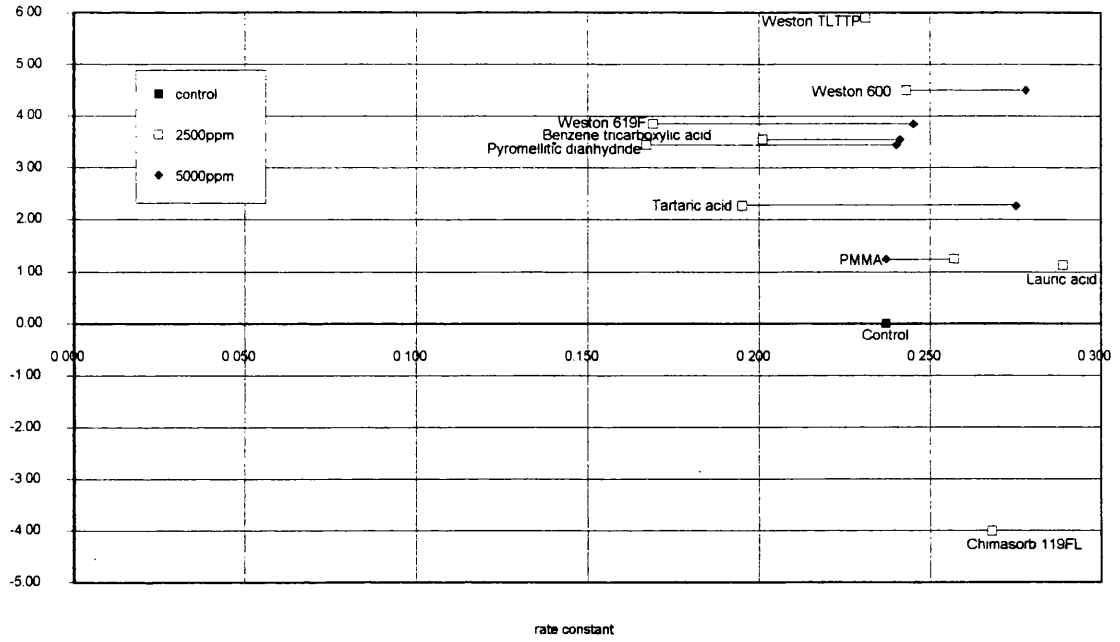

Figure 3.13 Oil bath stabilising factor vs. rate constant calculated by Fig.P. using $y=e^{k(t+d)}+c$ for 180°C data

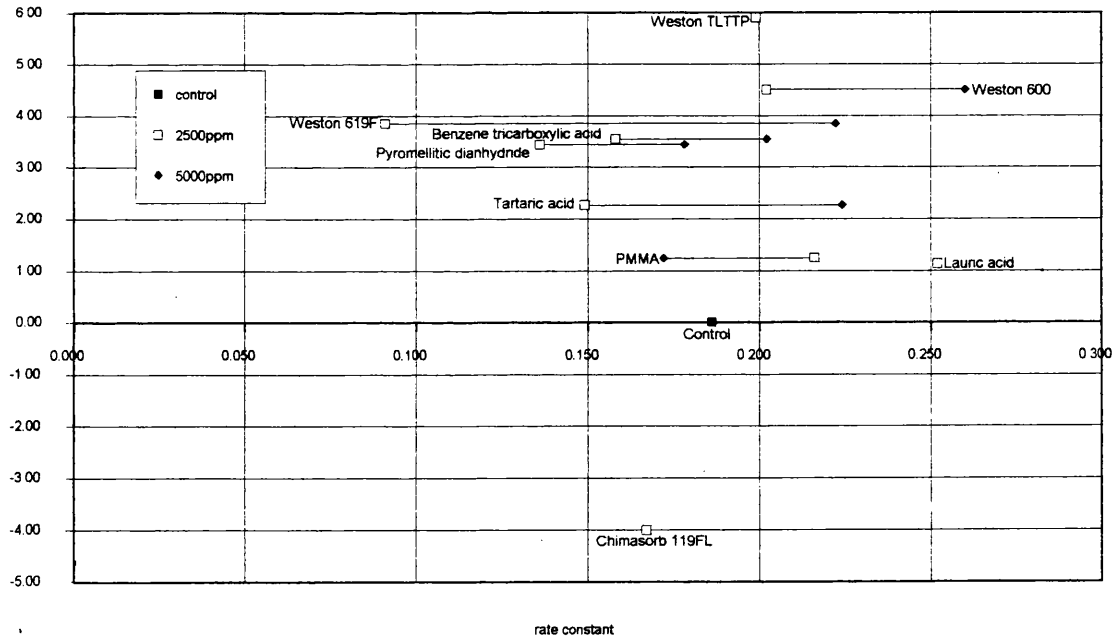

Figure 3.14 Oil bath stabilising factor vs. rate constant calculated by Fig.P. using $y=e^{k(t-d)}$ for 190°C data

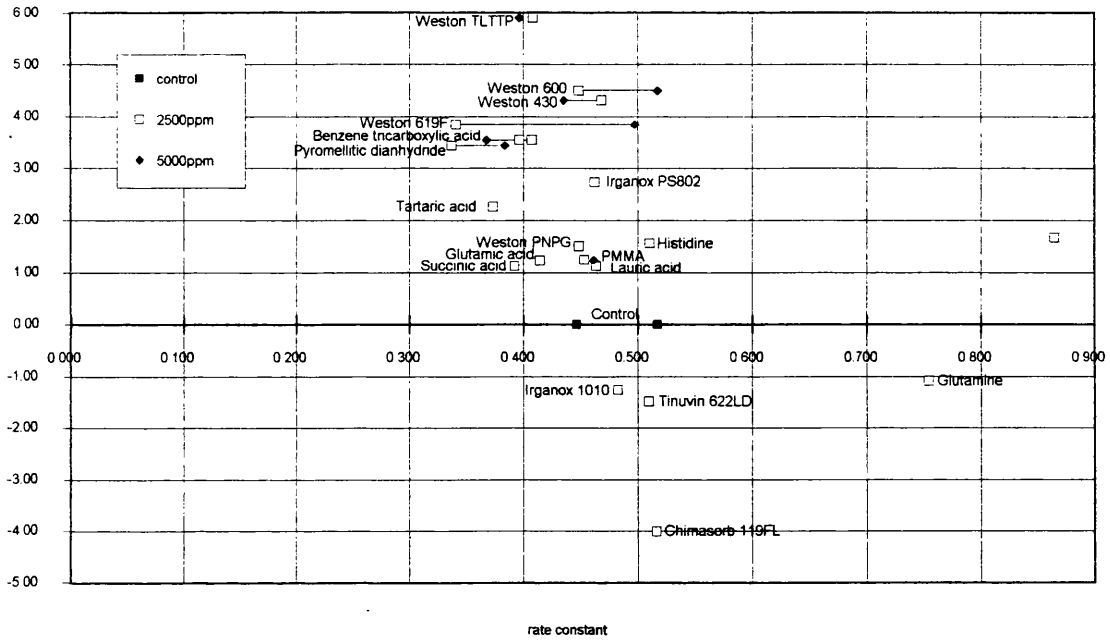

Figure 3.15 Oil bath stabilising factor vs. rate constant calculated by Fig.P. using $y=e^{k(t+d)}+c$ for 190°C data

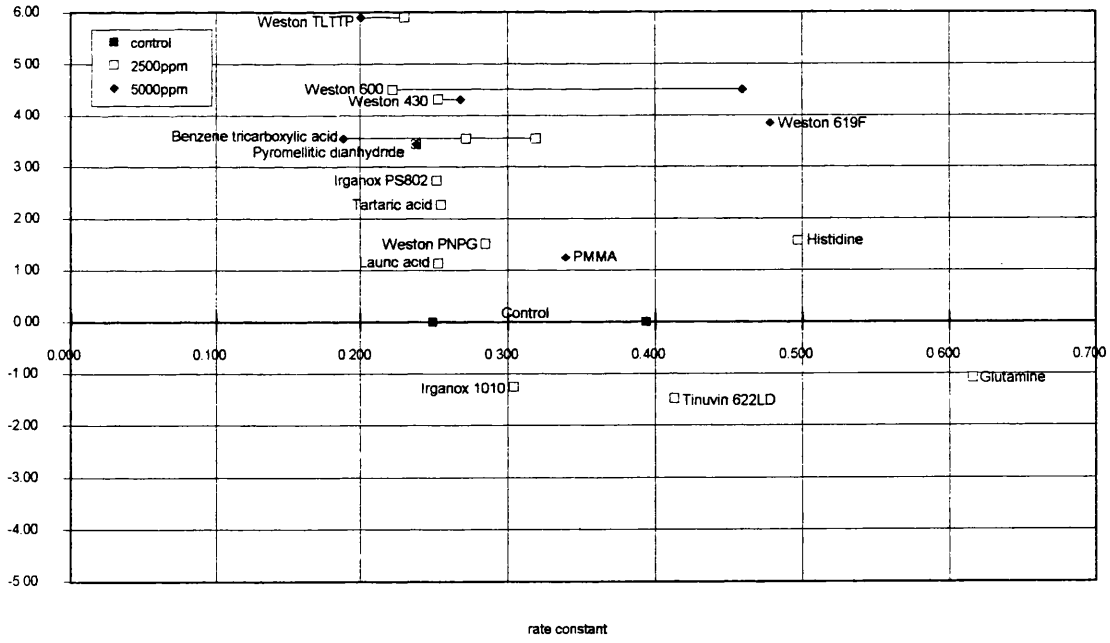

Weight loss vs. time

Initial attempts to elucidate the nature of the weight loss curve were unsuccessful as the apparatus used proved to be unreliable, producing large margins of error. A method using the oil bath apparatus was devised and used with great accuracy. The sample tubes were filled with 100mg of PHB and placed in the preheated oil bath at 200°C. A sample tube was removed every 15 minutes and weighed to ascertain the mass lost. An empty sample tube was inserted to replace the one removed to prevent anomalous eddies in the stirred oil. It had been discovered in earlier experiments that any irregularities in the flow of the stirred oil would cause uneven temperatures within the bath.

The results for PHB without additive (*see figure 3.16*) produced a very smooth curve suggesting that there was very little error in the procedure. The anomaly at 150 minutes (tube 10) was thought to be caused by a drop of silicone fluid falling from one of the other sample tubes as it was being lifted out. This curve shows remarkable similarity to the curves obtained by degrading the polymer in the heated gas cell (*see 'Degradation of PHB in heated gas cell' p54*). i.e. the rate of volatilisation increases with time then tails off as complete weight loss is approached. Therefore it can be assumed that the weight loss is due to the products observed in the heated gas cell experiments.

The experiment was repeated using PHB mixed with additive to discover if the additives affect the nature of this weight loss curve. Five additives were examined: Irganox PS802, oxalic acid, magnesium sulphate, pyromellitic dianhydride and Weston TLTTP. These were chosen to be representative of the types of additive that demonstrate stabilising effects.

Generally, the curves match that of the control, but with reduced weight loss, except for magnesium sulphate which appears to show a linear weight loss. This suggests that the polymer with magnesium sulphate added is degrading by a different mechanism to the others. Linear weight loss could be accounted for in two ways: one is that the weight loss is due to scission from the chain ends only as scission of the main chain would increase the number of ends from

which weight loss could occur thus increasing the rate of weight loss. The other is intramolecular ester exchange, in which a cyclic molecule of PHB is ejected from the main chain without a chain scission.

By drawing a first order plot([ln (A/A_0)=kt] *see p61*) for the data (figure 3.22) a rate constant was calculated for the case of each additive from the gradient of the best fit stright line, determined by the least squares method.

Table 3.14

Sample	First order rate constant (min^{-1})
Control	23.2×10^{-3}
Irganox PS802	9.4×10^{-3}
Oxalic acid	16.8×10^{-3}
Magnesium sulphate	16.4×10^{-3}
Pyromellitic dianhydride	12.3×10^{-3}
Weston TLTTP	10.5×10^{-3}

The rate contants show that the additives are performing as expected, with Irganox and Weston additives reducing the rate of degradation quite markedly.

From the figure (figure 3.22) it can be seen that the first order plot for magnesium sulphate is not linear. In the initial stages, the the rate of weight loss increases rapidly, but changes to a slower increase later on. Thus the rate constant calculated does not give a true picture of this particular degradation mechanism.

Figure 3.16 Weight loss vs. time for PHB without additive at 200°C in oil bath

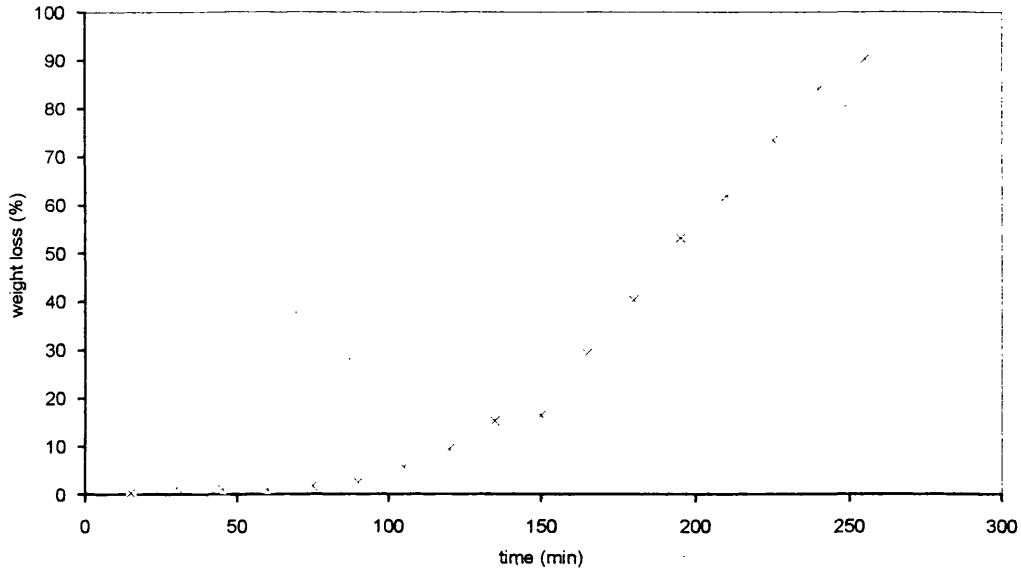

Table 3.16 Measurements from PHB degradation at 200°C in oil bath

Tube number	Heating time (min)	Initial mass of sample (g)	Mass lost on heating (g)	Mass lost (%)
1	15	0.1031	0.0004	0.4
2	30	0.0950	0.0014	1.5
3	45	0.1016	0.0011	1.1
4	60	0.1033	0.0012	1.2
5	75	0.1003	0.0018	1.8
6	90	0.1020	0.0027	2.6
7	105	0.1006	0.0058	5.8
8	120	0.1049	0.0099	9.4
9	135	0.1030	0.0158	15.3
10	150	0.1000	0.0165	16.5
11	165	0.1061	0.0312	29.4
12	180	0.0981	0.0396	40.4
13	195	0.1009	0.0537	53.2
14	210	0.1051	0.0652	62.0
15	225	0.1044	0.0767	73.5
16	240	0.0964	0.0812	84.2
17	255	0.1059	0.0957	90.4

Figure 3.17 Weight loss vs. time for PHB with 5000ppm oxalic acid at 200°C in oil bath

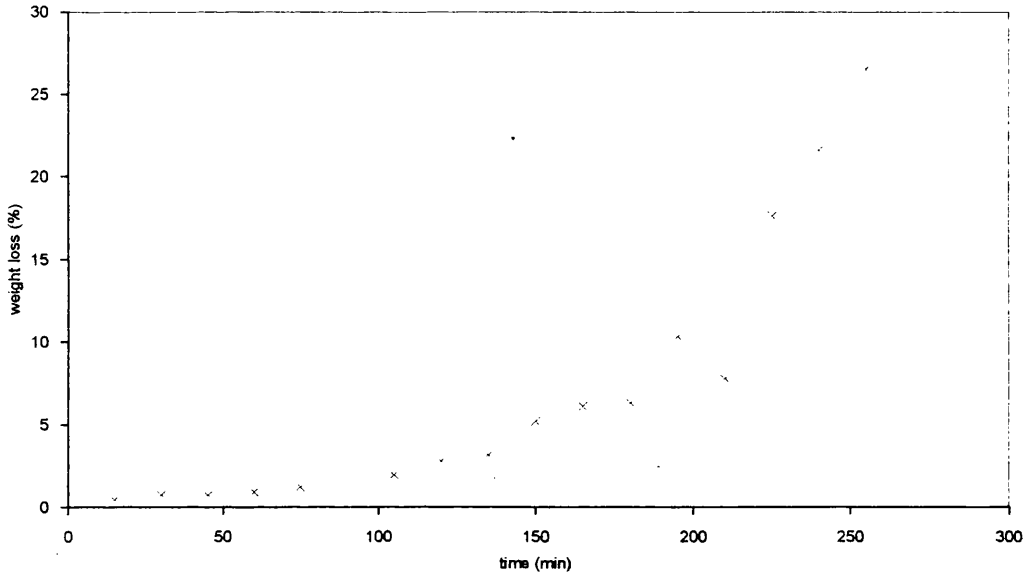

Table 3.17 Measurements taken from PHB with 5000ppm oxalic acid at 200°C in oil bath

Tube number	Heating time (min)	Initial mass of sample (g)	Mass lost on heating (g)	Mass lost (%)
1	15	0.0945	0.0004	0.42
2	30	0.0985	0.0007	0.71
3	45	0.0849	0.0006	0.71
4	60	0.0998	0.0009	0.90
5	75	0.0989	0.0012	1.21
6	90		(sample tube cracked)	
7	105	0.0985	0.0019	1.93
8	120	0.0970	0.0027	2.78
9	135	0.0954	0.0030	3.14
10	150	0.0983	0.0051	5.19
11	165	0.0981	0.0060	6.12
12	180	0.0998	0.0063	6.31
13	195	0.0998	0.0103	10.32
14	210	0.1024	0.0080	7.81
15	225	0.1033	0.0182	17.62
16	240	0.1028	0.0222	21.60
17	255	0.1025	0.0272	26.54

Figure 3.18 Weight loss vs. time for PHB with 5000ppm Weston TLTTP at 200°C in oil bath

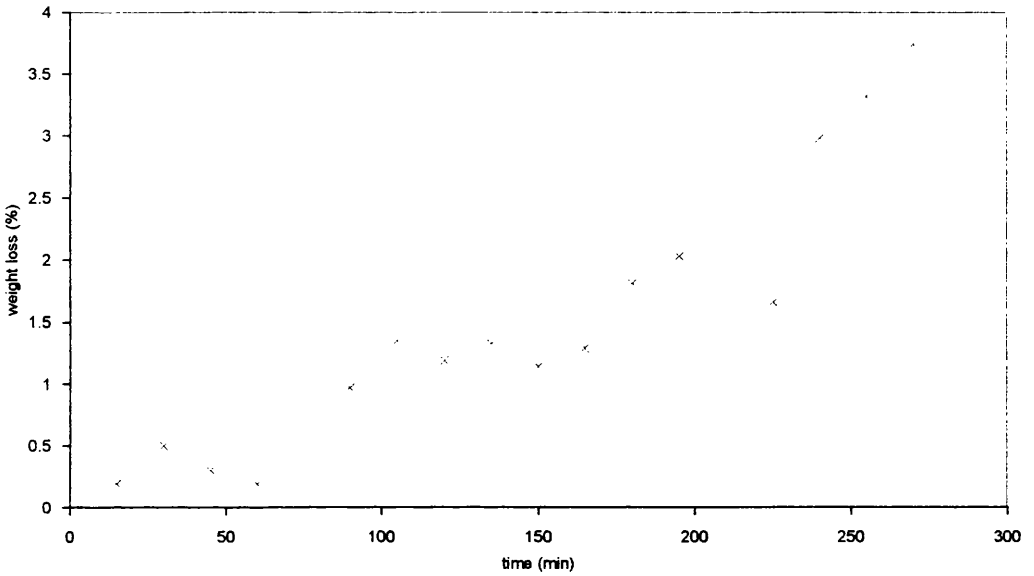

Table 3.18 Measurements taken from PHB with 5000ppm Weston TLTTP at 200°C in oil bath

Tube number	Heating time (min)	Initial mass of sample (g)	Mass lost on heating (g)	Mass lost (%)
1	15	0.1046	0.0002	0.19
2	30	0.1010	0.0005	0.50
3	45	0.1010	0.0003	0.30
4	60	0.1033	0.0002	0.19
5	75		(sample tube cracked)	
6	90	0.0929	0.0009	0.97
7	105	0.0962	0.0013	1.35
8	120	0.0926	0.0011	1.19
9	135	0.1054	0.0014	1.33
10	150	0.1057	0.0012	1.14
11	165	0.1006	0.0013	1.29
12	180	0.0996	0.0018	1.81
13	195	0.0986	0.0020	2.03
14	225	0.1087	0.0018	1.66
15	240	0.1041	0.0031	2.98
16	255	0.0965	0.0032	3.32
17	270	0.0989	0.0037	3.74

Figure 3.19 *Weight loss vs. time for PHB with 5000ppm magnesium sulphate at 200°C in oil bath (first run)*

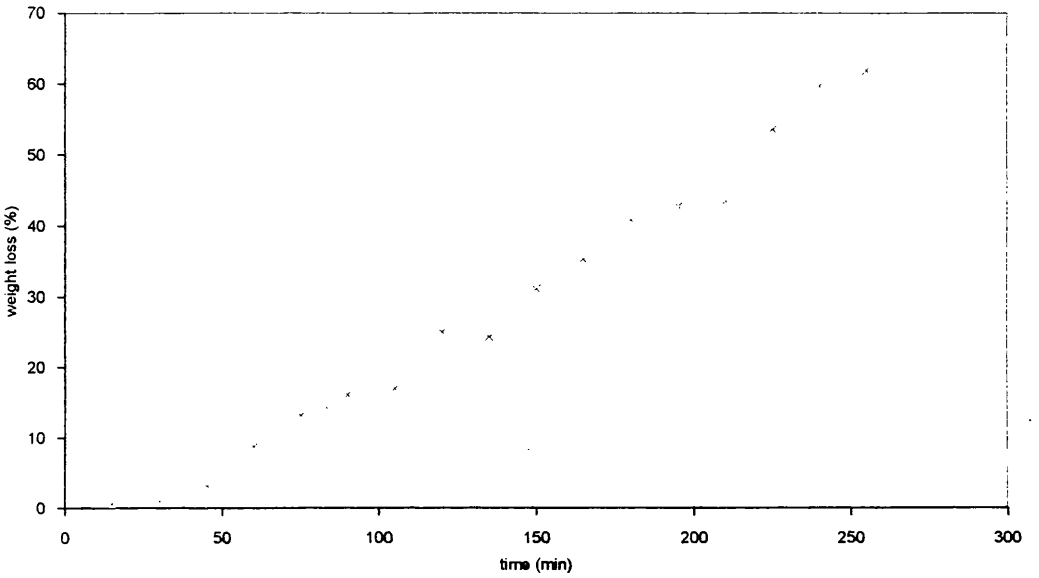

Table 3.19 *Measurements taken from PHB with 5000ppm magnesium sulphate at 200°C in oil bath (first run)*

Tube number	Heating time (min)	Initial mass of sample (g)	Mass lost on heating (g)	Mass lost (%)
1	15	0.1039	0.0006	0.58
2	30	0.0956	0.0009	0.94
3	45	0.0931	0.0029	3.11
4	60	0.1033	0.0091	8.81
5	75	0.1001	0.0132	13.19
6	90	0.0975	0.0157	16.10
7	105	0.1037	0.0176	16.97
8	120	0.0975	0.0244	25.03
9	135	0.0949	0.0231	24.34
10	150	0.1044	0.0325	31.13
11	165	0.1005	0.0355	35.32
12	180	0.0978	0.0399	40.80
13	195	0.0959	0.0410	42.75
14	210	0.1006	0.0438	43.54
15	225	0.0973	0.0521	53.55
16	240	0.1014	0.0605	59.66
17	255	0.1025	0.0635	61.95

Figure 3.20 Weight loss vs. time for PHB with 5000ppm Irganox PS802 at 200°C in oil bath

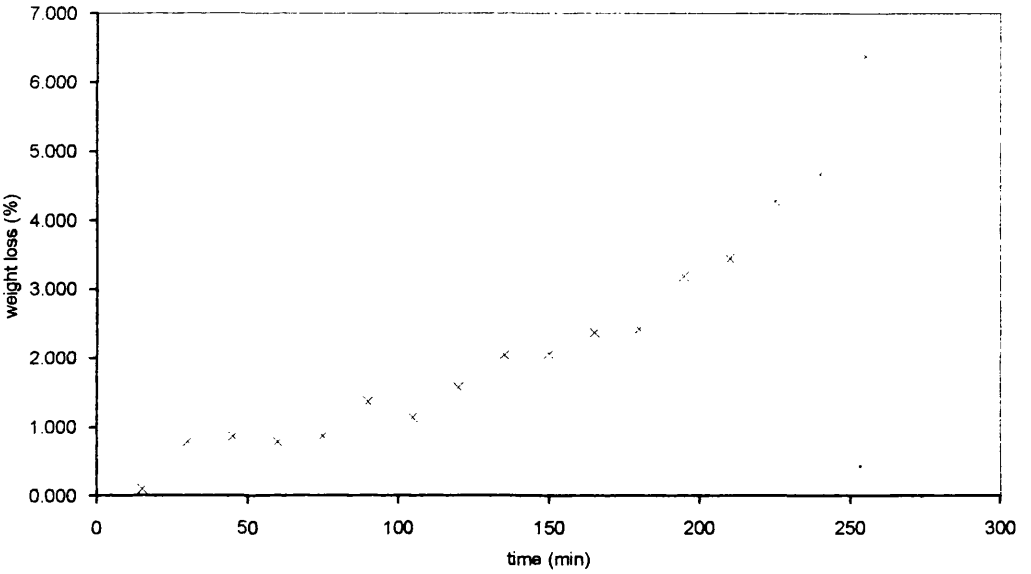

Table 3.20 Measurements taken from PHB with 5000ppm Irganox PS802 at 200°C in oil bath

Tube number	Heating time (min)	Initial mass of sample (g)	Mass lost on heating (g)	Mass lost (%)
1	15	0.1030	0.0001	0.10
2	30	0.1009	0.0008	0.79
3	45	0.1043	0.0009	0.86
4	60	0.1016	0.0008	0.79
5	75	0.1025	0.0009	0.88
6	90	0.1021	0.0014	1.37
7	105	0.0962	0.0011	1.14
8	120	0.0951	0.0015	1.58
9	135	0.1023	0.0021	2.05
10	150	0.1013	0.0021	2.07
11	165	0.0968	0.0023	2.38
12	180	0.0946	0.0023	2.43
13	195	0.0970	0.0031	3.20
14	210	0.1016	0.0035	3.44
15	225	0.1004	0.0043	4.28
16	240	0.0941	0.0044	4.68
17	255	0.0955	0.0061	6.39

Figure 3.21 *Weight loss vs. time for PHB with 5000ppm pyromellitic dianhydride at 200°C in oil bath*

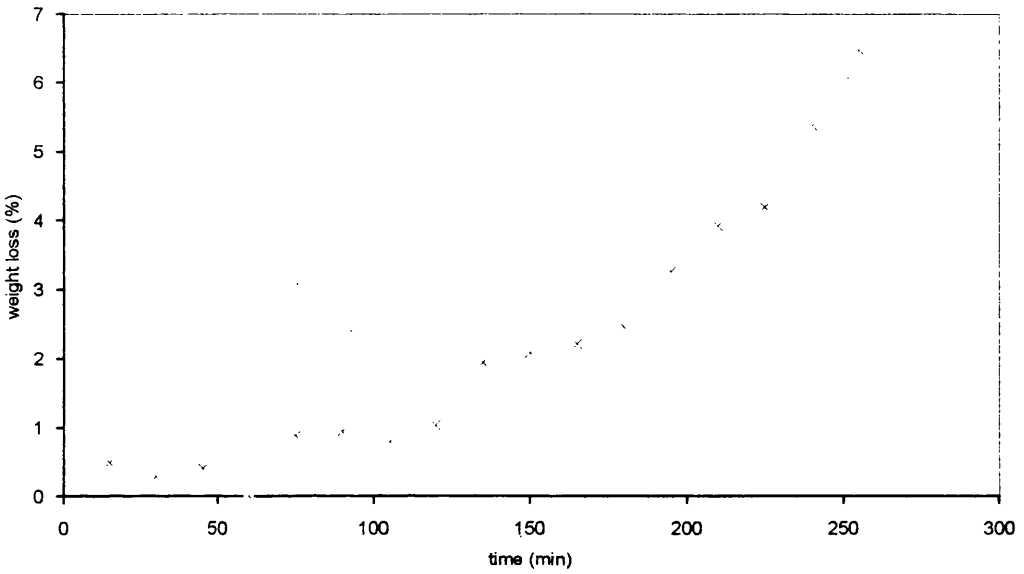

Table 3.21 *Measurements taken from PHB with 5000ppm pyromellitic dianhydride at 200°C in oil bath*

Tube number	Heating time (min)	Initial mass of sample (g)	Mass lost on heating (g)	Mass lost (%)
1	15	0.1022	0.0005	0.49
2	30	0.1046	0.0003	0.29
3	45	0.0976	0.0004	0.41
4	60		(sample tube cracked)	
5	75	0.1015	0.0009	0.89
6	90	0.1055	0.0010	0.95
7	105	0.1007	0.0008	0.79
8	120	0.0968	0.0010	1.03
9	135	0.0977	0.0019	1.94
10	150	0.1006	0.0021	2.09
11	165	0.0991	0.0022	2.22
12	180	0.0973	0.0024	2.47
13	195	0.0980	0.0032	3.27
14	210	0.1045	0.0041	3.92
15	225	0.1025	0.0043	4.20
16	240	0.1002	0.0054	5.39
17	255	0.0956	0.0062	6.49

Figure 3.22 First order plot of weight loss from PHB with various additives, heated in an oilbath at 200°C

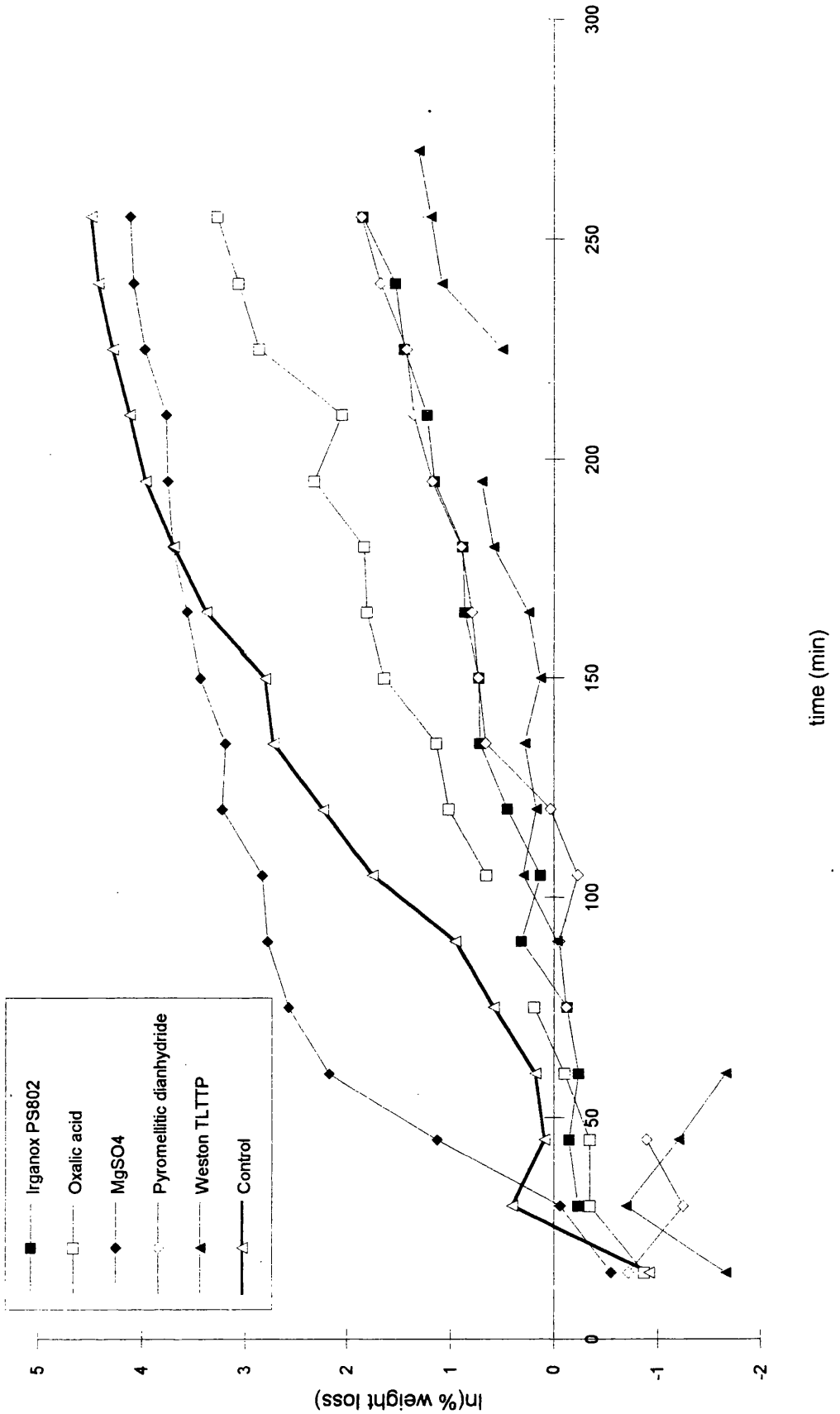

Molecular weight measurements

To complement the results from the weight loss versus time experiments, each sample was submitted to molecular weight analysis by gel permeation chromatography (GPC).

Again the results are as expected with the majority of additives improving the rate of fall of molecular weight with respect to the control(figure 3.23), but magnesium sulphate appears to show a prodegradant effect.

Table 3.22 Molecular weight measurements of PHB (with additive) heated at 200°C in an oil bath.

	Molecular weight (×1000)					
time (min)	Irganox PS802	Oxalic acid	Magnesium sulphate	Pyromellitic dianhydride	Weston TLTTP	Control
15	62.6	62.79	42.92	90.1	76.59	47.61
30	22.9	32.71	10.97	30.5	46.51	23.74
45	15.0	19.11	1.91	19.8	28.22	13.46
60	11.2	10.56	0.91	13.8	20.49	7.87
75	9.64	7.38	0.76	10.5	15.73	4.63
90	8.24	5.69	0.77	9.11	12.21	3.24
105	7.28	4.51	0.73	7.66	9.94	1.41
120	6.23	3.40		6.55	9.18	1.09
135	5.62	0.15		5.53	7.66	0.73
150	5.00			4.91	6.84	0.70
165	4.73			4.38	5.94	0.48
180	4.14			3.88	5.22	0.38
195	3.72			3.22	4.54	
210	3.44			2.91	4.15	
225	2.95			2.66	3.21	
240	2.87			2.42	2.91	
255	2.33			2.02	0.12	

First order plots for each additive (figure 3.24) confirms their relative stabilising effect by giving the following rate constants for the decrease in molecular weight.

Table 3.23 First order rate constants calculated from molecular weight measurements

Sample	First order rate constant (min^{-1})
Control	29.4×10^{-3}
Irganox PS802	10.4×10^{-3}
Oxalic acid	27.2×10^{-3}
Magnesium sulphate	43.9×10^{-3}
Pyromellitic dianhydride	12.5×10^{-3}
Weston TLTTP	12.8×10^{-3}

These rate constants match those for the weight loss very well. Again the Irganox, Weston and pyromellitic dianhydride additives are performing well.

Magnesium sulphate appears to be very much prodegradant in this case, contrary to the weight loss result. However the first order plot is not linear, as in the weight loss plot, again indicating that this additive causes the polymer to degrade by a different mechanism.

Figure 3.23 Molecular weight of PHB additive samples heated in an oilbath at 200°C

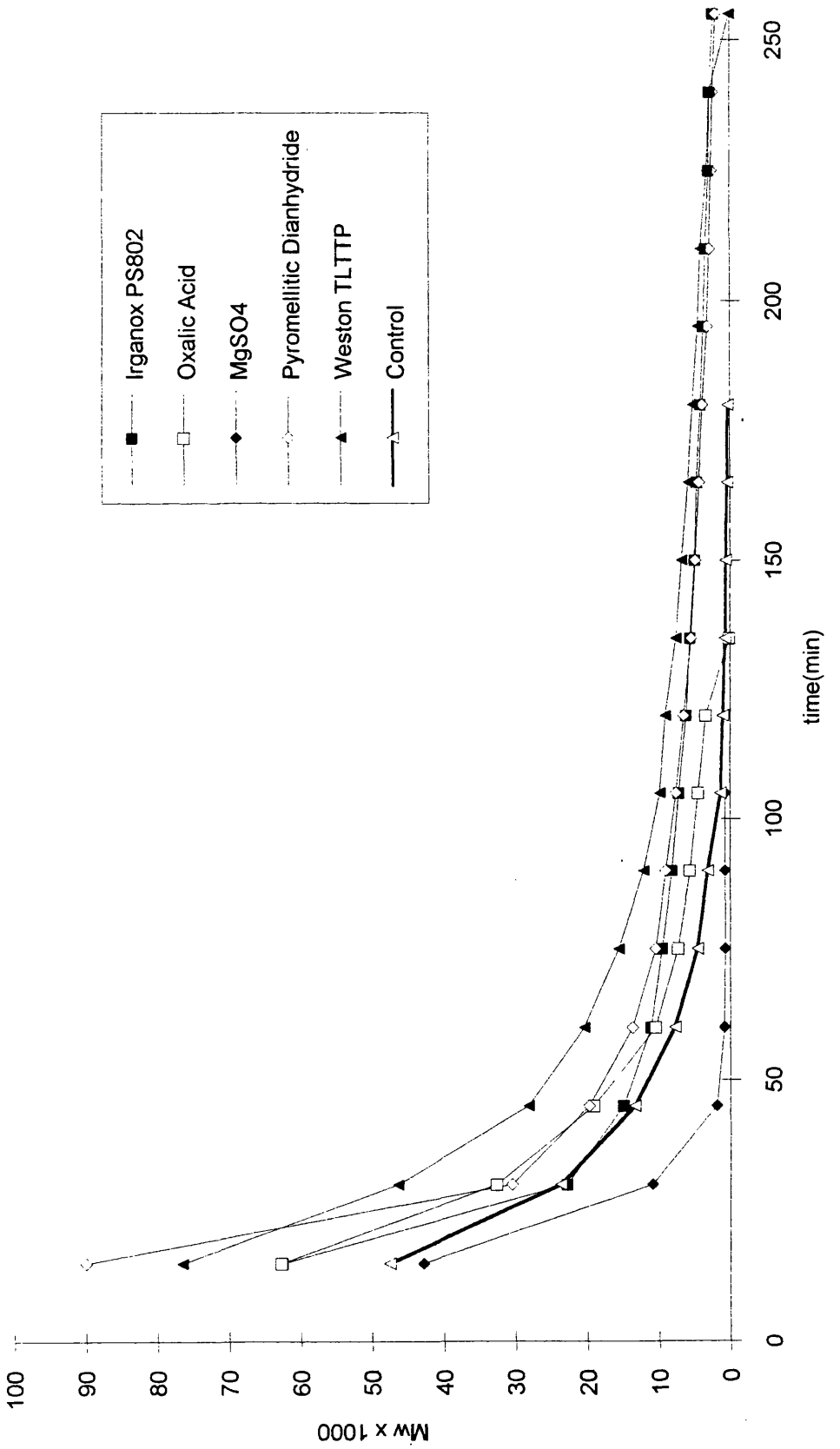

Figure 3.24 First order plot for decrease in molecular weight of PHB additive samples heated in an oilbath at 200°C

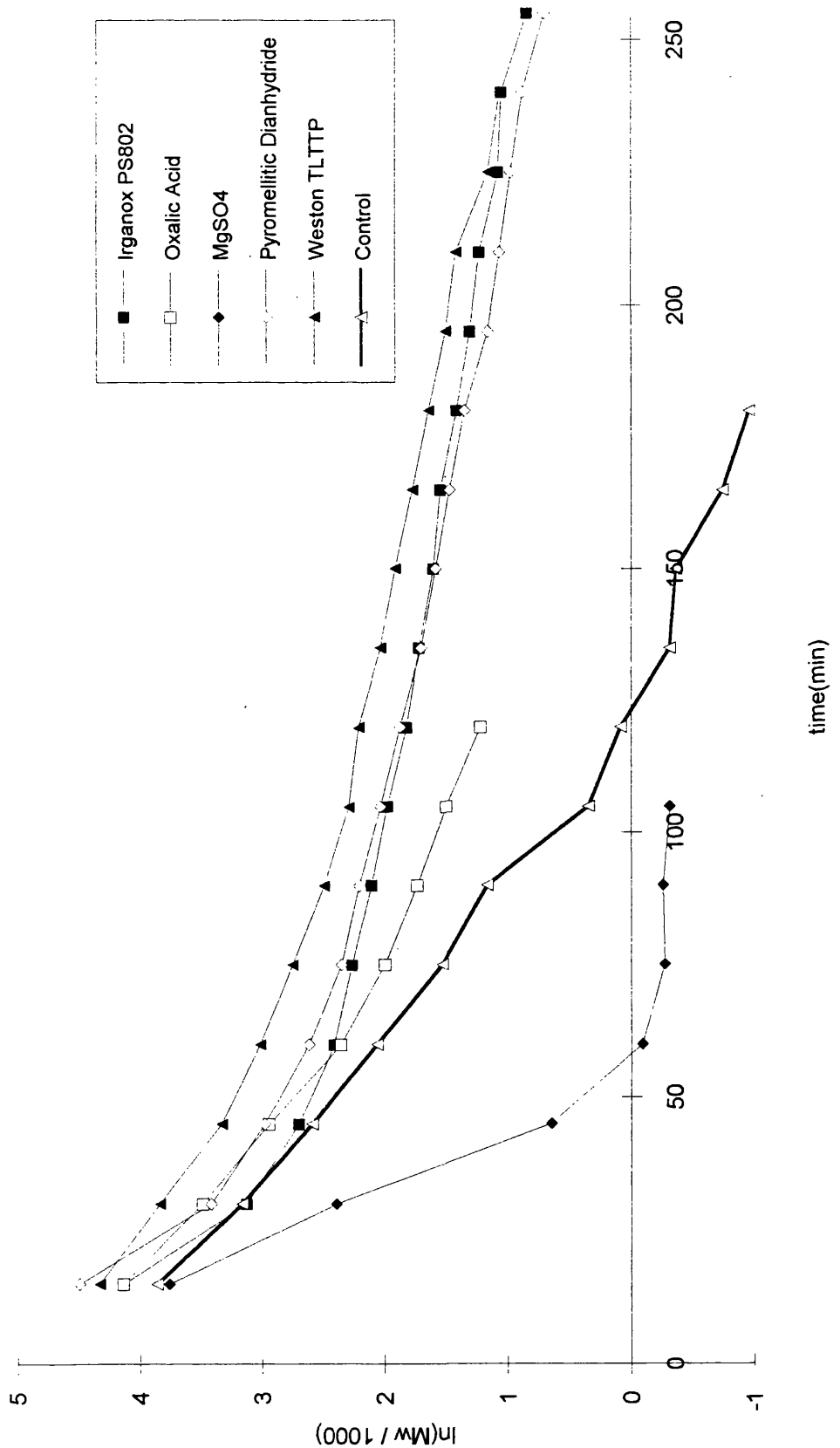

Direct comparison of stabilisers using molecular weight measurements

As stated previously, for the oil bath experiments results from two separate experiments cannot be directly compared as it is impossible to reproduce the experimental conditions exactly. For this reason a set of experiments was run to directly compare the additives. The experiments were run at three specified temperatures (180, 200 and 220°C) and for three specified periods of time (5, 10 and 20 minutes). Each additive was run in triplicate to reduce uncertainty, as in a typical oil bath experiment, and the experiment performed in the usual way (*see p89*) at the desired temperature and for the specified time. The molecular weight of each sample was then determined by GPC (gel permeation chromatography).

The average molecular weight was taken and used to calculate a stabilising/destabilising factor, as for the weight loss experiments. This is calculated as the ratio of the average molecular weight of the control samples to that of the samples with additive, or the reciprocal, whichever is greater than one. For convenience a stabilising factor is denoted as a positive number and a destabilising factor as a negative. To aid graph plotting the value one is subtracted from the stabilising/destabilising factor to give the fraction of improvement/depreciation. Thus, a stabilising factor of 1.5 gives an improvement fraction of 0.5 which means that the sample has molecular weight 50% greater than the control, or conversely a destabilising factor of -1.5 gives a depreciation fraction of -0.5 which means the sample has a molecular weight 50% less than the control.

Using this improvement/depreciation fraction graphical comparisons have been produced(figure 3.25). The charts show some correlation but some are vastly different. It is thought this may be due to poor experimental method as the some of the measured molecular weights varied enormously, i.e. there was a large amount of scatter, for different samples containing the same additive.

To quantify this scatter the relative variance (relative average deviation from the mean) was calculated for each additive type.

$$\text{Relative variance} = \frac{\sum|x-\bar{x}|}{n} \times \frac{1}{\bar{x}}$$
$$= \sum\left|\frac{x}{\bar{x}} - 1\right| \times \frac{1}{n}$$

This was summed for each sample type to give an overall value for the experiment. It can be seen that for many of the experiments this value is very low, less than 0.1 and the charts show a similar pattern, but when the value is high, greater than 0.2, then the charts are dissimilar to the rest. For the intermediate values, between 0.1 and 0.2, there is one similar to those with low scatter and one dissimilar.

For these reasons, it is believed that the chart for 10 minutes at 200 °C is a typical example with all additives except magnesium sulphate producing a significant stabilising effect. It appears that oxalic acid and pyromellitic diannydride have the largest effect, up to 50% improvement, whilst the Irganox and Weston additve a slightly smaller effect, with up to 30% improvement.

Figure 3.25 Direct comparison of stabilisers, by improvment factor, for various oilbath experiments, based on molecular weight measurements.

Additives used

A	Irganox PS802
B	Oxalic acid
C	Magnesium sulphate
D	Pyromellitic dianhydride
E	Weston TLTTP

180°C for 5mins

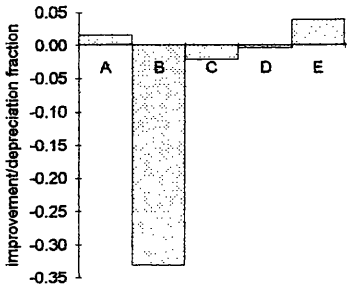

180°C for 10mins

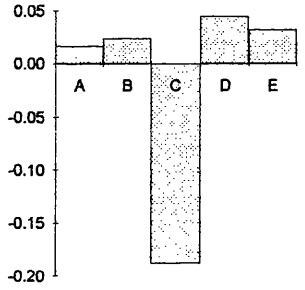

180°C for 20mins

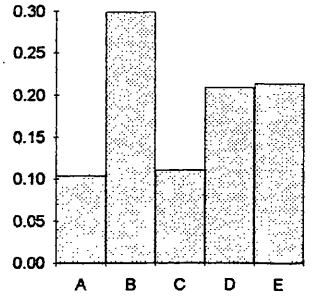

200°C for 5mins

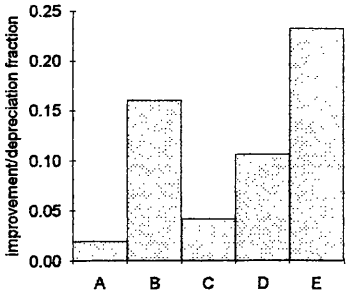

200°C for 10mins

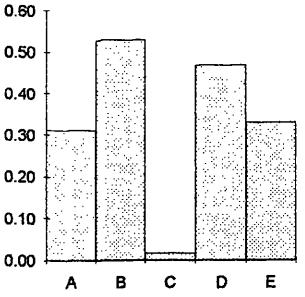

200°C for 20mins

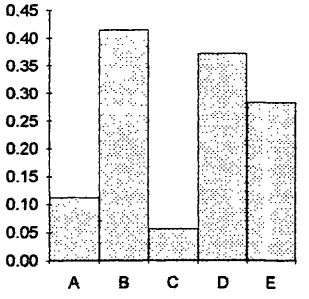

220°C for 5mins

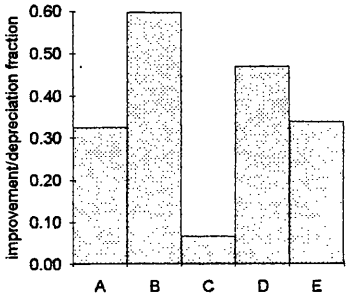

220°C for 10mins

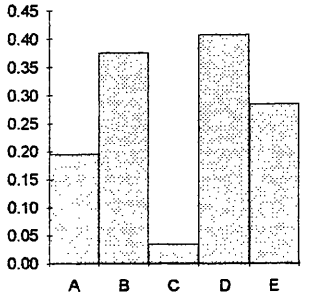

Table 3.24 Molecular weight measurements for 5 minutes at 180°C in oil bath

	Mw measurements (×1000)			Mean	relative variance	stabilising factor	improve -ment fraction
Irganox PS802	510	535	535	526.7	0.021	1.02	0.02
Oxalic acid	403	401	364	389.3	0.043	-1.33	-0.33
Magnesium sulphate	510	504	508	507.3	0.004	-1.02	-0.02
Pyromellitic dianhydride	512	503	533	516.0	0.022	-1.00	0.00
Weston TLTTP	546	540	529	538.3	0.012	1.04	0.04
Control	536	501		518.5	0.034		
total relative variance					0.136		

Table 3.25 Molecular weight measurements for 10 minutes at 180°C in oil bath

	Mw measurements (×1000)			Mean	relative variance	stabilising factor	improve ment fraction
Irganox PS802	419	422	440	426.8	0.020	1.02	0.02
Oxalic acid	421	431	439	430.0	0.014	1.02	0.02
Magnesium sulphate	352	351	357	353.5	0.007	-1.19	-0.19
Pyromellitic dianhydride	426	443	447	438.7	0.019	1.04	0.04
Weston TLTTP	436	417	447	433.3	0.025	1.03	0.03
Control	420	420		420.0	0.000		
total relative variance					0.085		

Table 3.26 Molecular weight measurements for 20 minutes at 180°C in oil bath

	Mw measurements (×1000)			Mean	relative variance	stabilising factor	improve ment fraction
Irganox PS802	168	174	173	171.7	0.014	1.10	0.10
Oxalic acid	191	196	219	202.0	0.056	1.30	0.30
Magnesium sulphate	166	177	175	172.7	0.026	1.11	0.11
Pyromellitic dianhydride	181	196	187	188.0	0.028	1.21	0.21
Weston TLTTP	193	203	170	188.7	0.066	1.21	0.21
Control	149	162		155.5	0.042		
total relative variance					0.232		

Table 3.27 Molecular weight measurements for 5 minutes at 200°C in oil bath

	Mw measurements (×1000)			Mean	relative variance	stabilising factor	improvement fraction
Irganox PS802	166	176	175	172.3	0.025	1.02	0.02
Oxalic acid	203	195	190	196.0	0.024	1.16	0.16
Magnesium sulphate	180	184	164	176.0	0.045	1.04	0.04
Pyromellitic dianhydride	186	187	188	187.0	0.004	1.11	0.11
Weston TLTTP	207	211	207	208.3	0.009	1.23	0.23
Control	185	153		169.0	0.095		
total relative variance					0.201		

Table 3.28 Molecular weight measurements for 10 minutes at 200°C in oil bath

	Mw measurements (×1000)			Mean	relative variance	stabilising factor	improvement fraction
Irganox PS802	89.6	89.6	86.1	88.4	0.018	1.31	0.31
Oxalic acid	100	103	105	103.1	0.020	1.53	0.53
Magnesium sulphate	69.2	69.0	67.6	68.6	0.010	1.02	0.02
Pyromellitic dianhydride	98.0	98.7	100	98.9	0.008	1.47	0.47
Weston TLTTP	88.2	91.7	88.9	89.6	0.016	1.33	0.33
Control	69.1	65.8		67.4	0.024		
total relative variance					0.095		

Table 3.29 Molecular weight measurements for 20 minutes at 200°C in oil bath

	Mw measurements (×1000)			Mean	relative variance	stabilising factor	improvement fraction
Irganox PS802	30.3	31.8	30.0	30.7	0.024	1.11	0.11
Oxalic acid	40.7	38.2	38.2	39.0	0.028	1.41	0.41
Magnesium sulphate	28.8	29.1	29.6	29.2	0.010	1.06	0.06
Pyromellitic dianhydride	37.8	38.8	37.0	37.9	0.016	1.37	0.37
Weston TLTTP	36.2	35.5	34.5	35.4	0.017	1.28	0.28
Control	27.5	27.7		27.6	0.004		
total relative variance					0.099		

Table 3.30 Molecular weight measurements for 5 minutes at 220°C in oil bath

	Mw measurements (×1000)			Mean	relative variance	stabilising factor	improvement fraction
Irganox PS802	68.8	63.4	63.7	65.3	0.036	1.32	0.32
Oxalic acid	82.9	75.6	77.7	78.7	0.035	1.60	0.60
Magnesium sulphate	54.6	52.0	51.1	52.6	0.026	1.07	0.07
Pyromellitic dianhydride	70.9	74.4	72.0	72.4	0.018	1.47	0.47
Weston TLTTP	63.8	67.9	66.2	66.0	0.022	1.34	0.34
Control	49.2	49.4		49.3	0.002		
total relative variance					0.139		

Table 3.31 Molecular weight measurements for 10 minutes at 220°C in oil bath

	Mw measurements (×1000)			Mean	relative variance	stabilising factor	improvement fraction
Irganox PS802	16.7	17.4	17.0	17.0	0.014	1.20	0.20
Oxalic acid	19.2	19.1	20.5	19.6	0.031	1.38	0.38
Magnesium sulphate	14.7	14.8		14.8	0.003	1.04	0.04
Pyromellitic dianhydride	19.8	20.3		20.1	0.012	1.41	0.41
Weston TLTTP	17.9	18.7		18.3	0.022	1.28	0.28
Control	14.1	14.4		14.3	0.011		
total relative variance					0.093		

Heated plate FT-IR

It is clear that the important part of the degradation, from an industrial point of view, is in the early stages where there has been little or no weight loss from the bulk material. So it makes sense to concentrate on analysing the polymer as it decomposes, rather than the volatile products, as it would yield more accurate information about the state of the polymer.

A system has been devised that enables the heating of a thin film and allows the recording of an infra red spectrum simultaneously.

The apparatus(Figure 3.32) fits into the FTIR spectrometer and deviates the IR beam onto a thin film of polymer, trapped behind a NaCl window. The beam reflects off a polished heating surface behind the film and returns to its original path. The beam, therefore, has effectively passed through the film twice and produces a typical absorbance spectrum of the polymer. The heating plate is accurately held at 200°C by a thermocouple feedback temperature controller.

The apparatus had to be redesigned a number of times. Initially it consisted of a single 25 watt soldering iron heating element which only heated to 130°C. Two of these 25W heating elements attained the desired operating temperature of 200°C but after around only 8 hours of use they fused and the apparatus had to be completely rebuilt with a single 150W cartridge heater.

The experimental procedure involves casting a very thin film of PHB from a chloroform solution onto the polished heating plate. When dry, a sodium chloride window is secured on front and the apparatus mounted in the sample chamber of the spectrometer. The mirrors are then aligned to direct the infra red beam onto the sample and to focus it onto the detector of the machine to obtain maximum signal strength and hence optimum sensitivity. The heater would be set to 200°C and the spectrometer control software set to collect a spectrum every five minutes. These spectra are stored for later reference and manipulation.

Figure3.32 Schematic diagram of heated plate FT-IR attachment

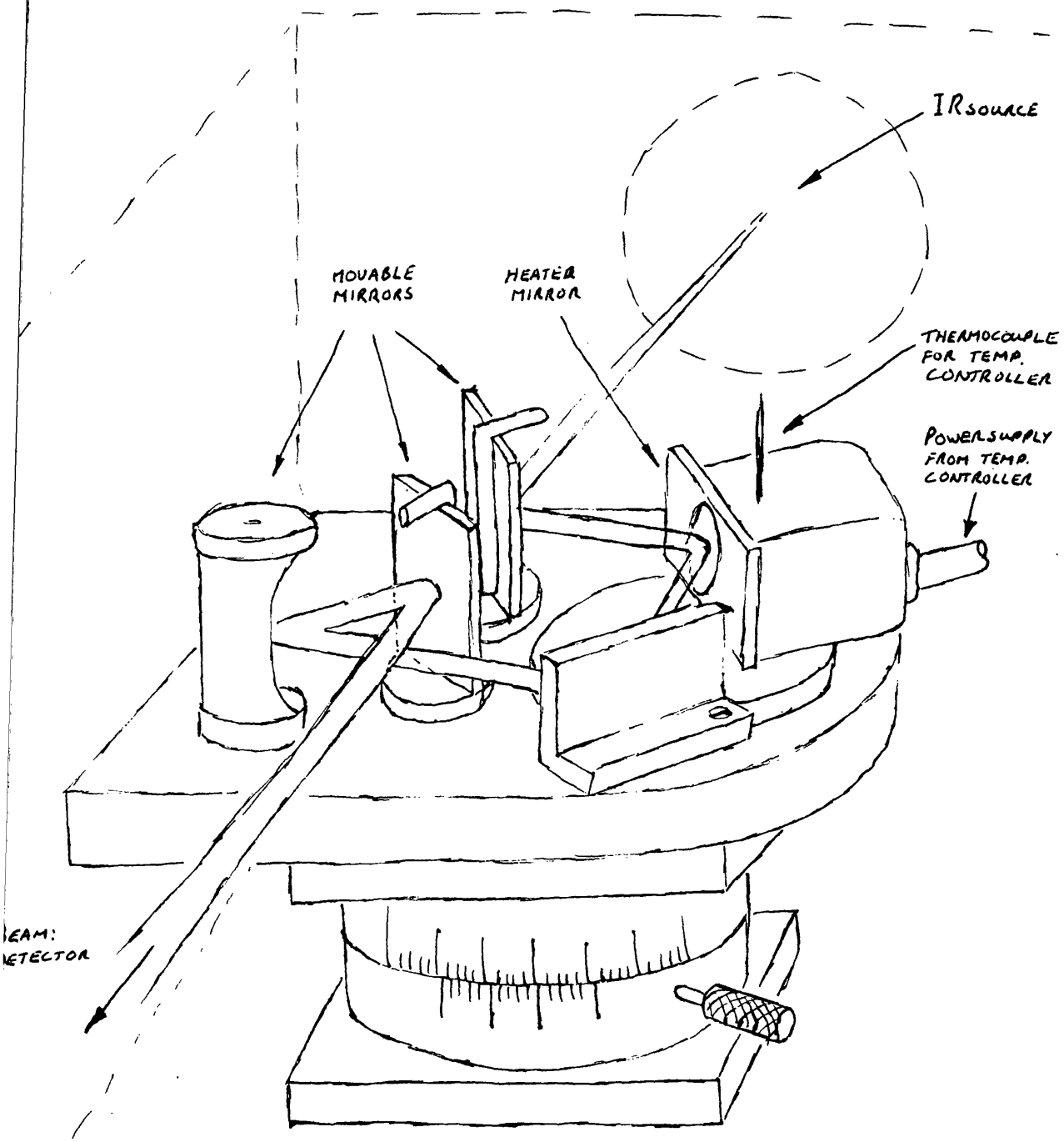

Degradation of poly(hydroxybutyrate) without additive

Prior to heating, the polymer film produces a spectrum typical of that for PHB. On heating, there is an initial change, attributed to melting, followed by steady reduction in the overall intensity of the spectrum. Towards the latter part of the series absorptions due to unsaturation begin to appear and the position of the carbonyl shifts and broadens, producing a spectrum very like that of the cold ring fraction collected from TVA experiments (*see 'TVA and PHB' p20*). This is followed by much diminished spectra indicating that most of the polymer has degraded and volatilised.

Figure 3.33 Comparison of starting material with products after four hours at 200°C in heated film FTIR apparatus

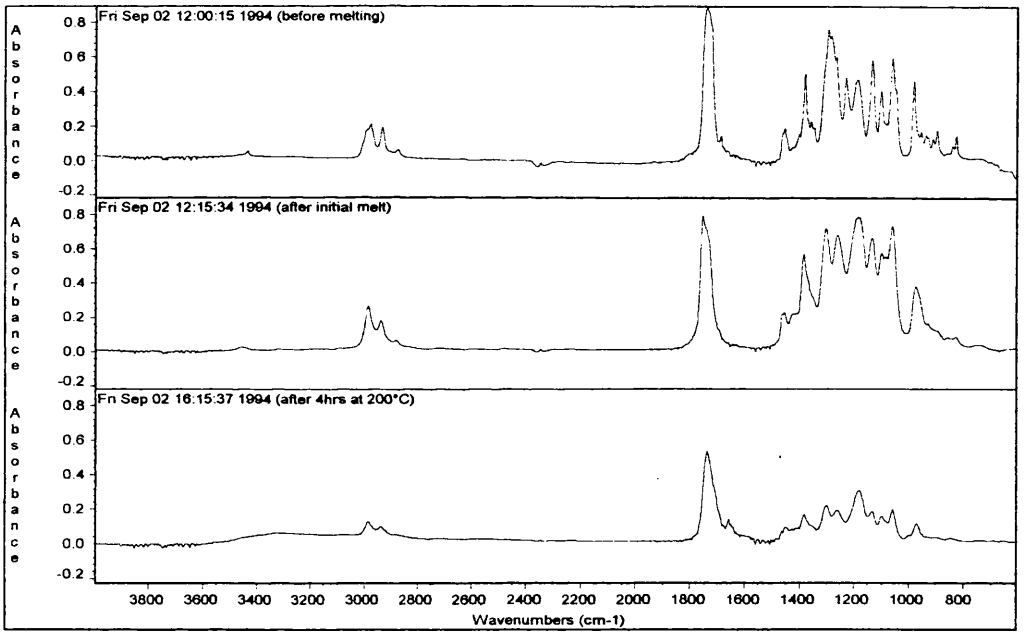

As with the heated gas cell experiments (*see 'Degradation of PHB in heated gas cell' p54*) the main advantage of this system is that it enables us to accurately monitor the relative quantities of compounds present with respect to time and can be visualised on a 3-dimensional plot. This is generated in a similar way to that for the heated gas cell using the Fortran programs and Microsoft Excel. The spectrometer data is converted to a comma separated

variable (CSV) format, which is then read, modified and re-written by the Fortran program which, in turn, is read by Excel, to plot the graph.

This data benefits enormously from the baseline and water vapour software corrections used for the heated gas cell data(*see 'Three dimensional representation of data' p55*). The Nicolet FTIR spectrometer is a single beamed instrument, so each sample spectrum is measured with reference to a background spectrum, recorded previously. Thus, any change in environmental conditions, such as humidity or temperature, can affect the spectra adversely and obscure fine details. The software correction moves the apparent baseline of the spectrum onto the x-axis and can remove absorbances due to water vapour. The benefits are apparent in the figures of PHB degradation, where after 'cleanup'(Figure 3.35), the formation and disappearance of the unsaturation bands (~1655cm^{-1}) can be seen clearly , while they are completely obscured in the 'crude' data(Figure 3.34).

From the 3 dimensional plot, after the initial melting stage, the carbonyl absorbance decreases in a smooth curve. This appears to be in good correlation with the heated gas cell(*see 'Degradation of PHB in heated gas cell' p54*) and weight loss data(*see 'Weight loss vs. time' p140*).

This heated film apparatus is potentially a very powerful tool for examining the degradation processes that take place in polymer melts and has been used to determine the effect of a few of the additives identified previously.

Figure 3.34 Raw data for C O region of PHB in heated plate FT-IR apparatus

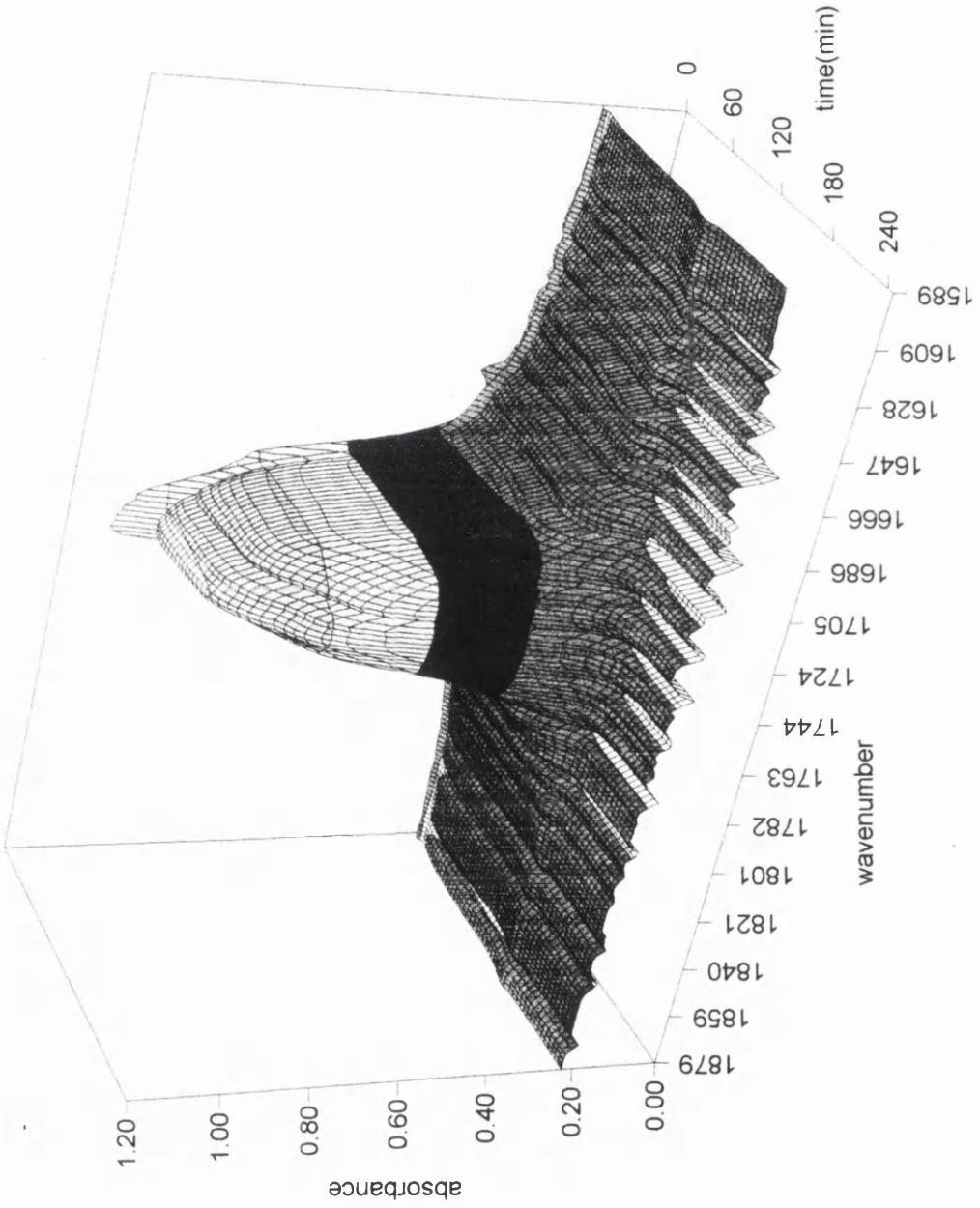

Figure 3.35 C O region for PHB in heated plate FT-IR apparatus after baseline and watervapour corrections

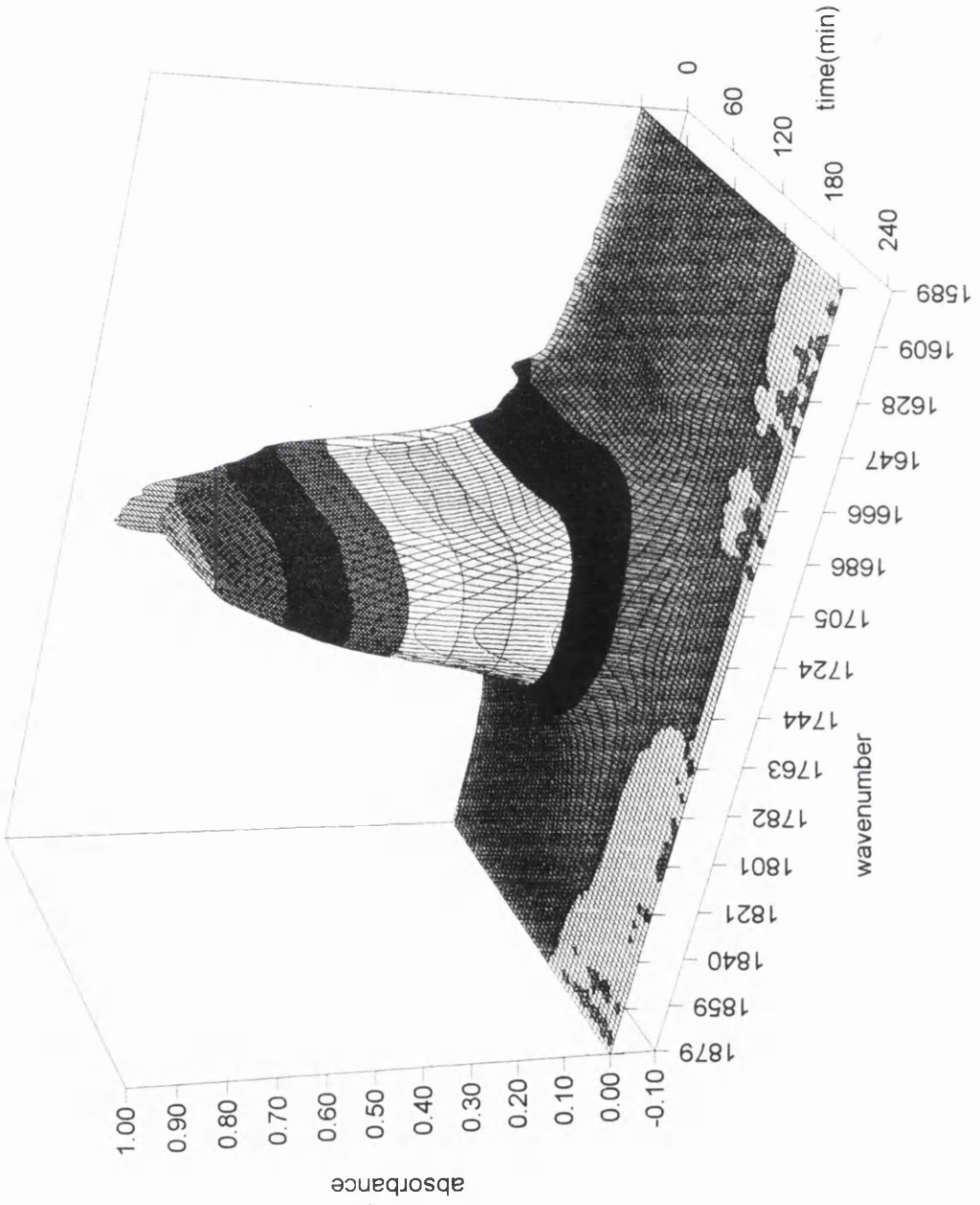

Weston TLTTP

A mix of PHB solution and Weston TLTTP was made up and cast onto the heating plate, and subjected to the above procedure. (Figure3.36)After an initial melting, the carbonyl peak halves in intensity and broadens considerably, over a period of about an hour. After this, there is no further change in the system over the duration of the experiment. There is no accumulation of unsaturation at all. The oil bath experiments show that there is very little weight loss from a mixture of PHB and Weston TLTTP, hence the observed drop in absorbance must be due to some other factor other than loss of material from the sample. The broadening of the peak suggests that the carbonyl groups are changing their environment, shifting the absorbance to a different wavelength. Although it is impossible to predict extinction coefficients exactly, the area under the peak in the carbonyl region is similar, throughout this change, which is consistent with this idea as the area under the peak would diminish if the carbonyl groups were being lost or destroyed.

The dramatic change in intensity and broadening of the carbonyl peak suggests that the additive is acting upon a large proportion of the carbonyl groups in the bulk polymer changing their nature. The sustained intensity of the carbonyl band along with the absence of any unsaturation absorbance suggests that the additive is quite successful at preventing degradation

Oxalic acid

A film was made by mixing solutions of PHB and oxalic acid which were then cast onto the heating plate. On heating it appears that the major changes occur in the first 30 minutes(Figure 3.37). A decrease in the carbonyl at 1749cm^{-1} is concurrent with an increase at 1632cm^{-1}. The band at 1632cm^{-1} can be attributed to oxalic acid which has only become apparent after melting. Following this stage the polymer would seem to be completely stable as the spectra are very similar, indicating that there is no further loss of material. This is similar situation to what was seen with Weston TLTTP

Magnesium sulphate

This film was made up as a 'sandwich' as the polymer and additive do not share a common solvent. A film of PHB was cast onto the heating plate, followed by an aqueous $MgSO_4$ solution , followed by another PHB film. On heating (Figure 3.37) there was an initial change at 1620-1680cm^{-1} region corresponding to an absorbance due to sulphate ions, but after this the intensity of the whole spectrum appears to decrease steadily which suggests volatilisation of the polymer. This would appear to confirm the linear weight loss that was seen in the oil bath experiments.

There are a number of intrinsic problems in the use of this apparatus.

The polymer is in direct contact with a sodium chloride window, which is known to be a pro degradant. An inert substance, such as quartz, would be much more satisfactory.

The thickness of the film cannot be controlled, a variable that is known to influence the degradation behaviour of PHB[59], but in the above cases the absorbances are of similar intensity and so the films are expected to be of comparable thickness.

It would also be much better to subtract any absorbances due to the additive, such that the polymer spectrum can be examined more easily. This would be a relatively simple procedure , working in much the same way as the water vapour correction using a spectrum of the pure additive instead of water vapour(*see p56*).

In spite of these problems, the changes observed for the above additives vary considerably suggesting that there is no common chemical mechanism, and confirming what has already been discovered about the effectiveness of these additives.

Figure 3.36 C=O region for PHB / Weston TLTTP in heatedplate FT-IR apparatus

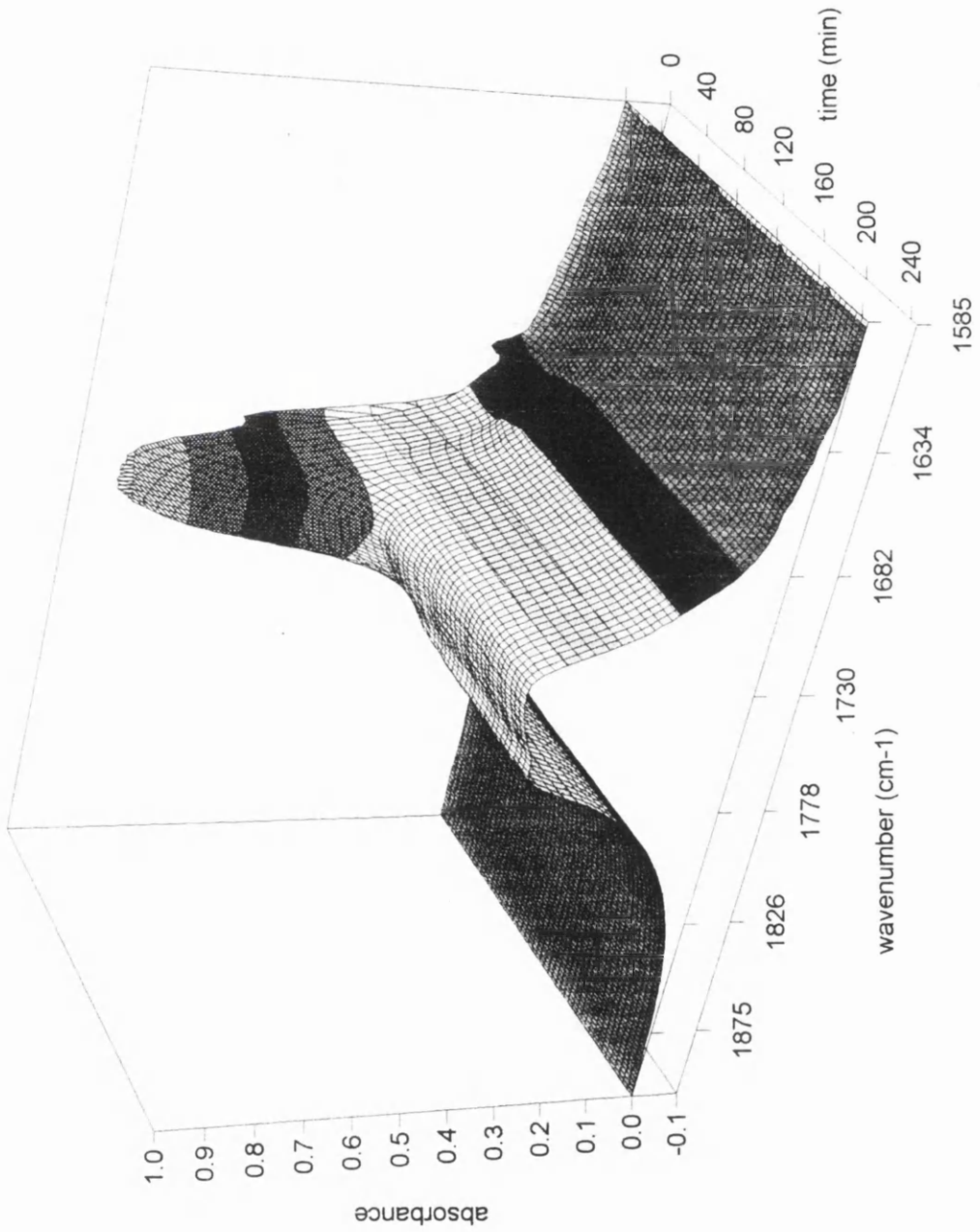

Figure 3.37 C=O region for PHB / oxalic acid in heatedplate FT-IR apparatus

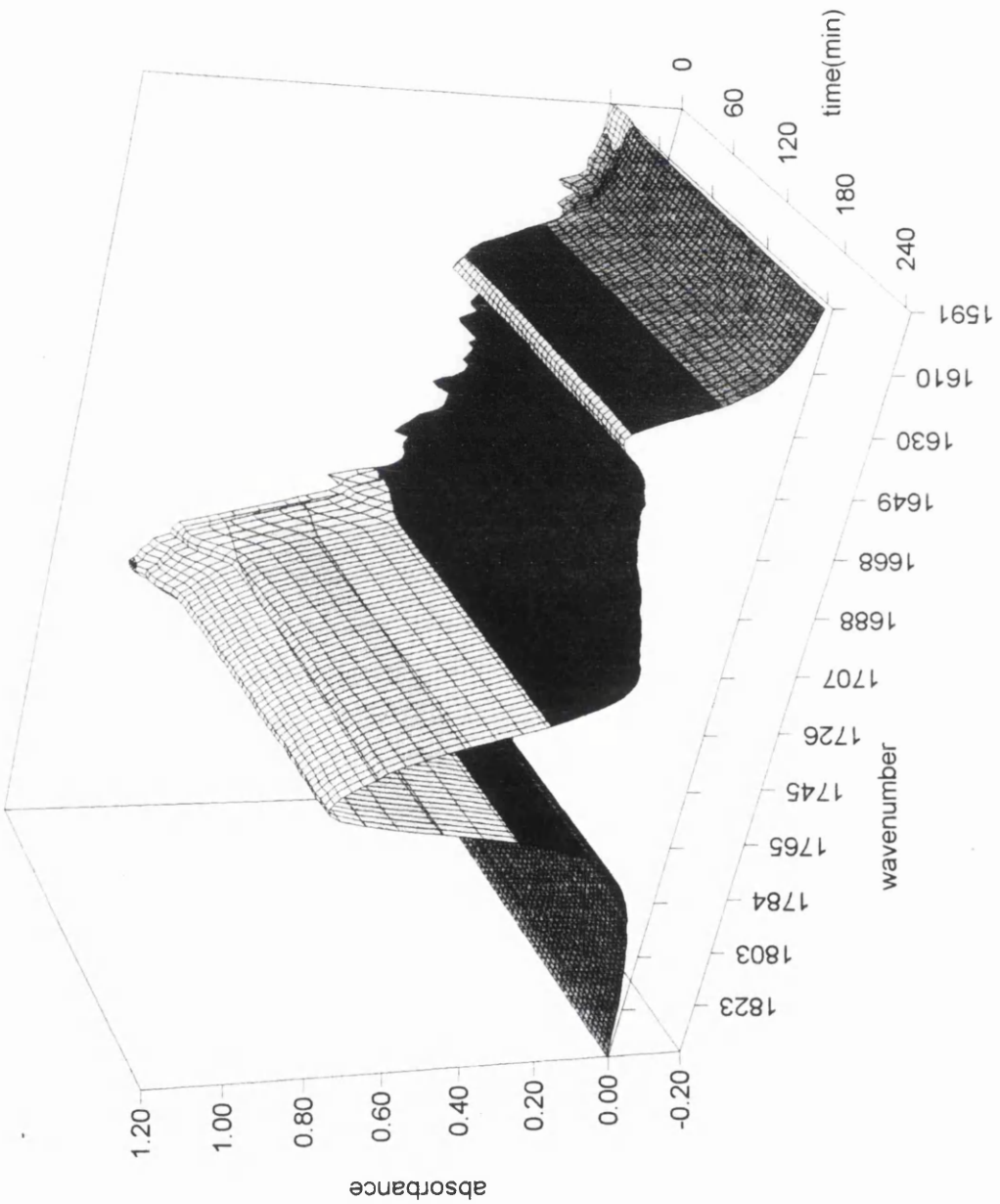

Figure 3.38 C=O region for PHB / magnesium sulphate in heatedplate FT-IR apparatus

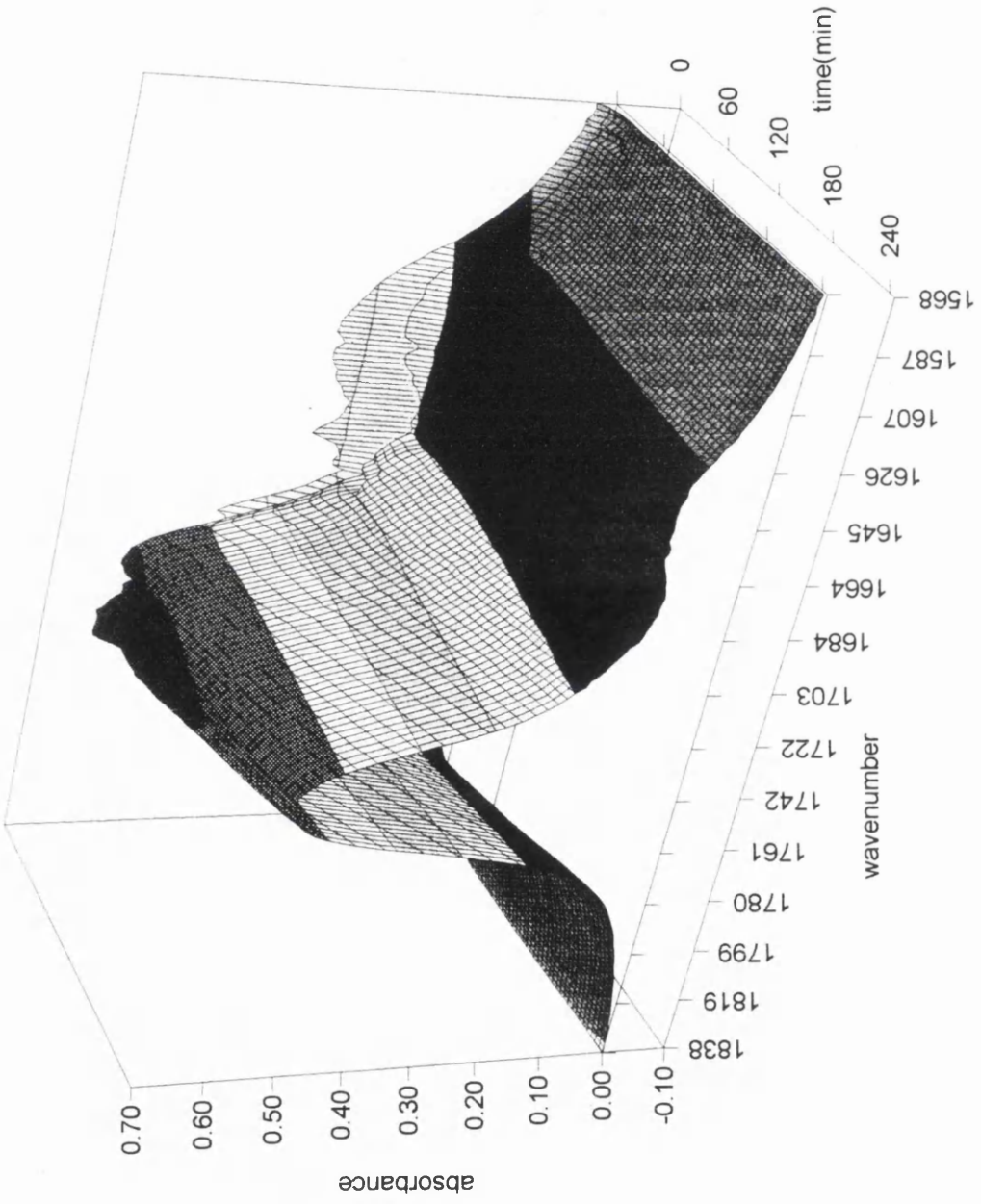

Conclusion

A number of new methods for analysing the degradation of polymers have successfully been devised.

These have included a number of modifications to the existing TVA apparatus. Internal thermocouples have been shown to be able to detect formation of cold ring fraction and the reproducibility of TVA experiments has been shown to be very precise. A thermal volatilisation mass spectrometry system was constructed, that allowed continuous recording of mass spectra of the volatile gases evolved from a sample under ramped heating conditions.

Similar systems were developed for FT-IR. By use of a heated gas cell, the IR spectra of volatile products could be recorded with respect to time, allowing both qualitative and quantitative measurements to be made. Kinetic information can also be deduced from these quantitative measurements. Heated mirror apparatus was designed to analyse polymer melts by IR. Again qualitative and quantitative measurements can be made, showing changes in its chemical nature and loss of material, thus allowing direct analysis of the polymer as it degrades. Software was written to 'clean up' the spectra from these systems, by removing noise and unwanted spectra, and to plot the data in three dimensions to make the data much easier to visualise.

These methods were applied to PHB, in an attempt to gain better understanding of the degradation processes that take place.

A large number of additives have been tested for suitability as stabilisers for PHB. This was done by measuring weight loss from samples of polymer after a number of other techniques were discarded because of poor reproducibility or being too unwieldy for repeated use. Additives that showed stabilising effects could be classified by the functional groups present. Within these classifications, it was discovered that not only did the structure of the compounds change the effectiveness, but the stereochemistry did also. A selection of these favourable additives were used in further trials, with

molecular weight, MFI (melt flow index) and kinetic measurements being made.

The heated mirror FT-IR apparatus was used to examine the effects of a few of the additives, indicating that there is not a common mechanism for all of the additives.

The techniques developed in this work proved to be successful in the observation of the degradation of PHB. However, they are not limited to the study of PHB but could easily be used or adapted for many other polymer systems. It is hoped that, in the future they shall be used for such.

Similarly, a number of compounds have been identified as having stabilising effects upon PHB, and although their effects are perhaps not as large as one might have hoped, they are very significant and will possibly find their way into the manufactured product, or at the least provide pointers to other compounds that will provide PHB with its maximum thermal stability.

References

1 Lemoigne, M., *Ann. Inst. Past.*, **39**, (1925), 144

2 Okamuka, K.; Marchessault, R.H., *'Conformation of Biopolymers'*, Ramachandran, G.N., (Ed), Academic Press, London, Vol 2, (1967), 709

3 Dawes, E.A.; Senior, P.J., *Ad. Microbial Phys.*, **10**, (1973), 138.

4 Lundgren, D.G.; Alper,R.; Schnaitman, C.; Marchessault, R.H., *J. Bacteriol.*, **89**, (1965), 245.

5 Holmes, P.A.;Wright, L.F.; Alderson, B.; Senior, P.J., (ICI plc.), Eur. Patent Appln. EP 15123, (1980).

6 Lafferty, R.M.; Heinzle, E, *Chem. Rundschau*, **30**, (1977), 14.

7 Lafferty, R.M., (Agroferm AG), US Patent 4,101,533, (1977).

8 Williamson, D.H.; Wilkinson, J.F., *J. Gen. Microbiol.*, **19**, (1958), 198.

9 Agostini, D.E.; Lando, J.B.; Shelton, J.R., *J. Polym. Sci.*, **9**, (1971), 2789.

10 Teranishi, K.; Iida, M.; Araki, T.;Yamashita, S.; Tani, H., *Macromolecules*, **7**, (1974), 421.

11 Inoue, S.; Tomoi, Y; Tsuruta, T.; Furukawa, J., *Makromol. Chem.*, **48**, (1961), 229.

12 Agostini, D.E.; Lando, J.B.; Shelton, J.R., *J. Polym. Sci.*, **9**, (1971), 2775.

13 Shelton, J.R., D.E.; Lando, J.B.; Agostini, *J. Polym. Sci.*, **9**, (1971), 173.

14 Vergara, J.; Figini, R.V., *Makromol. Chem.*, **178**, (1977), 267.

15 Iida, M.; Araka, T.; Teranishi, K.; Tani, H., *Macromolecules*, **16**, (1983), 275

16 Araki, T.; Hayase, S.J., *J. Polym. Sci, Polym. Chem. Ed.*, **17**, (1979), 1877.

17 Kung, F.E., US patent 2,361,036 (1944).

18 W.R. Grace and Co., US patent 3,044,942 (1962).

19 Baptist, J.N.; Werber, F.X., *Soc. Plast. Eng Trans*, **4**, (1964), 245.

20 Holmes, P.A., *'Dev. Cryst. Polym - 2'*, Basset, D.C., (Ed.), Elsevier, (1988), 1.

21 Holmes, P.A.; Wright, L.F.; Collins, S.H., (ICI plc), European Patent Application EP 52459 (1981).

22 Holmes, P.A.; Wright, L.F.; Collins, S.H., (ICI plc), European Patent Application EP 69497 (1983).

23 Nakagawa, Y.; Taniguchi, M.; Aizawa, T.; Hachifusa, K.; Yoshikawa, M., (Toppan Printing Co. Ltd.), Jpn. Kokai Tokkyo Koko JP 06,106,944 (1994).

24 Aizawa, T.; Hachifusa, K.; Nakagawa, Y.; Taniguchi, M.; Yoshikawa, M., (Toppan Printing Co. Ltd.), Jpn. Kokai Tokkyo Koko JP 06,106,679 (1994).

25 Yoshikawa, M.; Nakagawa, Y.; Hachifusa, K.; Aizawa, T.; Taniguchi, M.;, (Toppan Printing Co. Ltd.), Jpn. Kokai Tokkyo Koko JP 06,123,098 (1994).

26 Brunger, P.M.; Kemmish, D.J., (ICI plc.) PCT Int. Appl. WO 10,308 (1993).

27 Harusawa, Y.; Uchida, M.; Kaneda, T., (Three Bond Co. Ltd.), Jpn. Kokai Tokkyo Koko JP 04,331,294 (1992).

28 Hasegawa, R.; Fukunaya, K., (Nippon Kayaku Kk) Jpn. Kokai Tokkyo Koko JP 05,227,939 (1993).

29 Rieker, C.; Swessmuth, R., *GWF, Gaswasserfach: Wasser/Abwasser*, **133(4)**, (1992), 231.

30 *'New Scientist'*, IPC Magazines Ltd., number 1820, **184**, (1984), 20.

31 Niven, L.; Pournelle, J.; Flynn, M., *'Fallen Angels'*, Pan Books, (1991).

32 Macrae, R.M.; Wilkinson, J.F., *J. Gen. Microbiol.*, **19**, (1958), 210.

33 Grassie, N.; Murray, E.J.; Holmes, P.A., *Polym. Deg. Stab.*, **6**, (1984), 95.

34 Grassie, N.; Murray, E.J.; Holmes, P.A., *Polym. Deg. Stab.*, **6**, (1984), 47.

35 Grassie, N.; Murray, E.J.; Holmes, P.A., *Polym. Deg. Stab.*, **6**, (1984), 127.

36 McNeill, I.C.; Bounekhel, M., *Polym. Deg. Stab.*, **34**, (1991), 187.

37 Montaudo, G.; Puglisi, C., *'Comprehensive Polymer Science'*, Pergamon Press (1992), Chapter 11, 227.

38 Carothers, W.H.; Dorough, G.L.; Vanatta, F.J., *Am.Chem. Soc.*, **54**, (1932), 761.

39 Taylor, R., *'Chemistry of Functional Groups'*, Patai, S., (Ed.), Applied Science, (1979), Chapter 15.

40 Taylor, R., *J. Chem. Soc. Perkin II*, 1975, 1025.

41 Grassie, N., *Trans. Faraday Soc.*, **48**, (1952), 379.

42 Iwabuchi, S.; Jaacks, V.; Galil, F.; Kern, W., *Makro. Chem.*, **165**, (1973), 59.

43 Burnett, G.M., *High Polymers, Vol III: "Mechanism of Polymer Reactions"*, Interscience (1954), 325.

44 McNeill, I.C., *'Comprehensive Polymer Science'*, Chapter 1, Vol 6, Pergammon, London (1989).

45 Shad, F., Thesis submitted for B.Sc.(Hons), Glasgow University, (1992).

46 *'Handbook of Chemistry and Physics 76th Edition'*, CRC Press, (1995), 15-5.

47 McNeill, I.C.; Ahmed, S.; Memetea, L., *Polym. Deg. Stab.*, **48**, (1995), 89.

48 Lehrle, R.S.; Robb, J.C.; Suggate, J.R., *Eur. Poly. J.*, **18**, (1982), 443.

49 Miller, R.G.; Stace, B.C, (Editors), *'Laboratory methods in infra-red spectroscopy, 2nd Ed.'*, Heydon, (1972), Chapter 5, 48.

50 Philpotts, A.R.; Thain, W.; Smith, P.G., *Anal Chem*, **23**, (1951), 268.

51 Coggleshall, N.D.; Savier, E.L., *J. Appl. Phys.*, **17**, (1946), 450.

52 Esperron, J.H., *'Chemical kinetics and reaction mechanism'*, McGraw Hill, (1981), 24

53 Hudlicky, M., *J. Org. Chem.*, **45**, (1980), 77.

54 Kovats E., *Helv. Chim. Acta.*, 41, (1958), 1951.

55 McNeill, I.C.; Seeley, G., unpublished

56 McNeill, I.C.; Seeley G., unpublished

57 Private communication from Zeneca Bio Products

58 Miles, D.C., Briston, J.H., *'Polymer Technology'*, Temple Press, (1965)

59 Williams, R, Ph.D. thesis, School of Chemistry, Birmingham University (1994)